IntechOpen

Sustainable Air Conditioning Systems

Edited by Chaouki Ghenai and Tareq Salameh

SUSTAINABLE AIR CONDITIONING SYSTEMS

Edited by **Chaouki Ghenai**
and **Tareq Salameh**

Sustainable Air Conditioning Systems
http://dx.doi.org/10.5772/intechopen.68608
Edited by Chaouki Ghenai and Tareq Salameh

Contributors

Emna Aridhi, Abdelkader Mami, Zhenjun Ma, Haoshan Ren, Wenye Lin, Rosenberg Javier Romero Domínguez, Khaled Saleh, Mahmoud Badawy Elsheniti, Osama Elsamni, Raya Al-Dadah, Saad Mahmoud, Eman Elsayed, Yujiro Hirano, Shogo Nakamura, Kei Gomi, Takuya Togawa, Tsuyoshi Fujita, Makoto Ooba, Muhammad Mujahid Rafique, Shafiqur Rehman

Notice

First published in London, United Kingdom, 2018 by IntechOpen
eBook (PDF) Published by IntechOpen, 2019
IntechOpen is the global imprint of INTECHOPEN LIMITED, registered in England and Wales, registration number: 11086078, The Shard, 25th floor, 32 London Bridge Street
London, SE19SG – United Kingdom
Printed in Croatia

British Library Cataloguing-in-Publication Data
A catalogue record for this book is available from the British Library

Additional hard and PDF copies can be obtained from orders@intechopen.com

Sustainable Air Conditioning Systems
Edited by Chaouki Ghenai and Tareq Salameh

p. cm.

Print ISBN 978-1-78923-300-1

Online ISBN 978-1-78923-301-8

eBook (PDF) ISBN 978-1-83881-331-4

Meet the editors

Chaouki Ghenai is an associate professor at the Sustainable and Renewable Energy Engineering Department, College of Engineering; a coordinator of the Sustainable Energy Development Research Group at the Research Institute for Sciences and Engineering; and the chairman of the Research Funding Department at the University of Sharjah. He received his PhD and master's degrees in Mechanical Engineering from University of Orleans, France. Before joining the University of Sharjah, Dr. Ghenai was an assistant professor at Florida Atlantic University, Boca Raton, Florida, and a project manager at the Applied Research Center, Miami, Florida. He worked also as a postdoc at Cornell University (Ithaca, NY), Kansas State University (Manhattan, KS), and the University of California, Los Angeles (Los Angeles, CA). Dr. Ghenai has published more than 100 research papers in technical journals, book chapters, and books. His research interests are renewable energy, energy efficiency, sustainability, combustion, biofuels, alternative fuels, clean combustion technologies, waste to energy, eco-design, energy-water nexus, energy planning and climate change mitigation assessment, modeling and simulation of microgird power systems, and air pollution.

Dr. Tareq Salameh has been an assistant professor in Sustainable and Renewable Energy Engineering Department (SREE) at the College of Engineering at the University of Sharjah in the United Arab Emirates since 2013. Dr. Salameh had gotten many scholarships and research grants from local and international organizations. He is a reviewer for different international journals. He is a member in scientific committee for different conferences. His research interests focus on energy generation by conventional and renewable resources; mechanical, thermal, and electrical energy storage systems; hybrid and renewable energy systems; design of buildings and systems of high efficiency; nanotechnology for energy systems; simulation and modeling of energy systems and components; and numerical simulation and computational fluid dynamics (CFD) for the components of energy systems.

Contents

Preface

Heating, ventilation, and air conditioning (HVAC) system is one of the major energy consumers in modern buildings (40–70% of the energy consumption in commercial buildings). The demand of energy for air conditioning systems is expected to increase further in the next decades due to the population growth, the technological advancements, the new economic boom, the urbanization development, and the increase in the living standards. The increase in energy demand leads to increased greenhouse gas emissions associated with the burning of fossil fuels and contributes to global warming. More energy-efficient and renewable energy-based air conditioning systems to accomplish space cooling are needed.

This book intends to provide the reader with a comprehensive overview of the current state of the art in sustainable air conditioning technologies and focus on the most recent research and development on green air conditioning systems including energy-efficient and renewable energy-based air conditioning systems. The book is divided in three sections: (1) "Solar Air Conditioning Systems," (2) "Absorption and Adsorption Air Conditioning Systems," and (3) "Low-Carbon Air Conditioning Systems."

The first section of this book related to the integration of solar energy in the air conditioning systems has two chapters: (1) "Solar Air Conditioning Systems" and (2) "Solar-Assisted HVAC Systems with the Integration of Phase Change Materials (PCM). The second section about the absorption and adsorption air conditioning systems has two chapters: (1) "Design and Construction for Hydroxide-Based Air Conditioning System with Solar Collector for Confined Roofs (Suitable Devices for the Operation of Air Conditioning Absorption System Based on Hydroxide)" and (2) "Adsorption Refrigeration Technologies." The last section about low-carbon air conditioning systems has two chapters: (1) "Introduction of Low-Carbon Community Energy Systems by Combining Information Networks and Cogeneration-Type District Heating and Cooling Systems" and (2) "Renewable and Sustainable Air Conditioning Systems (Renewable Energy-Based Desiccant Cooling Systems)."

The integration of renewable energy systems, sustainable and alternative fuels, energy-efficient innovations, and low-carbon refrigerants in the HVAC systems will help to reduce the high energy demand for modern buildings, reduce the greenhouse gas emissions, and provide potential solutions to the biggest energy challenges facing the humanity.

Chaouki Ghenai, Associate Professor
Sustainable and Renewable Energy Engineering Department (SREE)
College of Engineering

Sustainable Energy Development Research Group Coordinator
Research Institute of Science and Engineering (RISE)
University of Sharjah, Sharjah, United Arab Emirates

Tareq Salameh, Assistant Professor
Sustainable and Renewable Energy Engineering Department (SREE)
College of Engineering

Member of the Sustainable Energy Development Research Group
Research Institute of Science and Engineering (RISE)
University of Sharjah, Sharjah, United Arab Emirates

Section 1

Solar Air Conditioning Systems

Chapter 1

Solar Air-Conditioning Systems

Emna Aridhi, Hmida Bemri and Abdelkader Mami

Additional information is available at the end of the chapter

http://dx.doi.org/10.5772/intechopen.72189

Abstract

The chapter presents the recent studies focusing on optimizing the efficiency of air-conditioning (AC) systems using solar energy. For this purpose, several advanced AC plants (absorption, adsorption, and desiccant) are designed. Their technology and components are described in this chapter. It also discusses the energy intake of the solar energy use in air-conditioning, especially in rural regions where the electricity shortage is frequent, as well as the reduction of the energy costs and the pollution rate. A comparison between solar AC systems and traditional AC systems at the level of the designs, costs, and effectiveness is made at the end of the chapter.

Keywords: solar energy, air-conditioning systems, energy savings, absorption systems, desiccant systems, adsorption systems

1. Introduction

In recent years, the demand for comfort has been accentuated due to the earth's changing climate. Therefore, the use of air-conditioning systems is increased, which leads to higher costs and consumption of energy. It also significantly contributes to the global warming. For instance, in the United States, air conditioners use about 6% of the entire electricity produced, at an annual cost of about $ 29 billion to homeowners. Consequently, roughly 117 million metric tons of CO_2, per year, are released into the atmosphere. On the other hand, 40% of energy consumption and 36% of CO_2 emissions in the EU are caused by buildings, according to United Nations Environment Programme (UNEP). As a result, an increasing interest has been concentrated on the design of modern sustainable AC systems powered by renewables, especially the solar energy that is a universally inexhaustible natural and clean resource [1]. Hence, it can offer a reduction of the consumption, the demand, and the costs of energy, without decreasing the desired comfort. These systems allow converting the solar thermal energy (in the form of

heat) into conditioned air and sometimes chilling storage water. They are outstandingly used in residential and other sectors (offices, hotels, restaurants, storage warehouses, schools, hospitals, etc.) [2], what makes them classified among the most energy consumers.

The present chapter reviews recent studies focusing on three technologies of solar AC systems: absorption, adsorption, and desiccant systems.

2. Solar absorption systems

The harmful effects of conventional AC systems (use of environmentally unfriendly refrigerants; CO_2 emission) and their high primary energy consumption lead scientists to invest in clean energy resources, especially the solar energy [3]. The absorption technology is the most used in air-conditioning [4–6]. It uses an absorber and a generator instead of the compressor. Therefore, no electrical power is needed to pressurize the refrigerant (water or ammonia) [7]. In fact, the refrigerant is first absorbed in an absorbing material and then pressurized in the absorbed liquid phase. The pressurized absorption mixture is then reheated in a solar-powered generator to regenerate the pressurized refrigerant vapor. After that, it is deliquesced in the condenser in order to become liquid, which is then expanded through an expansion valve. The chilled refrigerant causes the cooling effect in the evaporator. Finally, the refrigerant is transferred to the absorber and a new cycle is beginning. Thereby, absorption systems contribute to reducing the greenhouse gas emissions to the atmosphere and the energy costs. Nonetheless, they have a low coefficient of performance (COP) (between about 0.3 and 0.75 according to the cooling capacity) compared with the electrical vapor compression AC systems that their COP can reach up to 3 [7].

The operating principle of a solar air-conditioning system is illustrated in **Figure 1**.

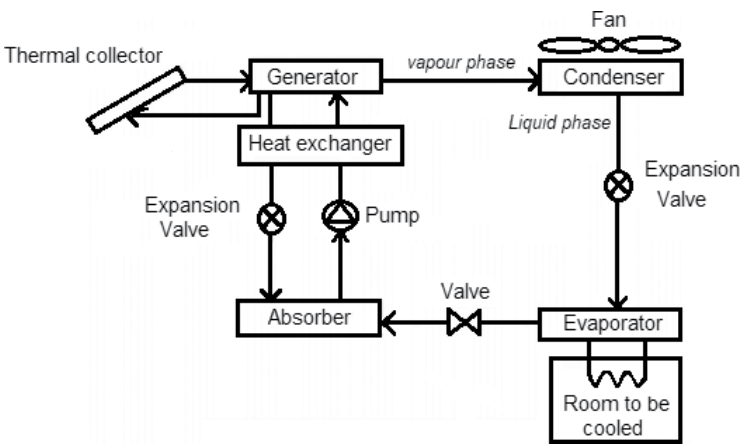

Figure 1. Absorption solar air-conditioning system.

http://dx.doi.org/10.5772/intechopen.72189

Several research studies around the world aimed to design various modern solar-powered plants with energy storage. They allow minimizing the environmental effects and satisfying the energy demand [4, 8, 9]. We find single-stage or double-stage absorption systems with and without crystallization [4]. The single-stage systems are equipped with two heat exchangers and two or three storage tanks. However, the double-stage systems are different from the preview systems by adding the two pairs of absorber/generator and evaporator/condenser. In addition, the crystallization process occurs that the refrigerant undergoes three-phase transformation (solid: usually crystallized salt, liquid, and vapor) [4]. Furthermore, these plants and their performance are closely linked to the climatic conditions (especially solar irradiance) of the regions where they are installed. For instance, Mediterranean countries are characterized by a hot climate, which encourages the use of solar air-conditioning systems [5]. In fact, Tunisia widely invests in solar energy that this country is characterized by a sunny climate over long periods of the year [10]. In this reference, an absorption solar installation is applied to a room of 150 m^2 to minimize the energy consumption during the summer. It consists of a water-lithium bromide absorption chiller having a capacity of 11 kW, a flat-plate solar collector having an area of 30 m^2, and a hot water storage tank having a volume of 0.8 m^3. The simulation results showed that the COP reached 0.725 for a cooling capacity of 16.5 kW as long as the heat source temperature increases, which causes the growth of the heat transfer between the system exchangers and then the quantity of heat distributed in the surroundings [11]. Moreover, another study analyzed the energy performance of a solar air-conditioning office building that maximum monthly consumes about 380 kWh [12]. It consists of insulating the walls and cooling the roof. Hence, it allows reaching an energy saving of 46 and 80% in winter and summer, respectively, as well as, reducing the cooling load from 14.09 to 8.68 kW. In the same framework, the studies [13, 14] aimed to improve the efficiency of a solar installation equipped with parabolic solar collectors (having an area of 39 m^2), an absorption chiller associated with a cooling tower, a backup heater, two tanks for storage and drain-back storage, and a set of fan coils installed in the building to be cooled [14]. The synoptic scheme presenting the main components of the proposed cooling system is illustrated in **Figure 2**, according to Ref. [14].

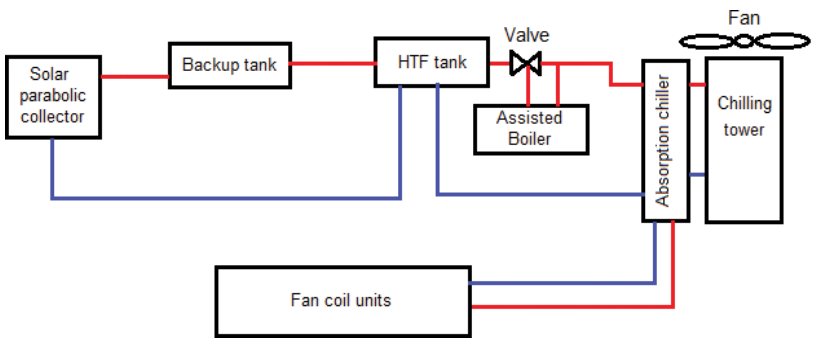

Figure 2. Synoptic schema of the solar cooling system using parabolic collectors.

The analysis of the system performance showed that the absorption chiller output could reach up to about 12 kW. Also, its COP is ranged between about 0.8 and 0.9 [15]. Furthermore, it allowed reducing the CO_2 emission of about 3000 kg during hot seasons and reaching an energy saving of 1154 l of gasoil. This type of solar air-conditioning plants was reviewed in Ref. [16] and performed in the investigation [17] for cooling and heating office buildings in Greece. It is characterized by lower thermal losses, high efficiency, and a small collecting surface of about 14 m^2. An energy saving of up to 50% can be obtained [17]. Nonetheless, the installation costs are higher (about 924 €/m^2 of the solar collector), especially for large areas [17]. Moreover, the maintenance is frequent and also expensive. Reference 18 reports the performance statistics of a solar AC system constituted by thermal parabolic collectors (having an area of 588 m^2) and a double-effect absorption chiller. The system has an annual average efficiency of 40% and a peak efficiency of 58% [18]. It also allows chilling water contained in a storage tank of 23.000 l that is used as a buffer tank. The annual average COP of the absorption chiller, which is a water-cooled double-effect chiller, can reach 1.1. Nonetheless, its costs are very high and reach up to $ 680.000 that can be paid after about 21 years [18].

In Algeria, the solar energy was also harnessed to cool houses in hot climates [19]. In this investigation, the authors developed a model of the air conditioner and the absorption cooling system of 10 kW, which is constituted by solar collectors (having a surface of 28 m^2) and a 900-l hot storage tank, as well as a cooling tower and a thermally driven chiller. The results obtained showed that the solar system with a thermal COP equal to 0.73 can satisfy the required conditioned air of a house having a surface of 120 m^2 [20]. The study [21] proposed a very efficient hybrid combined cooling, heating, and power system driven by solar energy and biomass applied to a building with a 100-kW electricity load. It consists of a biomass gasification subsystem, solar evacuated collector (having an area of 96 m^2 for an 800 W/m^2 solar irradiance), internal combustion engine, and dual-source powered mixed-effect absorption water chiller. In fact, the system allowed an energy saving of about 57%, a reduction of the carbon emission ratio of about 95%, and providing about 200 kW of cooling power. In addition, the COP of the system is high (1.1) [21].

Furthermore, the high ambient temperatures in Gulf countries cause a ceaseless demand for cooling, which allows achieving a significant scientific development in the solar AC field. For instance, in Saudi Arabia, the investigation [22] focused on optimizing the performance of a solar-powered LiBr-water absorption AC system. It is equipped with a flat-plate collector and storage tanks of cold and refrigerant, which ensure a continuous operation of 24 h/7 days. The chiller has a cooling capacity of 5 kW. The authors also give its complete mathematical model using unsteady time-dependent values of the solar intensity and the ambient temperature that are assumed to be constant over given small time intervals Δt. In fact, the generalized energy equation over each Δt, assuming uniform flow processes, is given by Eq. 1 [22].

$$Q - W = \left(\sum m \,.\, h\right)_{out} - \left(\sum m \,.\, h\right)_{in} + m\left(u_f - u_i\right)_{system} \tag{1}$$

where Q and W are the net thermal and mechanical energies, m is the mass inside the volume (V) of each system component, and $(u_f - u_i)$ is the change in internal energy per unit mass inside the volume (V) during the time Δt (u_f is the final internal energy per unit mass inside the volume (V) at the end of the time step (Δt), while u_i is the initial value).

http://dx.doi.org/10.5772/intechopen.72189

Moreover, the governing equations of the mass flow rates of the weak and strong refrigerant-absorbent solutions (ws and ss, respectively) for lithium bromide-water are given by Eq. (2) [22].

$$\begin{aligned} \dot{m}_{ss} &= X_{ws}/(X_{ss} - X_{ws}) \,.\, \dot{m}_r \\ \dot{m}_{ws} &= X_{ss}/(X_{ss} - X_{ws}) \,.\, \dot{m}_r \end{aligned} \tag{2}$$

where X_{ws} and X_{ss} are the mass concentrations for weak and strong solutions.

The generator and evaporator heat and pump work are written in Eq. (3) [22].

$$\begin{aligned} Q_G &= \left(\dot{m}_r h_1 + \dot{m}_{ws} h_8 - m_{ss} h_7\right) . \Delta t \\ Q_E &= \left(\dot{m}_r (h_4 - h_3)\right) . \Delta t \\ W_P &= \left(m_{ss} (h_6 - h_5)\right) . \Delta t \end{aligned} \tag{3}$$

where Δt is a 1-h time-step interval and the enthalpy h(1 to 10) is based on the thermodynamic state shown in **Figure 3**, according to Ref. [22].

For a collector area of 48 m^2, a hot storage mass of 1500 kg, and a constant load, the simulation results using Engineering Equation Solver (EES) software indicated that the COP of the system is about 0.85. However, the experimental results showed that it can reach 0.9 [22]. At the level of the size of system components (collector and tanks), they become smaller in summer that the solar intensity is high. Thus, the required mass storage will be reduced and the COP will be enhanced.

In the same context, many related studies were carried out in Australia. For example, in Ref. [23], the author modeled a building (having a volume of 60 m^3) equipped with an autonomous solar photovoltaic-battery air conditioner in order to satisfy the desired comfort with the minimum energy consumption. The conditioned supply air temperature T_s and the humidity ratio HR_s are computed using Eq. (4) [23].

$$\begin{aligned} T_s &= T_b - \frac{Q_s}{\dot{m}\, c_p} \\ HR_s &= HR_b - (Q_t - Q_s)/\dot{m}\, h_{fg} \end{aligned} \tag{4}$$

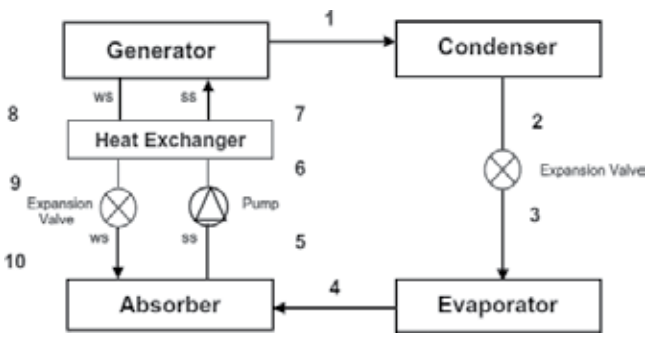

Figure 3. Thermodynamic state of the LiBr-H_2O absorption system.

where Q_s and Q_t are, respectively, the sensible and total cooling power, h_{fg} is the heat of vaporization of water, T_b is the building air temperature (it must be higher than 25°C to activate the air-conditioning process), and $\dot{m}$ is the supply air flow rate (0.275 kg/s) [23].

Thanks to the presence of the battery, the system can be used during peak times to provide the energy required. Indeed, the energy stored in the battery $E_{battery}$ is determined using Eq. (5) [23].

$$\frac{dE_{battery}}{dt} = \eta_c P_c - \frac{1}{\eta_d P_d} \tag{5}$$

where P_c is the battery charging power, P_d is the battery discharging power, η_c is the charge efficiency, and η_d is the discharge efficiency.

The simulation results of the internal temperature and humidity were carried out for different types of buildings and climates using TRNSYS software. The system increased the solar fraction of 30% [23]. Moreover, medium-temperature, concentrated solar thermal collectors are used in an air-conditioning system with an auxiliary heater (used to compensate for a lack of energy) and a double-effect absorption chiller [24] to cool a building. The main components of the proposed AC system are shown in **Figure 4**, according to Ref. [24].

For a collector area of 2.4 m^2/kW of cooling capacity and a storage tank volume of 40 L/m^2, the simulation results using TRNSYS software show that the system is able to cover 50% of the load needs of the building [24]. In addition, the COP system is 1.4, which reveals the system efficiency.

On the other hand, the investigation [25] couples the solar energy to a traditional vapor compression air conditioner to perform a new hybrid solar-driven AC system. The proposed system was modeled and controlled using TRNSYS software in order to improve its energy efficiency. It is constituted of three main parts (a vapor compression system, a solar vacuum collector, and a solar storage tank). At steady-state conditions, the compressor power consumption was decreased from 1.45 to 1.24 kW, which is traduced by a global energy saving of about 14 and 7.1% for only the compressor. Likewise, an energy saving achieved by the condenser fan is about 2.6% [25], which allows increasing the COP. Hence, the authors reported that the system is able to satisfy efficiently the cooling requirements.

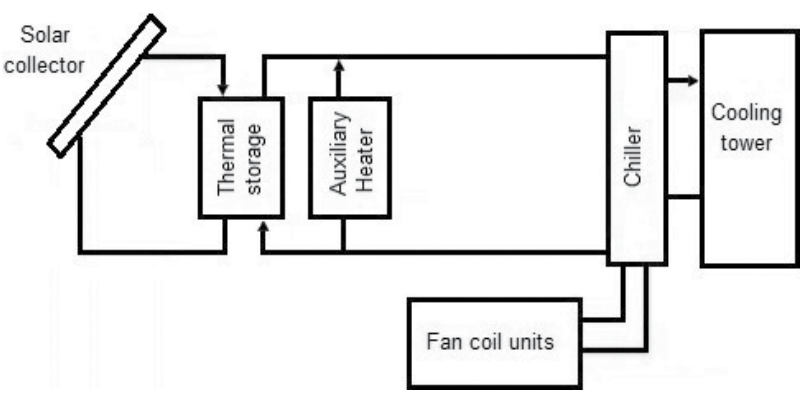

Figure 4. General scheme of the components constituting the solar AC system.

3. Solar adsorption systems

These systems have long-term environmental benefits and significant energy efficiency like the absorption AC systems [26]. In fact, they use natural refrigerants such as the water [27] and can be driven by a low-temperature heat source [28].

Several studies have been focused on the design of solar adsorption AC systems. Nonetheless, their design is complex and some parameters, like the heat rejection, are not easy to be determined using classical tools [27]. In this investigation, the authors developed a dynamic model to simulate a solar cooling system equipped with a backup unit, a heat rejection unit (having a thermal capacity of 35 kW), and adsorption chillers, which are driven by solar collectors distributed over an area of 27.52 m^2 to cool a flat building area of 130 m^2 in Italy.

The authors expressed the thermal performance of the solar collectors as [27]:

$$\frac{Q}{A} = G\left(\eta_0 - 1.485\frac{(T_m - T_a)}{G} - 0.002\frac{(T_m - T_a)^2}{G}\right) \tag{6}$$

where Q is the power of solar collectors, A is their area, G is the intensity of the solar radiation, η_0 is the ratio of the efficiency measured at actual admitted irradiance to vertical admitted irradiance, T_m is the collector average temperature, and T_a is the ambient temperature.

The system also cooled about 1000 l of water that can be used in numerous activities. However, the COP of the chiller is much low compared with the electric one: 0.35 and 2.5, respectively. They are computed using Eq. (7) [27].

$$\begin{aligned} COP_{chiller} &= \frac{Q_{ev}}{Q_s + Q_{heater}} \\ COP_{electric} &= \frac{Q_{ev}}{E_{el,tot}} \end{aligned} \tag{7}$$

where Q_{ev} is the evaporation energy representing the useful effect of the chiller, Q_s is the energy supplied by the solar collectors, Q_{heater} is the energy supplied by the backup unit, and $E_{el,tot}$ is the total electric consumption of all the system components.

The ratio between the energy supplied by the thermal collectors and the total energy required by the complete system, called solar fraction, is given by Eq. (8) [27].

$$SF = \frac{Q_s}{Q_s + Q_{heater}} \tag{8}$$

In addition, the installation costs are very high, about $ 29.022. They can be paid back after about 13 years. In fact, about $ 1085 and 3942.45 kWh of electric energy are saved per year. Another adsorption cooling system using a tubular solar 1-m^2 double-glazed collector/adsorber was designed, as shown in **Figure 5**, according to Ref. [28]. The main objective is to decrease the energy consumption of cooling systems in the sub-Sahara regions in Algeria. Indeed, an energy saving of about 28.3 MWh could be reached during August [28]. However, the solar COP is too low (about 0.21).

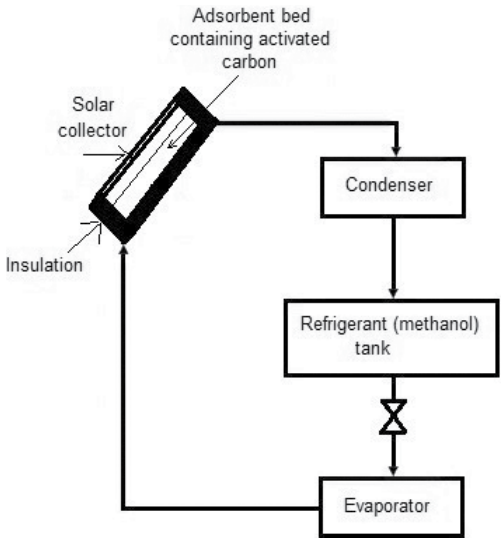

Figure 5. Synoptic schema of the adsorption solar cooling system.

In the investigation [29], a reduction of the energy consumption of about 50% was achieved, especially in hot and wet climates due to the use of solar energy for the production of cold. The authors used a traditional cooling system with a dehydrating cooling cycle that can be adapted to the fixed solar cells to air-condition a housing volume of 330 m^3 using 20 m^2 flat-plate collector and 2 m^3 hot water tank [30], which can be employed in household activities. However, the COP of the cooling system is low (about 0.6) and the indoor climate does not fulfill standard comfort criteria for few hours during the cooling season. A new water/air-conditioning system for buildings is presented in Ref. [31]. It is constituted by a solar-driven adsorption chiller, a solar chimney (having 12 m^2 of area), and a cooling channel (having 24 m^2 of area), through which the hot air is cooled and distributed in the test room (having 200 m^3 of volume) under hot and humid, and hot and arid climate. The cyclic cooling capacity and the COP of the chiller reached their maximum values (about 16 kW and 0.71, respectively) during the day (between 15 and 16 h). This allowed decreasing the room temperature by 26.8%. Furthermore, the electric energy consumed by the system is 37% less than that consumed by a split inverter air conditioner having the same cooling power [31].

Absorption and adsorption technologies can be combined in the same AC system in order to further improve its performance. This is the subject of [32] in which the authors proposed novel solar poly-generation systems, based on both adsorption and absorption chiller technologies fed by dish-shaped concentrating and flat photovoltaic/thermal collectors instead of conventional solar collectors. They developed a computer code to determine the optimal system configurations taking into account the operating parameters and the climatic conditions. The systems are applied to buildings (office and residential spaces) located in different climatic European regions. They provided electricity and hot water, as well as they ensured the heating and cooling of the air-conditioned spaces.

4. Solar desiccant systems

On the environmental front, desiccant systems rank among the top efficient cooling systems [33]. In fact, they can decrease the greenhouse gas emissions and improve the energy savings given that they do not use any ozone-depleting refrigerants and consume less energy as compared with the vapor compression systems [34–36]. Their benefits are meaningful when they interact with renewable energy technologies, such as solar collectors [37, 38]. They also reduce moisture from the indoor air and enhance its quality [39–41]. For instance, liquid desiccant dehumidification solar systems are used to supply fresh air in humid climate locations using the calcium chloride liquid and a flat-plate solar collector (having an area of 86.16 m^2). It allows reducing their latent heat load and then enhancing their efficiency [42, 43]. During the entire cooling season, the proposed system in this study provides 10 [44] and 40 kW for cooling a typical house and a small restaurant, respectively. However, the COP of the desiccant unit is too low (0.41 for the house and 0.45 for the restaurant). The costs of the installation powered by natural gas can be paid back after 11 years if the gas price is 0.5638 $/kg [43]. In addition, this kind of system (having 1 m^2 of dehumidifier area and 80 m^2 of solar collector area) has been tested under hot and dry climate conditions, and a Multi-Population Genetic Algorithm (MPGA) is developed to optimize the system parameters to reach a maximum energy saving and a minimum payback period. It is shown in **Figure 6** according to Ref. [45].

In fact, 38% of electricity saving and a payback period of 14 years are achieved [45]. Furthermore, a solar desiccant cooling unit equipped with evacuated solar collectors (having 16 m^2 of area), in which the regeneration thermal energy is supplied by a natural gas boiler, and with a conventional air-handling device is enough to obtain a reduction of primary energy consumption and CO_2 emissions of 50.2% and 49.8%, respectively. Moreover, the system costs can be paid back after 17 years [36]. A liquid desiccant solar system is combined with two evaporative coolers (a regenerative indirect evaporative cooler and a direct evaporative cooler with an adjustable bypass flow) [46]. This has the objective to improve the performance of the desiccant system by using low-grade heat for air-conditioning [46]. The liquid desiccant system is characterized by a self-cycle solution at dehumidification. Its performance was analyzed through a mathematical model that studies the impact of varying five parameters (solution self-cycle ratio, working to intake air flow ratio, regeneration temperature, ambient air temperature, and humidity ratio). The system can decrease the air temperature of the cooled space to 17.9°C. Nonetheless, the obtained thermal COP is low (0.5) for the design conditions [46]. In addition, the system has the advantage of using lower temperature heat source compared with a conventional AC system. The same technology was also invested for hot climates in Saudi Arabia [47]. The investigation shows that the desiccant evaporative AC system presents a modest performance in dry climates and does not operate in very wet conditions.

On the other hand, three models of solar solid desiccant AC system were performed in Ref. [48] under cold, humid, hot, and dry climates in Tunisia and applied to a building having a volume of 48 m^3. The authors used a fixed solid desiccant bed in place of a rotary desiccant wheel. The solar flat-plate collectors (having an area of 2 m^2) consist mainly of a transparent cover, a plate absorber, tubes fixed and set under the absorber plate, and insulation on the back side of them.

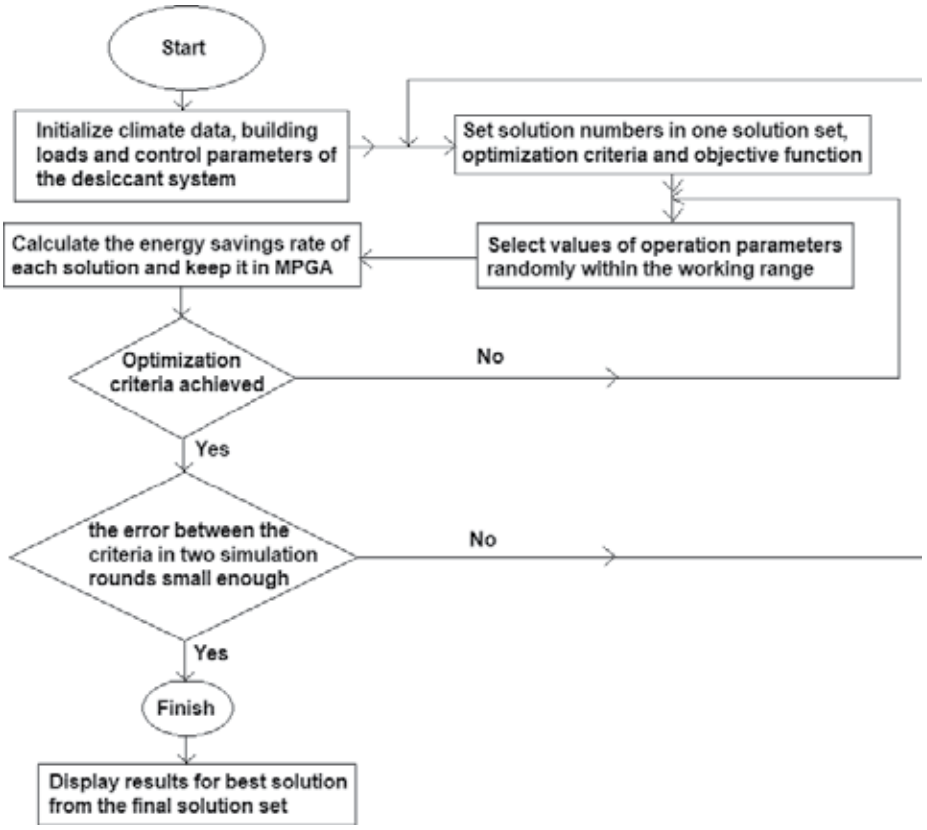

Figure 6. Multi-population genetic algorithm (MPGA) to optimize the desiccant AC system.

They are made of copper. Water circulates into the tubes in order to be heated. The solar collectors are coupled to the desiccant system (it consists of a desiccant dehumidifier, an air–air heat exchanger, a water-air heat exchanger, and a humidifier). This provides the heat required to regenerate it, precisely the desiccant dehumidifier. The coupling is ensured by a water storage tank and a heating coil inserted in the return air stream of the desiccant system [48].

The authors expressed the thermal balance for the absorber as follows [48]:

$$\begin{aligned}\rho_{abs}\,\delta_{abs}\,C_{abs}\frac{dT_{abs}}{dt} = {} & G\,\tau_{abs}\,\alpha_{abs} + h_{r_{abs\_tc}}\left(T_{tc}-T_{abs}\right) + h_{conv_{a-abs}}\left(T_{a}-T_{abs}\right) \\ & + \left(\frac{S_{abs-tube}}{S_{abs}}\right)h_{cond_{abs-tub}}\left(T_{tube}-T_{abs}\right) + \left(\frac{S_{abs-insulation}}{S_{abs}}\right)h_{cond_{abs-insulation}}\left(T_{insulation}-T_{abs}\right) \\ & + \lambda_{abs}\,\delta_{abs}\left(\frac{\partial^{2}T_{abs}}{\partial x^{2}} + \frac{\partial^{2}T_{abs}}{\partial y^{2}}\right)\end{aligned} \tag{9}$$

where 'abs' refers to absorber, ρ is the intrinsic average density, σ is the thickness, C is the specific heat, G is the solar global radiation, τ is the transmission coefficient, α is the absorption coefficient, *hr.* is the radiation heat transfer coefficient, T_{tc} is the temperature of the transparent cover, T_a is the air temperature, S is the surface area, and λ is the conductivity.

Solar air-conditioning systems				
		Absorption systems [3–25]	**Adsorption systems [26–32]**	**Desiccant systems [33–48]**
Design values		*Small storage water volume:* minimum 0.8 m^3 *Collector area:* 14–96 m^2 *Building volume (or surface)*: up to 150 m^2	*Small storage water volume:* up to 2 m^3 *Collector area:* 1–20 m^2 *Building volume (or surface)*: minimum 130 m^2, up to 330 m^3	*Small storage water volume:* up to 2 m^3 *Collector area:* 2–80 m^2 *Building volume (or surface)*: minimum 48 m^3
Design optimization		• Insulating the walls and cooling the roof of the building. • Using parabolic and concentrated thermal collectors. • Combining solar energy and biomass. • Small size of collectors and tanks • Adding batteries	• Using low-temperature heat source. • Using sustainable adsorption chillers. • Using tubular solar double-glazed collector/adsorber.	• Using dehumidifier to reduce moisture from the cooled air. • Using multi-population genetic algorithm to optimize the system parameters. • Using a natural gas boiler to regenerate thermal energy.
Cooling capacity		From 5 to 16.5 kW	About 16 kW	About 40 kW
Effectiveness	COP	From 0.3 to 0.75 and sometimes up to 1.4	From 0.2 to 0.7	From 0.41 to 0.5
	Environmental benefits	Reduction of the energy consumption up to 80% (especially during the summer). Reduction of the CO_2 emissions up to 95% (up to 3000 kg).	Energy saving: up to 28.3 MWh. Up to 50%.	Reduction of the energy consumption up to 52%. Reduction of the CO_2 emissions up to 49.8%.

Table 1. Design values and effectiveness of absorption, adsorption, and desiccant solar AC systems.

$$h_{cond_{abs-tube}} = \frac{1}{\frac{\delta_{abs}}{\lambda_{abs}} + \frac{\delta_{tube}}{\lambda_{tube}}}: \text{conductive heat transfer coefficient between absorber plate and tube}$$

$$h_{cond_{abs-insulation}} = \frac{1}{\frac{\delta_{abs}}{\lambda_{abs}} + \frac{\delta_{insulation}}{\lambda_{insulation}}}: \text{conductive heat transfer coefficient between absorber plate and insulation}$$

$$h_{conv_{a-abs}} = \frac{Nu_a \lambda_a}{\delta_a}: \text{the convective heat transfer coefficient between air gap and the absorber}$$

For the tube, the thermal balance is written as [48]:

$$\rho_{tube} S_{tube} C_{tube} \frac{dT_{tube}}{dt} = Sc_{abs-tube} h_{cond_{abs-tub}} (T_{abs} - T_{tube}) + P_{tube} h_{conv_{tube-insulation}} (T_{insulation} - T_{tube}) + Sc_{tube-insulation} h_{cond_{tub-insulation}} (T_{insulation} - T_{tube}) + \lambda_{tube} S_{tube} \frac{\partial^2 T_{tube}}{\partial y^2} \quad (10)$$

where P is the perimeter.

$h_{conv_{a-abs}} = \frac{Nu_{tube} \lambda_f}{D_{h,tube}}$: the convective heat transfer coefficient between tube and circulating fluid (water)

$h_{cond_{tube-insulation}} = \frac{1}{\frac{\delta_{tube}}{\lambda_{tube}} + \frac{\delta_{insulation}}{\lambda_{insulation}}}$: conductive heat transfer coefficient between tube and insulation

The value of the Nusselt number Nu_{tube} depends on the Reynolds number Re as follows [48]:

$$\text{Re} < 2300 \Rightarrow Nu_{tube} = 4.364$$
$$\text{Re} > 2300 \Rightarrow Nu_{tube} = 0.023\,\text{Re}^{0.8}\,\text{Pr}^{0.4}$$

The numerical values of the temperature and humidity show that the desired comfort is reached by the three proposed models under different climatic conditions.

Table 1 summarizes the design values and the effectiveness of the three technologies of solar AC systems investigated in the present chapter.

5. Comparative study of solar air-conditioning systems vs. traditional ones

From research studies reviewed in this chapter, we conclude that whatever the technology, solar AC systems have many environmental benefits compared with those that are driven by conventional vapor compression cycles. In fact, traditional AC systems operate with chlorofluorocarbons and hydrofluorocarbon refrigerants that impact on ozone depletion [49]. Hence, solar AC systems present an interesting solution to inhibit the harmful effects on the environment. It is observed that they significantly lower the emission of greenhouse gases into the atmosphere, achieve the desired comfort, and reach a considerable saving of energy of up to 80%. They also can be installed in all regions and operating under all climatic conditions. On the other hand, the solar air-conditioning can effectively mitigate peak load pressures occurred with the use of conventional air conditioners, thanks to the heat storage process. Indeed, the heat is especially stored when the solar irradiance is high and can be after harnessed when the solar radiation becomes deficient [50]. This fact ensures the continuous operation of the solar AC systems. In terms of COP, the thermal COP of a solar AC system is generally lower than those of a conventional AC system without decreasing the solar system performance. All these benefits make solar AC systems attractive and extensively integrated into modern buildings. This comparative study is illustrated in the following **Table 2**.

		Solar air-conditioning systems	Conventional air-conditioning systems
Designs of installations		Complex installations and new components are added to them according to the technology adopted (solar collectors, boiler, absorber, adsorber, generator, desiccant bed, rotary wheel and so on).	Simple installations based on the vapor compression cycles
Costs		Maintenance is frequent and expensive, especially for the desiccant AC systems. - 924 €/m^2 of the solar collector (for solar absorption AC systems). - Up to $ 29.022 that can be paid back after 13 years (for solar adsorption AC systems). - Gas price up to 0.5638 $/kg can be paid after 11–17 years (for solar desiccant AC systems).	Low costs
Effectiveness	COP	Low COP (according to the technology of the solar AC system)	High COP
	Environmental benefits	Use lower temperature heat source	Use harmful refrigerants
		Continuous operation of the solar AC systems	Depend on a supply of electricity
		Driven by an exhausted clean energy resource (solar)	Driven by a vapor compression cycle
		Reduce the CO_2 emissions into the atmosphere	Contribute to the global warming
		Can be installed in regions where the electricity is unavailable (desert, etc.)	Impact on ozone depletion
		Reduce the energy consumption	High energy consumption

Table 2. Advantages and disadvantages of solar AC systems compared with conventional AC ones.

6. Conclusions

The solar AC systems reported in this chapter present an interesting worldwide solution to reduce the harmful effects (high energy consumption and pollution) of traditional AC systems. In fact, research studies revealed that absorption, adsorption, and desiccant systems allowed saving energy up to 80, 50, and 52%, respectively, thanks to the optimization of their designs at the level of using environmentally unfriendly refrigerants, investing in the free and clean solar energy to power them, as well as at the level of the choice of the components that comprise them. Therefore, these systems also reduced the pollution rate

up to 95% (about 3000 kg of CO_2), especially the absorption systems. In addition, their use is remarkably suitable in rural regions where the electricity is not available or its shortage is frequent. Some solar AC systems are also equipped with chilled or hot water tanks, which can be used in various activities (household, agricultural, and so on). However, their coefficient of performance is lower than 1 in most cases compared with the traditional AC systems that their coefficient can reach the value 3. Moreover, the installation and maintenance costs of the most solar AC systems are relatively high. They can reach up to $ 29.000 and be paid back after at least 9 years. Hence, we can reach a long-term sustainability. Nonetheless, the design of these systems, especially adsorption and desiccant AC systems, is complex.

Author details

Emna Aridhi[1,2]*, Hmida Bemri[3] and Abdelkader Mami[2]

*Address all correspondence to: aridhi_emna@yahoo.fr

1 Ecole des Sciences et Technologies Avancées de Borj Cédria, Université de Carthage, Tunis, Tunisie

2 Laboratoire d'Application de l'Efficacité Énergétique et des Énergies Renouvelables-LAPER, Faculté des Sciences de Tunis, Université de Tunis El Manar, Tunis, Tunisie

3 Laboratoire de Recherche en Automatique (LARA), Ecole Nationale d'Ingénieurs de Tunis, Université de Tunis El Manar, Tunis, Tunisie

References

[1] Suman S, Khan MK, Pathak M. Performance enhancement of solar collectors—A review. Renewable and Sustainable Energy Reviews. 2015;**49**:192-210

[2] Ilie A, Dumitrescu R, Girip A, Cublesan V. Study on technical and economical solutions for improving air conditioning efficiency in building sector. In: Sustainable solutions for energy and environment, EENVIRO 2016; 26-28-10-2016; Bucharest, Romania. Energy Procedia. 2017:537-544

[3] Todorovic MS, Kim JT. In search for sustainable globally cost-effective energy efficient building solar system—Heat recovery assisted building integrated PV powered heat pump for air-conditioning, water heating and water saving. Energy and Buildings. 2014;**85**:346-355

[4] Ibrahim NI, Al-Sulaiman FA, Ani FN. Solar absorption systems with integrated absorption energy storage—A review. Renewable and Sustainable Energy Reviews Forthcoming. DOI: 10.1016/j.rser.2017.07.005

[5] Allouhi A, Kousksou T, Jamil A, Bruel P, Mourad Y, Zeraouli Y. Solar driven cooling systems: An updated review. Renewable and Sustainable Energy Reviews. 2015;**44**:159-181

[6] Jasim KK, Kadhum JA. A comparative study of solar thermal cooling and photovoltaic solar cooling in different Iraqi regions. International Journal of Enhanced Research in Science, Technology & Engineering. 2016;**5**:63-72

[7] Aman J, Ting DSK, Henshaw P. Residential solar air conditioning: Energy and exergy analyses of an ammonia-water. Applied Thermal Engineering. 2014;**52**:424-432

[8] Shirazi A, Pintaldi S, White SD, Morrison GL, Rosengarten G, Taylor RA. Solar-assisted absorption air-conditioning systems in buildings: Control strategies and operational modes. Applied Thermal Engineering. 2016;**92**:246-260

[9] Porumb R, Porumb B, Bălan M. Baseline evaluation of potential to use solar radiation in air conditioning applications. In: Sustainable solutions for energy and environment, EENVIRO-YRC 2015; 18-20-11-2015; 2015. Bucharest, Romania: Energy Procedia; 2016. p. 442-451

[10] Balghouthi M, Trabelsi SE, Ben Amara M, Bel Hadj A, Guizani AA. Potential of concentrating solar power (CSP) technology in Tunisia. Renewable and Sustainable Energy Reviews. 2016;**56**:1227-1248

[11] Balghouthi M, Chahbani MH, Guizani A. Feasibility of solar absorption air conditioning in Tunisia. Building and Environment. 2008;**43**:1459-1470

[12] Soussi M, Balghouthi M, Guizani A. Energy performance analysis of a solar-cooled building in Tunisia: Passive strategies impact and improvement techniques. Energy and Buildings. 2013;**67**:374-386

[13] Balghouthi M, Bel Hadj Ali A, Trabelsi SE, Guizani A. Optical and thermal evaluations of a medium temperature parabolic trough solar collector used in a cooling installation. Energy Conversion and Management. 2014;**86**:1134-1146

[14] Balghouthi M, Chahbani MH, Guizani A. Investigation of a solar cooling installation in Tunisia. Applied Energy. 2012;**98**:138-148

[15] Beccali M, Cellura M, Longo S, Guarino F. Solar heating and cooling systems versus conventional systems assisted by photovoltaic: Application of a simplified LCA tool. Solar Energy Materials and Solar Cells. 2016;**156**:92-100

[16] Cabrera FJ, Fernandez-Garcia A, Silva RMP, Perez-Garcia M. Use of parabolic trough solar collectors for solar refrigeration and air-conditioning applications. Renewable and Sustainable Energy Reviews. 2013;**20**:103-118

[17] Drosou V, Kosmopoulos P, Papadopoulos A. Solar cooling system using concentrating collectors for office buildings: A case study for Greece. Renewable Energy. 2016;**97**:697-708

[18] Greenaway T, Kohlenbach P. Assessment of potential energy and greenhouse gas savings in the Commercial Building Sector by using solar energy for air-conditioning purposes. Procedia Engineering. 2017;**180**:715-724

[19] Djelloul A, Draoui B, Moummi N. Simulation of a solar driven air conditioning system for house in dry and hot climate of Algeria. Journal: Courrier de Savoir. 2013;**15**:31-39

[20] Siddiqui MU, Said SAM. A review of solar powered absorption systems. Renewable and Sustainable Energy Reviews. 2015;**42**:93-115

[21] Wang J, Yang Y. Energy, exergy and environmental analysis of a hybrid combined cooling heating and power system utilizing biomass and solar energy. Energy Conversion and Management. 2016;**124**:566-577

[22] El-Shaarawi MAI, Al-Ugla AA. Unsteady analysis for solar-powered hybrid storage LiBr-water absorption air-conditioning. Solar Energy. 2017;**144**:556-568

[23] Goldsworthy MJ. Building thermal design for solar photovoltaic air-conditioning in Australian climates. Energy and Buildings. 2017;**135**:176-186

[24] Li Q, Zheng C, Shirazi A, Mousa OB, Moscia F, Scott JA, Taylor RA. Design and analysis of a medium-temperature, concentrated solar thermal collector for air-conditioning applications. Applied Energy. 2017;**190**:1159-1173

[25] Ha QP, Vakiloroaya V. Modeling and optimal control of an energy-efficient hybrid solar air conditioning system. Automation in Construction. 2015;**49**:262-270

[26] Islam MP, Morimoto T. Thermodynamic performances of a solar driven adsorption system. Solar Energy. 2016;**139**:266-277

[27] Vasta S, Palomba V, Frazzica A, Di Bella G, Freni A. Techno-economic analysis of solar cooling systems for residential buildings in Italy. Journal of Solar Energy Engineering. 2013; **135**:021002

[28] Hadj Ammar MA, Benhaoua B, Balghouthi M. Simulation of tubular adsorber for adsorption refrigeration system powered by solar energy in sub-Sahara region of Algeria. Energy Conversion and Management. 2015;**106**:31-40

[29] Henning HM, Erpenbeck T, Hindenburg C, Santamaria IS. The potential of solar energy use in desiccant cooling cycles. International Journal of Refrigeration. 2001;**24**:220-229

[30] Zhang N, Lior N, Han W. Performance study and energy saving process analysis of hybrid absorption compression refrigeration cycles. Journal of Energy Resources Technology. 2016;**138**:061603

[31] Jafari A, Poshtiri AH. Passive solar cooling of single-storey buildings by an adsorption chiller system combined with a solar chimney. Journal of Cleaner Production. 2017;**141**:662-682

[32] Buonomano A, Calise F, Palombo A. Solar heating and cooling systems by absorption and adsorption chillers driven by stationary and concentrating photovoltaic/thermal solar collectors: Modelling and simulation. Renewable and Sustainable Energy Reviews. 2018; **81**:1112-1146

[33] Duong HC, Hai FI, Al-Jubainawi A, Ma Z, He T, Nghiem LD. Liquid desiccant lithium chloride regeneration by membrane distillation for air conditioning. Separation and Purification Technology. 2017;**177**:121-128

[34] Sahlot M, Riffat S. Desiccant cooling systems: A review. International Journal of Low-Carbon Technologies. 2016;**11**:489-505

[35] Rjibi A, Kooli S, Allah Guizani A. A solid-desiccant cooling system for greenhouses. In: 3rd International Conference on Automation, Control, Engineering and Computer Science; Tunisia. Proceedings of Engineering & Technology (PET); 2016. pp. 320-325

[36] Kojok F, Fardoun F, Younes R, Outbib R. Hybrid cooling systems: A review and an optimized selection scheme. Renewable and Sustainable Energy Reviews. 2016;**65**:57-80

[37] Angrisani G, Roselli C, Sasso M, Tariello F. Selection of solar collectors technology and surface for a desiccant cooling system based on energy, environmental and economic analysis. In: 1st International e-Conference on Energies; Italy. Sciforum Electronic Conference Series; 2014

[38] Sabek S, Ben Nasr K, Chouikh R, Allah Guizani A. Analytical study of a heat recovery/desiccant cooling system under Tunisian climatic conditions. Journal of Clean Energy Technologies. 2015;**3**:159-164

[39] Abdel-Salam AH, McNevin C, Crofoot L, Harrison SJ, Simonson CJ. A field study of a low-flow internally cooled/heated liquid desiccant air conditioning system: Quasi-steady and transient performance. Journal of Solar Energy Engineering. 2016;**138**:031009

[40] Alizadeh S. A feasibility study of using solar liquid-desiccant air conditioner in Queensland, Australia. Journal of Solar Energy Engineering. 2008;**130**:021005

[41] Yong L, Sumathy K, Dai YJ, Zhong JH, Wang RZ. Experimental study on a hybrid desiccant dehumidification and air conditioning system. Journal of Solar Energy Engineering. 2006;**128**:77-82

[42] Mago P, Goswami DY. A study of the performance of a hybrid liquid desiccant cooling system using lithium chloride. Journal of Solar Energy Engineering. 2003;**125**:129-131

[43] Ghaddar N, Ghali K, Najm A. Use of desiccant dehumidification to improve energy utilization in air conditioning in Beirut. International Journal of Energy Research. 2003;**27**:1317-1338

[44] Qasem NAA, El-Shaarawi MAI. Improving ice productivity and performance for an activated carbon/methanol solar adsorption ice-maker. Solar Energy. 2013;**98**:523-542

[45] Ronghui Q, Lin L, Yu H. Parameter analysis and optimization of the energy and economic performance of solar-assisted liquid desiccant cooling system under different climate conditions. Energy Conversion and Management. 2015;**106**:1387-1395

[46] Zhang F, Yin Y, Zhang X. Performance analysis of a novel liquid desiccant evaporative cooling. Building and Environment. 2017;**117**:218-229

[47] Brumana G, Franchini G. Solar-powered air conditioning for buildings in hot climates: Desiccant evaporative cooling vs. absorption chiller-based systems. In: 71st Conference of the Italian Thermal Machines Engineering Association; 14-16-09-2016; Italia. Turin: Energy Procedia; 2016. pp. 288-296

[48] Zouaoui A, Zili-Ghedira L, Ben Nasrallah S. Solid desiccant solar air conditioning unit in Tunisia: Numerical study. International Journal of Refrigeration. 2017;**74**:662-681

[49] Gugulothu R, Somanchi NS, Banoth HB, Banothu K. A review on solar powered air conditioning system. In: Procedia Earth and Planetary Science, editors. Global Challenges, Policy Framework & Sustainable Development for Mining of Mineral and Fossil Energy Resources (GCPF 2015); 17-18-04-2015; Karnataka, India. Elsevier; 2015. pp. 361-367

[50] Hao EKJ, Ghaffarian Hoseini A. Solar vs. conventional air-conditioning systems: Review of LIMKOKWING University Campus, Cyberjaya, Malaysia. Journal of Creative Sustainable Architecture & Built Environment. 2012;**2**:23-32

Chapter 2

Solar-Assisted HVAC Systems with Integrated Phase Change Materials

Zhenjun Ma, Haoshan Ren, Wenye Lin and Shugang Wang

Additional information is available at the end of the chapter

http://dx.doi.org/10.5772/intechopen.72187

Abstract

Solar-assisted heating, ventilation and air-conditioning (HVAC) systems are receiving increasing attention. This chapter presents the development of HVAC systems with integrated solar photovoltaic-thermal (PVT) collectors and phase change materials (PCMs) to reduce building energy consumption while providing satisfactory indoor thermal comfort. PVT collectors, which can generate both thermal energy and electricity simultaneously, are a promising technology for developing high-performance buildings. As solar energy is intermittent, the integration of phase change materials (PCMs) with PVT-driven HVAC systems can provide an opportunity to effectively utilise solar energy and maximise the performance of HVAC systems. The results showed that the coefficient of performance (COP) of an air source heat pump system with integrated PVT collectors and PCMs was 5.2, which was higher than the use of the air source heat pump only (i.e., 3.06) during the test period investigated.

Keywords: HVAC system, photovoltaic-thermal collector, phase change material, thermal energy storage, solar energy, performance evaluation

1. Introduction

Building heating, ventilation and air-conditioning (HVAC) system is one of the major energy consumers in modern buildings. Promoting the energy efficiency of building HVAC systems is therefore essential to reduce building energy consumption and carbon footprint. Over the last several decades, many efforts have been made for the development of cost-effective HVAC technologies and solutions, including, but not limited to, desiccant cooling, heat recovery, renewable energy integration, optimal design, intelligent control, advanced fault detection and diagnosis and thermal energy storage. Among them, solar photovoltaic-thermal (PVT)

collectors and thermal energy storage (TES) using phase change materials (PCMs) are receiving increasing attention for developing high-performance HVAC systems.

Solar PVT collector is a combination of photovoltaics and solar thermal systems, which can generate both electricity and thermal energy simultaneously from one integrated component [1]. Compared to the use of separate solar technologies for heat and electricity generation, using solar PVT collectors is more cost-effective [2]. Phase change material (PCM) with a high energy storage density and the capacity to store thermal energy at a relatively constant temperature is being considered as a future technology to reduce building operating cost and provide better indoor thermal comfort [3, 4]. PCM has been used to increase the local thermal mass of building envelopes or incorporated into building HVAC systems to provide functional purposes and enhance overall system efficiency. As solar energy is intermittent and has a low energy density, the integration of PCMs with PVT collectors may provide an alternative solution to effectively use solar energy and enhance the performance of building HVAC systems. For instance, Su et al. [5] investigated the performance of an air-based PVT collector integrated with PCMs using different configurations. The results indicated that by attaching a PCM layer on the upper side of the air channel of the PVT collector, the overall efficiency of the PVT collector can be improved by 10.7% in comparison to the use of the same PVT without using the PCM. The electrical and thermal performance of a water-based PVT collector incorporating PCMs was also studied [6]. The results showed that the energy output of the PVT collector can be maximised by incorporating a PCM layer with a thickness of 3.4 cm and a melting point of 40°C under the weather conditions in Nanjing, China.

This chapter is structured as follows. Section 2 presents a brief introduction to solar PVT collectors and PCMs. Section 3 provides an overview of solar-assisted HVAC systems with integrated PCMs. Section 4 presents the development of two HVAC systems with integrated PVT collectors and PCMs. Section 5 provides a summary of this chapter.

2. Introduction to photovoltaic-thermal collectors and phase change materials

2.1. Photovoltaic-thermal collectors

According to the heat extraction methods used, PVT collectors can be categorised into air-based PVT, liquid-based PVT, heat pipe-based PVT, PCM-based PVT and thermoelectric-based PVT [7], among which air-based PVT and liquid-based PVT have been commonly studied. The research on PVT collectors has been primarily focussing on the model development and performance analysis, collector design and optimisation, and the integration of PVT collectors with building HVAC systems. **Figure 1** presents an air-based PVT collector, which consists of a PV panel, an absorber plate, a bottom plate and an insulation layer. An air channel is created between the absorber plate and the bottom plate to allow the air flowing through to take away the heat to increase the efficiency of electricity generation. The heated air can be directly used for space heating or to drive desiccant cooling systems. **Figure 2** provides the air-based PVT collectors implemented in a net-zero energy office building, in which the heated air from the PVT collectors was directed into the building, in winter, for space heating.

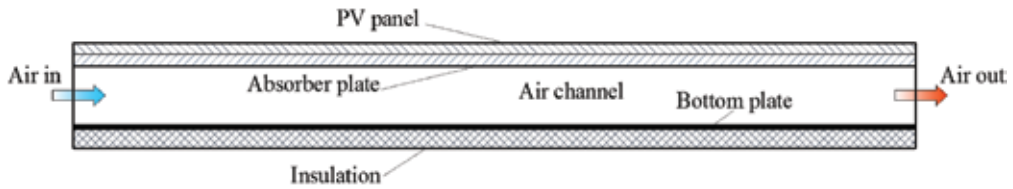

Figure 1. Illustration of an air-based PVT collector.

The performance of air-based PVT collectors is highly influenced by the factors such as solar irradiation, air flow rate, the slope and the orientation of the collectors. **Figure 3** shows the measured solar irradiance, ambient air temperature, the inlet air temperature and outlet air temperature of a PVT collector tested in a laboratory-scale test rig (**Figure 4**) under the two summer test days in 2014 with a fan operating frequency of 10 Hz (i.e. ~50 L/s). It can be seen that, during the daytime, a maximum temperature rise of 14.0°C was achieved when the air flowed through the PVT collectors. During the night-time, a reduction in the air temperature of 1–2°C was achieved in the two test days through night-time radiative cooling. **Figure 5** illustrates the instantaneous thermal energy collected, electricity generated and the electrical efficiency of the PVT collectors under the two summer test days. There was a slight delay between the electricity generation and thermal energy generation due to the low response of temperature to the changes in solar radiation. The maximum instantaneous thermal energy collected from the PVT collectors and the maximum instantaneous electricity generation in the two summer test days were 840 W and 408 W, respectively. The electrical efficiency of the PV cells was relatively stable except during the morning of the first test day due to large variations in solar irradiance.

The above-mentioned results showed that, besides electricity generation, a substantial amount of thermal energy can also be collected. The thermal energy collected during the winter daytime can be directly used for space heating, and the thermal energy collected during the summer night-time can be directly used for space cooling. However, the thermal energy collected during the summer daytime cannot be directly used for space conditioning unless it is used to drive air conditioning systems such as rotary desiccant cooling systems.

Figure 2. Air-based PVT collectors implemented in a net-zero energy office building.

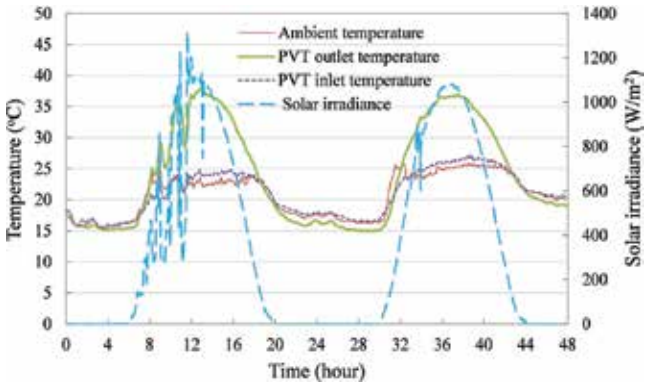

Figure 3. Weather condition and PVT inlet and outlet air temperatures under the two summer test days.

2.2. Phase change materials

PCMs are substances that can absorb, store and release a large amount of thermal energy at relatively constant temperatures and are well suited for heat transfer and energy conservation applications [3, 8]. Over the last several decades, different types of PCMs with different melting temperatures and heat of fusion, as shown in **Figure 6** [9, 10], have been developed. PCMs can be generally grouped into three categories based on their chemical composition, including organic compounds, inorganic compounds, and inorganic eutectics or eutectic mixtures [11].

PCMs as thermal energy storage (TES) should possess desirable thermophysical, kinetic and chemical properties. To characterise the thermophysical properties of PCMs, thermal conductivity analyser and differential scanning calorimetry (DSC) are often used to measure the thermal conductivity and the phase change temperature/heat of fusion of PCMs, respectively. **Figure 7** presents an example of the DSC test results of a commercial PCM product of RT24 [12] under different scanning rates of 0.5, 0.3 and 0.1 K/min, respectively.

PCMs can be incorporated into building envelopes to increase thermal mass and reduce indoor temperature fluctuations as well as to reduce/shift the building heating and cooling demand. PCMs can also be integrated into building HVAC systems as centralised thermal energy storage units to enhance the operating efficiency of HVAC systems through effective load management.

Figure 4. Illustration of the laboratory-scale PVT test rig.

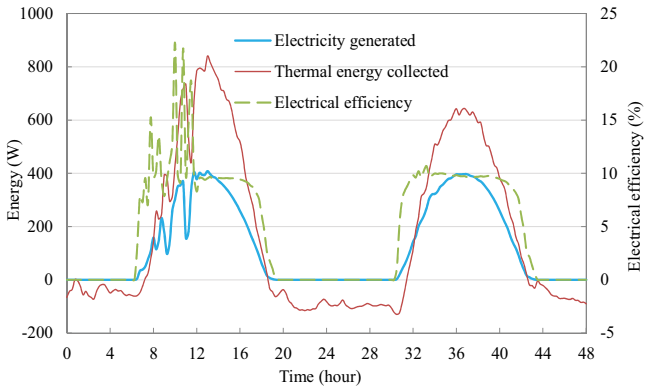

Figure 5. Thermal energy and electricity generation as well as electrical efficiency of the PVT collectors under the two summer test days.

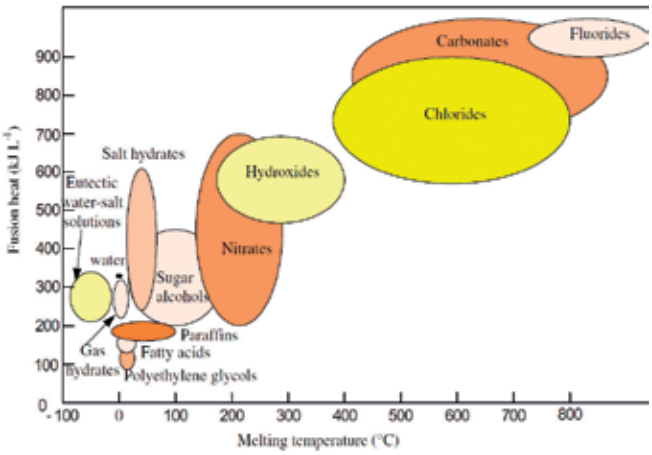

Figure 6. Melting temperature and heat of fusion of different PCMs [9, 10].

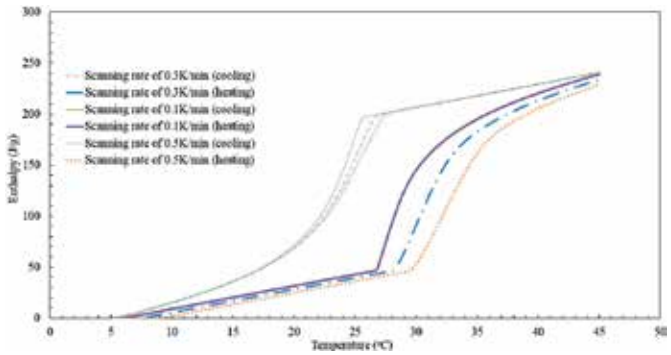

Figure 7. DSC test results of PCM RT24 with the scanning rates of 0.5, 0.3 and 0.1 K/min, respectively.

Figure 8 presents the charging and discharging performance of an air-based PCM thermal energy storage unit, which was tested based on a laboratory-scale rig (**Figure 9**) when the air flow rate was 100 L/s. The PCM tested was a commercial product of PCM S21 [13]. It can be seen that at the beginning of the charging process, both the air temperatures at the inlet and outlet of the PCM TES unit increased rapidly. Then, the outlet air temperature (measured by the temperature sensor #5) increased gradually until approaching to the inlet air temperature of 42°C at the end of the charging process, and the PCM in the TES was melted into the liquid phase during this process. During the discharging process, the outlet air temperature (measured by the temperature sensor #2) from the PCM TES unit first decreased and then slightly increased due to supercooling of the PCM and then continuously decreased to around 14°C at the end of the discharging process. It is worthwhile to mention that, during the experimental tests, the air flow directions in the charging mode and discharging mode were opposite in order to ensure a good heat transfer performance during the discharge of the PCM TES unit.

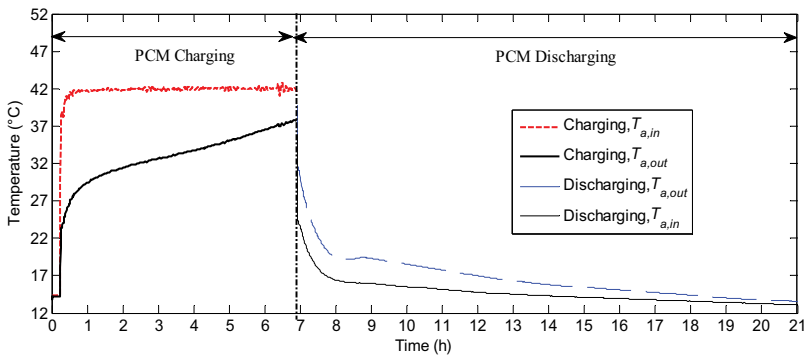

Figure 8. Air temperatures at the inlet and outlet of the PCM TES unit.

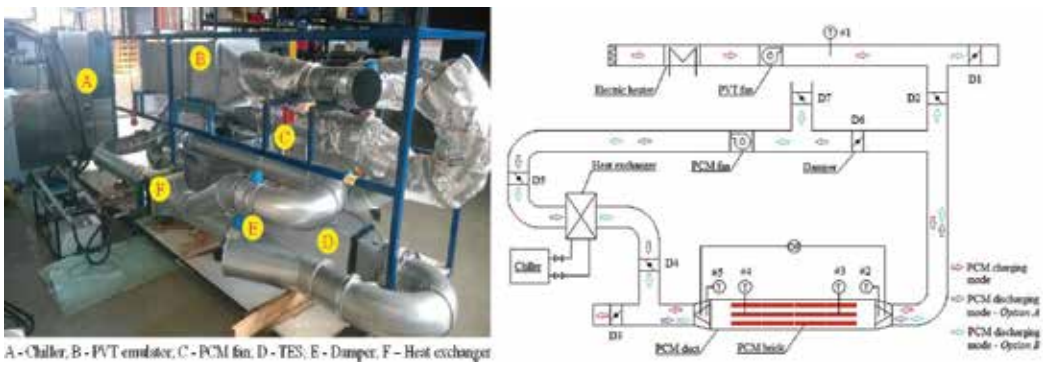

Figure 9. Laboratory-scale test rig of the PCM TES system.

3. Overview of solar-assisted HVAC systems with integrated PCMs

Many different solar-assisted HVAC systems such as solar-driven ejector air conditioners [14], direct current air conditioning systems integrated with photovoltaic (PV) systems [15], solar-driven absorption air conditioning systems [16] and solar-assisted desiccant cooling systems [17, 18] have been developed over the last two decades. As shown in **Figure 10**, in this section, the review mainly focuses on the solar-assisted HVAC systems with integrated PCMs for thermal energy regulation and space conditioning.

A solar-driven adsorption cooling system with an integrated PCM TES unit was investigated by Poshtiri and Jafari [19] in order to provide 24-h air conditioning. The system consisted of an adsorption cooling system, solar collectors, a water storage tank, a PCM TES unit and an auxiliary heater. The thermal energy generated by the solar collectors can be either used to power the adsorption cooling system or stored in the PCM TES unit. The solar energy stored in the PCM TES unit during the daytime was used to power the adsorption cooling system during the night-time if needed. The simulation results showed that the hourly electricity consumption of this system was approximately 30% less than that of a conventional air conditioner during the daytime, and the PCM TES unit reduced the night-time energy consumption of the auxiliary heater by about 31%.

A solar adsorption cooling system integrated with a PCM cold storage system was studied by Zhai et al. [20]. When sunshine was sufficient, the PCM TES unit will be charged using the regenerated coolness from the adsorption chiller. The cooling energy in the PCM can be discharged for space cooling through a radiant cooling terminal unit during the night-time. The results from the experimental test showed that the average charging and discharging rates of the PCM TES unit were 56.7 W and 79.1 W, respectively. The cooling capacity loss only accounted for 7.11% of the total coolness stored.

A solar heating and cooling system with an absorption chiller and a compact PCM TES unit with capillary tubes was proposed by Helm et al. [21]. Through integrating the PCM TES unit

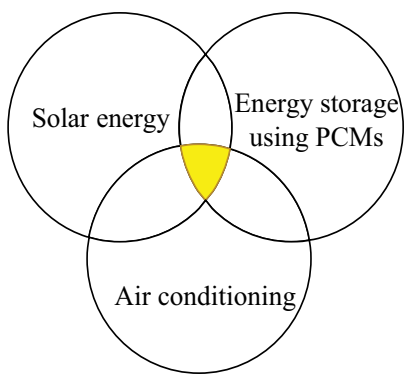

Figure 10. Scope of the review.

into the heat rejection system of the absorption chiller, a fraction of the rejected heat of the absorption chiller can be buffered under the cooling operation, which can allow a lower coolant temperature during the peak demand period, leading to an increased system efficiency. The heat stored in the PCM can be discharged during night-time or off-peak periods. The pilot running of this system showed that, during the hot ambient conditions, up to 50% of the daily rejected heat load can be covered by the PCM TES unit. The overall electrical coefficient of performance (COP) including the regeneration of the PCM TES unit during the night-time was varied between 4.5 and 8.0.

A solar-driven ejector cooling system with an integrated PCM cold TES unit was proposed by Allouche et al. [22]. A simulation study was performed based on an office with a total floor area of 25 m^2 under Tunisian summer weather conditions. The results showed that the use of the PCM TES unit significantly improved the cooling cycle COP of the ejector cooling system and the solar thermal ratio by up to 100%.

Eicker and Dalibard [23] developed a PVT system for night-time radiative cooling of buildings. The system consisted of water-based PVT collectors, a PCM ceiling, an activated floor and a reversible heat pump. During the night-time, the main priority of the PVT collectors was to regenerate the PCM ceiling and then to cool down a storage tank, which was used as a heat sink of the reversible heat pump. The results showed that the PVT-driven PCM ceiling can cover 27% of the total building cooling demand.

An active and responsive solar façade module with integrated PV panels and PCMs was developed by Favoino et al. [24]. In summer, the PCM was used as a passive thermal storage, and a ventilated cavity was used as an outdoor air curtain. In winter, the PCM was used as an active latent heat TES by heating the PCM through electric heat foils when the heating demand was low, and the stored thermal energy was used later when heating demand increased. The ventilated cavity can also be used to preheat the ventilation air in winter. The results showed that this system was able to prevent excessive heat gains in summer and to preheat fresh air for ventilation purposes in winter.

A heat pump with integrated solar collectors and a PCM TES unit was developed by Aydin et al. [25]. The thermal energy generated by the solar collectors was stored in the PCM unit through a closed cycle. The PCM TES unit was then used as the heat sink of the heat pump or as a heat source of hot water for space heating. The results showed that the first law efficiencies of the solar collectors and the PCM TES unit were 70.4% and 74%, respectively, while the second law efficiencies were 2.5% and 37%, respectively. It was also found that the quality of thermal energy was significantly decreased due to the entropy generation.

A solar hot water-driven low-temperature radiant floor heating system consisting of PCMs and polyethylene coils/capillary mat was evaluated by Zhou and He [26]. It was found that the use of the PCM reduced the temperature variations in the floor structure, in comparison with the use of sand for thermal mass. Compared with polyethylene coils, the capillary mat provided a more uniform vertical temperature distribution. A similar floor heating system with capillary plaits and a macro-packaged PCM layer was investigated by Huang et al. [27]. It was found that the PCM floor was able to release 37677.6 kJ heat within 16 h during the pump-off period for a room with a floor area of 11.02 m^2, which accounted for 47.7% of the energy supplied by solar water.

A space heating system with integrated solar air heaters and a fluidised bed TES unit using PCMs was proposed by Belmonte et al. [28]. The use of PCM fluidised bed enabled faster charging and discharging of the TES unit. The results showed that this system can supply approximately 50% of the heating demand of a single-family house under Barcelona and Madrid weather conditions when the TES unit used 2000 kg of the granular PCM.

The performance of a roof-integrated solar heating system using a PCM TES unit was investigated by Saman et al. [29]. The existing roof was used as a solar air heater. A PCM TES unit was used to store the thermal energy generated during the daytime, and the heat stored in the PCM was discharged during the night-time or when there was no sunshine. The simulation results showed that the effect of sensible heat cannot be neglected, and a higher inlet air temperature and a higher air flow rate can reduce the melting time.

A PCM-enhanced house with the PVT ventilation for space heating and cooling was developed by Lin et al. [30]. The PCM was embedded into building envelopes to increase local thermal mass, and PVT collectors were used to generate both electricity and the low-grade thermal energy for space conditioning. The simulation results showed that using the PCM in the building envelope reduced the indoor temperature fluctuations, and the combination of the PVT ventilation and PCM can substantially increase the indoor thermal performance of the house.

A ceiling ventilation system integrated with solar PVT collectors and PCMs was proposed by Lin et al. [31] (see **Figure 11**). The PVT collectors were used to generate electricity and provide the low-grade heating and cooling energy for buildings by using winter daytime solar radiation and summer night-time sky radiative cooling, respectively. The PCM was integrated into the building ceiling as part of the ceiling insulation and at the same time, as a centralised thermal energy storage to temporally store the thermal energy collected from the PVT collectors. The simulation results carried out based on a Solar Decathlon house showed that the thermal performance of the house under the heating conditions was improved significantly by using this system, in comparison with the original house without using PVT collectors and PCMs and the house using the PCM only but without using the PVT collectors.

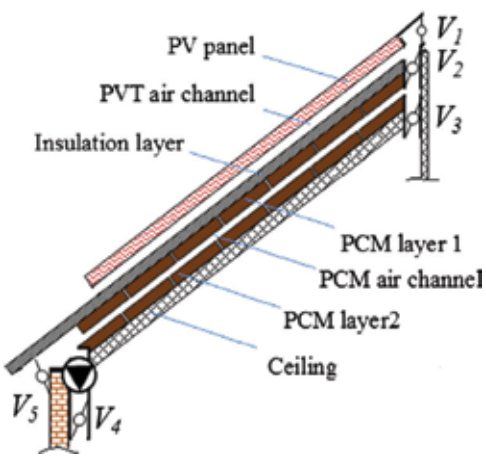

Figure 11. PCM-enhanced ceiling ventilation system with PVT collectors [31].

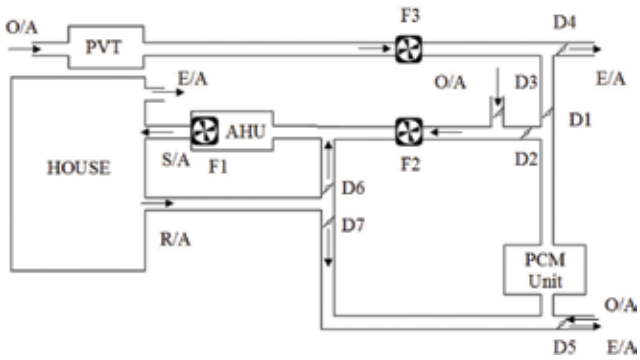

Figure 12. Schematic of the solar-assisted HVAC system (where S/A—supply air, O/A—outside air, R/A—return air, E/A—exhaust air, F—fan and D—damper) [32].

An air conditioning system with integrated PVT collectors and a PCM TES unit (see **Figure 12**) was developed by Fiorentini et al. [32] for a Solar Decathlon house. A hybrid model predictive control strategy was also developed to optimise the operation of this system [33]. The experimental results showed that the control strategy developed was capable of effectively managing and optimising the efficiency of this system.

From the above-mentioned review, it can be seen that solar-assisted HVAC systems with integrated PCMs offered more flexibility to maximise the system operation through the rational utilisation of solar energy. However, the research in this area is far from sufficient, and more prototypes are needed to demonstrate the practical performance of such systems.

4. Development of solar-assisted HVAC systems with integrated PCMs

In this section, two different HVAC systems with integrated PCMs and air-based PVT collectors are presented.

4.1. A rotary desiccant cooling system using PVT collectors and PCMs

Rotary desiccant cooling systems have been considered as one of the alternative approaches to replacing conventional vapour compression systems as such systems do not use chlorofluorocarbons and have the capability of independent temperature and humidity control [34, 35]. Compared to traditional vapour compression systems, rotary desiccant cooling systems are more energy efficient and environmentally friendly [34]. In a rotary desiccant cooling system, the cooling process is achieved by removing the moisture from the process air using a desiccant wheel and reducing the temperature of the process air using evaporative cooling and other cooling technologies.

Figure 13 presents the schematic of a rotary desiccant cooling system integrated with a hybrid photovoltaic thermal-solar air heater (PVT-SAH) and a PCM TES unit. In this system, the hybrid PVT-SAH (see **Figure 14**), in which the PVT collector and the SAH were connected in

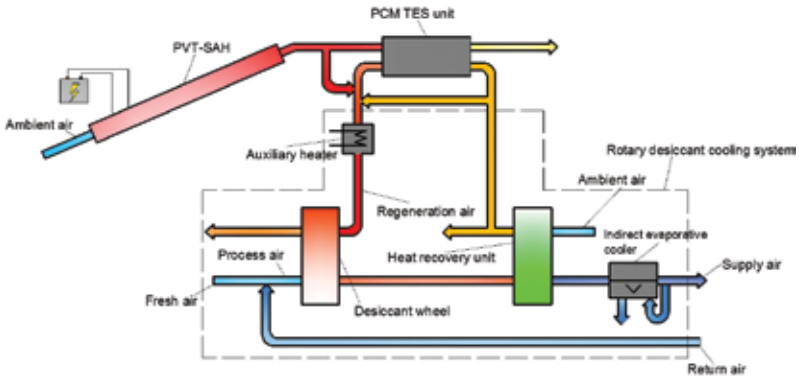

Figure 13. Schematic of the desiccant cooling system with integrated PVT-SAH and a PCM TES unit.

series, was used for both electricity and low-grade thermal energy generation. A glass cover and fins were used to improve the thermal efficiency of the device. The thermal energy collected from the PVT-SAH can be used to drive the desiccant wheel regeneration in cooling conditions or for space heating in heating conditions. The use of such a hybrid system is to achieve a relatively higher air temperature from the PVT-SAH while still maintaining the necessary electricity generation. An air-based PCM TES unit was used to regulate the discrepancy between the thermal energy generated from the PVT-SAH and the thermal energy demand for the desiccant wheel regeneration. A number of PCM arrays were arranged in parallel to create air channels and form the PCM TES unit. A desiccant wheel and an indirect evaporative cooler as well as a heat recovery unit were used to condition the process air.

This system can be used for both daytime and night-time cooling dependent on the building cooling demand. During the daytime, if there is a cooling demand, the heated air from the PVT-SAH will be directly used for the desiccant wheel regeneration. Otherwise, the heated air from the PVT-SAH will be used to charge the PCM TES unit. During the night-time, the heat stored in the PCM TES unit will be used for the desiccant wheel regeneration if there is a cooling demand of the building. It is worthwhile to note that the night-time radiative cooling of the PVT-SAH could be potentially used for space cooling directly. However, such scenario was not considered in this study. During the winter daytime, the heated air from the PVT-SAH can be directly used for space heating or to charge the PCM TES unit. The main potential operation modes of this proposed system are presented in **Table 1**.

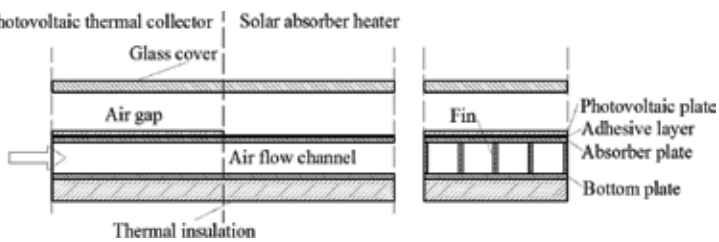

Figure 14. Schematic of the hybrid PVT-SAH system.

Operation mode	Description
Mode I: regeneration with PVT-SAH direct supply	The heated air from the PVT-SAH will be directly used for desiccant wheel regeneration. The electric heater will be used if the air temperature does not reach the required setting
Mode II: regeneration with PVT-SAH direct supply and TES charging	A fraction of the heated air from the PVT-SAH will be used for the desiccant wheel regeneration, and the rest will be used for TES charging
Mode III: TES charging	The heated air from the PVT-SAH is used for charging the PCM TES unit if there is no demand during the daytime
Mode IV: regeneration with TES discharging	The PCM TES unit is discharged for desiccant wheel regeneration if there is a cooling demand during night-time
Mode V: space heating	The heated air from the PVT-SAH is directly used for space heating or is directed into the TES unit (note: PCM with a different melting temperature should be used). The heat in the PCM can be used later for space heating

Table 1. Operation models of the desiccant cooling system with the PVT-SAH and PCM TES unit.

The performance of this system was evaluated based on a simulation system developed using TRNSYS [36]. The building load was calculated based on a DesignBuilder [37] model reported in a previous study [38]. The details about the models used can be found in Ref. [39]. **Figure 15** illustrates the simulated performance of this system under five consecutive Brisbane (Australia) summer working days when the system was operated under the operation modes III and IV. In this test, it was assumed that, during the working days, the house was occupied from 17:00 to 8:00 next day, and the cooling was provided if needed. Under the operation mode III, the ambient air was heated by the PVT-SAH and then used for charging the PCM TES unit during the daytime, and the charging process was suspended if the outlet air temperature of the PVT-SAH was lower than the average surface temperature of the PCM bricks in the TES unit. Under the operation mode IV, the PCM TES unit was discharged using the preheated air from the heat recovery unit. The outlet air from the PCM TES unit was then used for the desiccant wheel regeneration, and the electric heater was used if the outlet air temperature was lower than the desiccant wheel regeneration temperature (i.e. 65°C) required. At the process air side, the return air from the indoor space was first mixed with the fresh air and then used as the process air in order to improve the system efficiency. The results from **Figure 15** showed that the supply air temperature and humidity ratio can be generally controlled below 20°C and 0.008 kg/kg dry air, respectively. During the majority of the test period, the heat from the PVT-PCM system satisfied the heat required for the desiccant wheel regeneration. The total contribution of the solar energy for the desiccant wheel regeneration during the whole test period was 96.5%.

4.2. A heat pump system with integrated PVT collectors and PCMs

The schematic of a heat pump system with integrated PVT collectors and PCMs laminated onto the building ceiling is shown in **Figure 16**. This system was mainly designed for winter space heating, as the main benefit of using the low-grade thermal energy derived from the PVT collectors is for space heating, although the night-time radiative cooling effect of PVT collectors in summer can also be used to improve the energy performance of the proposed system for indoor space cooling. The system consisted of the PVT collectors, two PCM layers,

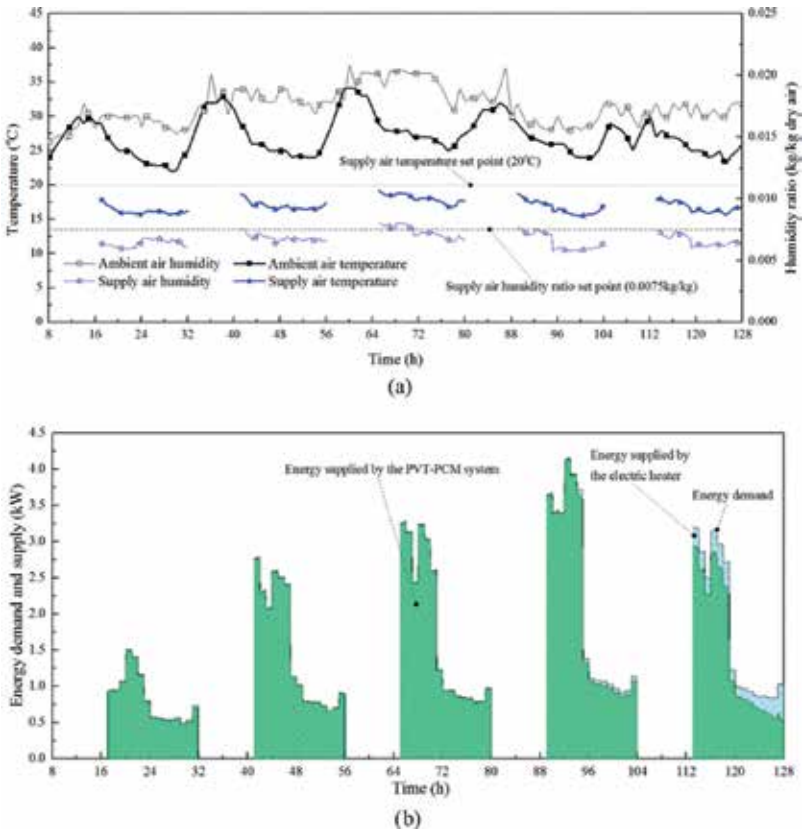

Figure 15. Simulation results of the rotary desiccant cooling system using PVT collectors and PCMs. (a) Ambient air and supply air conditions of the desiccant cooling system. (b) Energy required for desiccant wheel regeneration and energy supplied by the PVT-PCM system.

a PVT fan, a PCM fan and an air source heat pump. The PVT collectors were used to generate electricity and low-grade thermal energy simultaneously. The two PCM layers with an air channel between them were integrated into the building ceiling to increase the local thermal mass and to serve as a centralised TES unit to temporarily store the thermal energy collected from the PVT collectors for later use to facilitate the indoor space heating in winter.

As shown in **Figure 17**, the system can operate under different modes depending on the weather conditions, the thermal energy stored in the PCM and the indoor heating demand through ON/OFF control of the dampers of D1-D8, the PVT fan, the PCM fan and the air source heat pump system. The details of the operation modes are summarised in **Table 2**. During the daytime, the heated hot air from the PVT collectors can be directed into the PCM TES unit for thermal energy charging by switching on the PVT fan and opening the dampers D2 and D3 or it can be exhausted directly by switching on the PVT fan and opening the damper D1. The thermal energy stored in the PCMs can be used to facilitate the space heating via preheating the return air for the indoor unit of the air source heat pump by switching on the PCM fan and opening the dampers D4, D6 and D8 or could directly be used for space heating by switching on the PCM fan and opening the dampers D4, D6 and D7. In the normal air conditioning mode, only the air source heat pump will be used to maintain the indoor

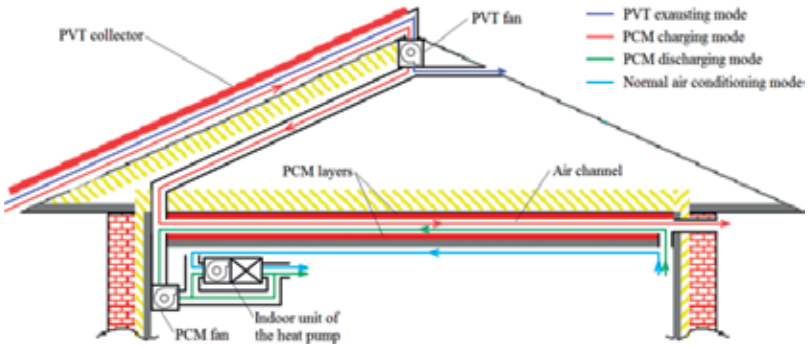

Figure 16. Schematic of the heat pump system with integrated PVT collectors and PCMs.

thermal comfort through opening the dampers D5 and D8. It should be noted that the PVT direct heating mode may cause overheating during the daytime. However, under some cold weather conditions, the direct heating mode could be considered.

The performance of this system was evaluated through numerical simulation. The heating demand of the house was simulated using TRNSYS, and the indoor thermostat setting was specified according to NatHERS [40]. A two-layer PCM TES model (**Figure 18**) and a PVT model developed in a previous study [41] were used to facilitate the performance simulation of the proposed system. The governing equations for the energy balance of the PCM layers and the fluid air in the PCM TES unit are described in Eqs. (1) and (2), respectively. In the model of the PVT collector, six nodes were vertically discretised, including the glass cover, PV plate, absorber plate, fins, fluid air and the bottom plate. The governing equations for the glass cover and the fluid air are described in Eqs. (3) and (4), respectively, while the governing equations of the other nodes can be described in the same way.

$$\rho_{PCM} \frac{\partial h_{PCM}}{\partial t} = k_{PCM} \frac{\partial^2 T_{PCM}}{\partial y^2} \tag{1}$$

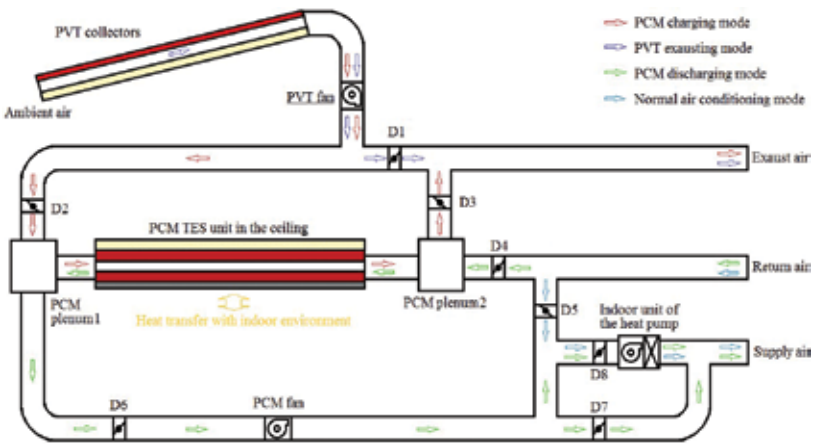

Figure 17. Illustration of the system operating modes.

Operation mode	ON/OFF status of the dampers, fans and heat pump										
	D1	D2	D3	D4	D5	D6	D7	D8	PCM fan	PVT fan	Heat pump
PCM charging	OFF	ON	ON	OFF	—**	OFF	OFF	—	OFF	ON	—
PVT exhausting	ON	OFF	OFF	—	—	—	—	—	—	ON	—
PCM discharging	—	OFF	OFF	ON	OFF	ON	ON/OFF*	OFF/ON*	ON	—	OFF/ON*
PVT direct heating	OFF	ON	OFF	OFF	OFF	ON	ON	OFF	ON	ON	OFF
Normal air conditioning	—	—	—	OFF	ON	OFF	OFF	ON	OFF	—	ON

*If the PCM discharging mode can maintain the required indoor thermal comfort, the heat pump is switched off, damper D8 is OFF and damper D7 is ON. Otherwise, the heat pump will be used, damper D8 is ON and damper D7 is OFF.
**The ON/OFF status is not related to the operation mode.

Table 2. Operation models of the heat pump system with PVT collectors and PCMs.

$$\frac{\partial T_{air}}{\partial t} = u_{air}\frac{\partial T_{air}}{\partial x} + \frac{1}{\rho_{air}\, c_{p,air}\, \delta_{air}}\left(q_{PCM1-air} - q_{air-PCM2}\right) \tag{2}$$

$$c_{p,g}\, m_g \frac{\partial T_{g,i}}{\partial t} = A_{air}\left(\alpha_g I_t + q_{nc,PV-g,i} + q_{rad,PV-g,i} - q_{wind} - q_{sky}\right) \tag{3}$$

$$c_{p,air}\, \rho_{air}\, A_{air}\, \delta_{air}\frac{\partial T_{air,i}}{\partial t} = c_{p,air}\, M\left(T_{air,in,i} - T_{air,out,i}\right) + A_{air}\left(q_{conv,p-air,i} + q_{conv,b-air,i}\right) + 2\, A_{fin}\, q_{conv,fin-air,i} \tag{4}$$

where ρ is the density, h is the specific enthalpy, k is the thermal conductivity, u is the velocity, c_p is the specific heat capacity, δ is the thickness, q is the heat flux, M is the mass flow rate, A is the heat transfer area, m is the mass, the subscripts *PCM1* and *PCM2* represent the two PCM layers respectively, the subscripts *g*, *PV* and *b* represent the glass cover, the PV panel and

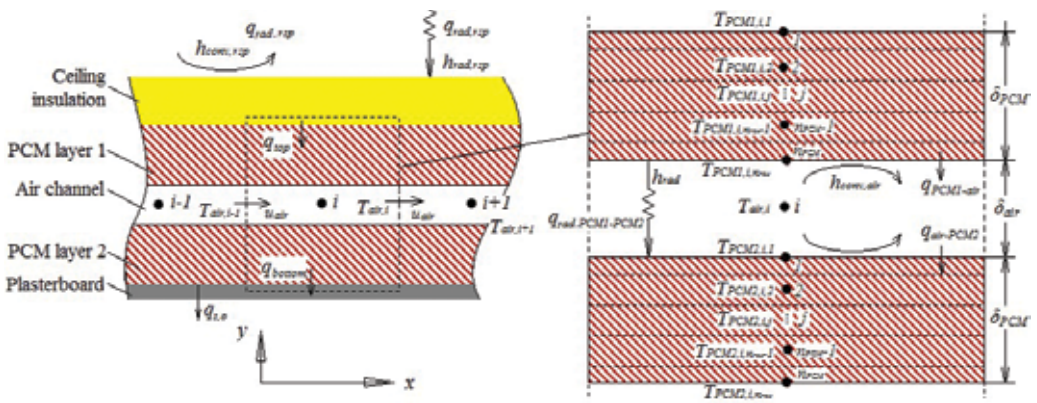

Figure 18. Schematic of the PCM TES model.

the bottom plate of the PVT collectors, and the subscripts *conv*, *rad*, *nc*, *wind* and *sky* indicate convective, radiative, natural convective, wind-driven and sky radiative, respectively. More details about the PVT model and the model validation can be found in Ref. [41].

The coefficient of performance (COP) of the heat pump system with the integrated PVT collectors and PCMs is determined by Eq. (5).

$$COP = \frac{Q_{heating}}{E_{HP} + E_{PVT,fan} + E_{PCM,fan}}. \tag{5}$$

where E is the electrical energy consumed, and $Q_{heating}$ is the heating energy demand.

To evaluate the performance of this system, two cases were designed and simulated under winter weather conditions in Melbourne. In the *baseline* case, only an air source heat pump was used to condition an Australian house. In the *PVT-PCM* case, the air source heat pump integrated with PVT and PCMs was used for space heating. **Figure 19** presents the one-week winter weather conditions used for performance tests.

Figure 20 compares the accumulated electricity generation and consumption during the test days and **Figure 21** illustrates the operation status of the heat pump unit under the two test cases. It is worthwhile to note that the PVT direct heating mode was not considered in this study. It can be seen that the accumulated electricity consumption under the PVT-PCM case was 42.3 kWh, which was much lower than the baseline case of 72.0 kWh. In comparison to the baseline case, the electricity saving was 41.1%, which was achieved through decreasing the operating time of the air source heat pump. The total electricity generation of the PV panels was 156.5 kWh under the *PVT-PCM* case. The average COP of the heat pump system with the integrated PCM layers in the building ceiling and PVT collectors for space heating during the selected week was 5.21, which was higher than that of the air source heat pump system in the *baseline* case (i.e. 3.06). The above-mentioned results indicated that this integrated heat pump system with PCMs and PVT collectors can substantially reduce the electricity consumption for winter space heating.

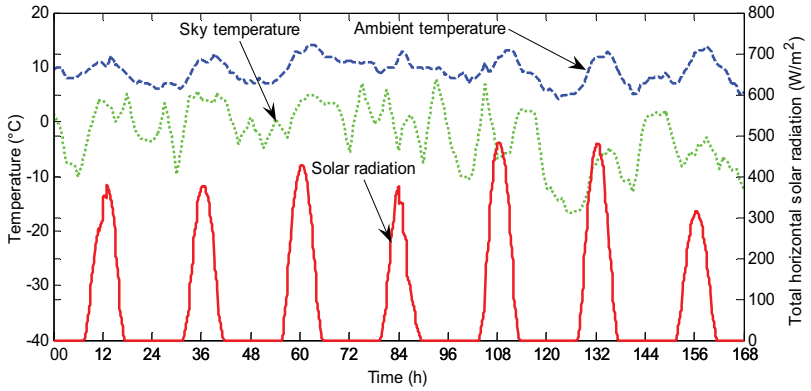

Figure 19. Weather data of a winter week.

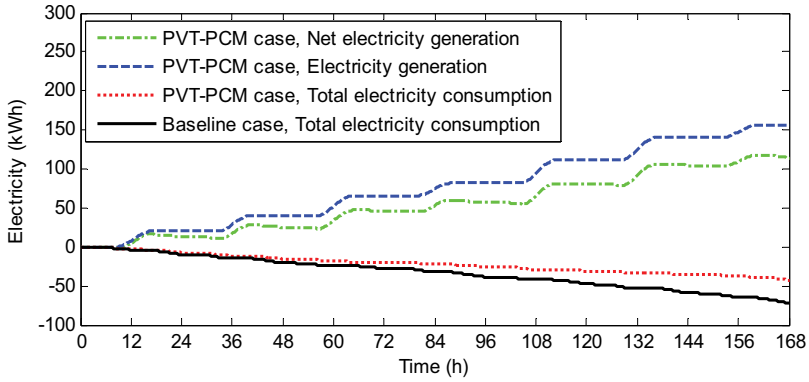

Figure 20. Accumulated electricity generation and consumption under the *PVT-PCM* case and the *baseline case*.

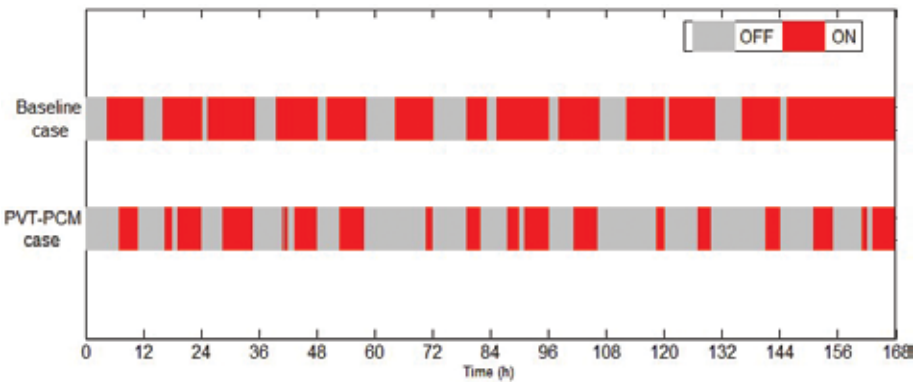

Figure 21. ON/OFF state of the heat pump under the PVT-PCM case and the *baseline* case.

5. Conclusion

Solar-assisted HVAC system with integrated PCMs are a good alternative to conventional fossil fuel-driven vapour compression systems. Due to the intermittency of solar energy, the integration of PCM thermal energy storage units with solar-assisted HVAC systems provides a great opportunity to maximise the utilisation of solar energy and thus to increase the efficiency of HVAC systems. Two different HVAC systems with integrated PCMs and solar photovoltaic thermal collectors were presented, and their performance was investigated. The results showed that the solar thermal contribution for the desiccant wheel regeneration was 96.5% when using integrated PVT collectors and PCMs during the test period. The average COP of the heat pump system with integrated PVT collectors and PCMs for space heating was 5.21 during the test period, which was higher than the baseline case with a COP of 3.06. The results showed that the system performance can be improved through the integration of PCMs. For solar-assisted HVAC systems, control will be essential to ensure that the system can always operate at the optimal performance.

Author details

Zhenjun Ma[1]*, Haoshan Ren[1], Wenye Lin[1] and Shugang Wang[2]

*Address all correspondence to: zhenjun@uow.edu.au

1 Sustainable Buildings Research Centre, University of Wollongong, Australia

2 Faculty of Infrastructure Engineering, Dalian University of Technology, China

References

[1] Chow TT. A review on photovoltaic/thermal hybrid solar technology. Apply Energy. 2010;**87**:365-379

[2] Kumar R, Rosen MA. A critical review of photovoltaic–thermal solar collectors for air heating. Apply Energy. 2011;**88**:3603-3614

[3] Ma Z, Lin W, Sohel M. Nano-enhanced phase change materials for improved building performance. Renewable and Sustainable Energy Reviews. 2016;**58**:1256-1268

[4] Khudhair AM, Farid MM. A review on energy conservation in building applications with thermal storage by latent heat using phase change materials. Energy Conversion and Management. 2004;**45**:263-275

[5] Su D, Jia Y, Alva G, Liu L, Fang G. Comparative analyses on dynamic performances of photovoltaic–thermal solar collectors integrated with phase change materials. Energy Conversion and Management. 2017;**131**:79-89

[6] Su D, Jia Y, Lin Y, Fang G. Maximizing the energy output of a photovoltaic–thermal solar collector incorporating phase change materials. Energy and Buildings. 2017;**153**:382-391

[7] Makki A, Omer S, Sabir H. Advancements in hybrid photovoltaic systems for enhanced solar cells performance. Renewable and Sustainable Energy Reviews. 2015;**41**:658-684

[8] Salunkhe PB, Shembekar PS. A review on effect of phase change material encapsulation on the thermal performance of a system. Renewable and Sustainable Energy Reviews. 2012;**16**:5603-5616

[9] Mehling H, Cabeza LF. Heat and Cold Storage with PCM: An up to Date Introduction into Basics and Applications. Berlin Heidelberg: Springer-Verlag; 2008

[10] Li G, Hwang Y, Radermacher R. Review of cold storage materials for air conditioning application. International Journal of Refrigeration. 2012;**35**:2053-2077

[11] Beatens R, Jelle BP, Gustavsen A. Phase change materials for building applications: A state-of-the-art review. Energy and Buildings. 2010;**42**:1361-1368

[12] Rubitherm PCMs. www.rubitherm.com [Accessed: 7 June 2016]

[13] Phase Change Material products Limited. http://pcmproducts.net/home.htm [Accessed: 23 March 2016]

[14] Varga S, Oliveira AC, Palmero-Marrero A, Vrba J. Preliminary experimental results with a solar driven ejector air conditioner in Portugal. Renewable Energy. 2017;**109**:83-92

[15] Daut I, Adzrie M, Irwanto M, Ibrahim P, Fitra M. Solar powered air conditioning system. Energy Procedia. 2013;**36**:444-453

[16] Ibrahim NI, Al-Sulaiman FA, Ani FN. Solar abosorption systems with integrated absorption energy storage—A review. Renewable and Sustainable Energy Reviews. 2018;**82**(1):0602-1610

[17] Mohaisen A, Ma Z. Development and modelling of a solar assisted liquid desiccant dehumidification air-conditioning system. Building Simulation. 2015;**8**(2):123-135

[18] Guo J, Lin S, Bilbao JI, White SD, Sproul AB. A review of photovoltaic thermal (PV/T) heat utilisation with low temperature desiccant cooling and dehumidification. Renewable and Sustainable Energy Reviews. 2017;**67**:1-14

[19] Poshtiri AH, Jafari A. 24-hour cooling of a building by a PCM-integrated adsorption system. International Journal of Refrigeration. 2017;**79**:57-75

[20] Zhai X, Wang X, Wang C, Wang R. Experimental investigation of a novel phase change cold storage used for a solar air conditioning system. HVAC&R Research. 2014;**20**(3):302-310

[21] Helm M, Keil C, Hiebler S, Mehling H, Schweigler C. Solar heating and cooling system with absorption chiller and low temperature latent heat storage energetic performance and operational experience. International Journal of Refrigeration. 2009;**32**(4):596-606

[22] Allouche Y, Varga S, Bouden C, Oliveira AC. Dynamic simulation of an integrated solar-driven ejector based air conditioning system with PCM cold storage. Applied Energy. 2017;**190**:600-611

[23] Eicker U, Dalibard A. Photovoltaic–thermal collectors for night radiative cooling of buildings. Solar Energy. 2011;**85**:1322-1335

[24] Favoino F, Goia F, Perino M, Serra V. Experimental analysis of the energy performance of an ACTive, RESponsive and solar (ACTRESS) façade module. Solar Energy. 2016;**133**: 226-248

[25] Aydin D, Utlu Z, Kincay O. Thermal performance analysis of a solar energy sourced latent heat storage. Renewable and Sustainable Energy Reviews. 2015;**50**:1213-1225

[26] Zhou G, He J. Thermal performance of a radiant floor heating system with different heat storage materials and heating pipes. Applied Energy. 2015;**138**:648-660

[27] Huang K, Feng G, Zhang J. Experimental and numerical study on phase change material floor in solar water heating system with a new design. Solar Energy. 2014;**105**:126-138

[28] Belmonte JF, Izquierdo-Barrientos MA, Molina AE, Almendros-Ibáñez JA. Air-based solar systems for building heating with PCM fluidized bed energy storage. Energy and Buildings. 2016;**130**:150-165

[29] Saman W, Bruno F, Halawa E. Thermal performance of PCM thermal storage unit for a roof integrated solar heating system. Solar Energy. 2005;**78**:341-349

[30] Lin W, Ma Z, Cooper P, Sohel MI, Yang L. Thermal performance investigation and optimization of buildings with integrated phase change materials and solar photovoltaic thermal collectors. Energy and Buildings. 2016;**116**:562-573

[31] Lin W, Ma Z, Sohel MI, Cooper P. Development and evaluation of a ceiling ventilation system enhanced by solar photovoltaic thermal collectors and phase change materials. Energy Conversion and Management. 2014;**88**:218-230

[32] Fiorentini M, Cooper P, Ma Z. Development and optimization of an innovative HVAC system with integrated PVT and PCM thermal storage for a net-zero energy retrofitted house. Energy and Buildings. 2015;**94**:21-32

[33] Fiorentini M, Wall J, Ma Z, Braslavsky JH, Cooper P. Hybrid model predictive control of a residential HVAC system with on-site thermal energy generation and storage. Applied Energy. 2017;**187**:465-479

[34] La D, Dai YJ, Li Y, Wang RZ, Ge TS. Technical development of rotary desiccant dehumidification and air conditioning: A review. Renewable and Sustainable Energy Reviews. 2010;**14**:130-147

[35] Jani DB, Mishra M, Sahoo PK. Solid desiccant air conditioning—A state of the art review. Renewable and Sustainable Energy Reviews. 2016;**60**:1451-1469

[36] Klein A, Beckman A, Duffie A, Duffie N, Freeman T. TRNSYS 17—A Transient System Simulation Program. Madison: Solar Energy Laboratory, University of Wisconsin; 2011

[37] Tindale A. Designbuilder Software. Gloucestershire, Design-Builder Software Ltd: Stroud; 2017

[38] Fiorentini M. Hybrid model predictive control of residential heating, ventilation and air conditioning systems with on-site energy generation and storage [PhD thesis]. University of Wollongong. 2016

[39] Ren H, Ma Z, Lin W, Fan W, Li W. Integrating photovoltaic thermal collectors and thermal energy storage systems using phase change materials with rotary desiccant cooling systems. Sustainable Cities and Society. 2018;**36**:131-143

[40] NatHERS software accreditation protocol. http://www.nathers.gov.au/. [Accessed: 26 October 2017]

[41] Fan W, Kokogiannakis G, Ma Z, Cooper P. Development of a dynamic model for a hybrid photovoltaic thermal collector–solar air heater with fins. Renewable Energy. 2017;**101**:816-834

Section 2

Absorption and Adsorption Air Conditioning Systems

Chapter 3

Design and Construction for Hydroxides Based Air Conditioning System with Solar Collectors for Confined Roofs

Yuridiana Rocio Galindo Luna,
Rosenberg Javier Romero Domínguez,
Jonathan Ibarra Bahena, Moises Montiel González,
Jesús Cerezo Román, José Eduardo Jasso Almazán,
Antonio Rodríguez Martínez,
Karina Solano Olivares, Ana María Hernández Jasso,
Sotsil Silva Sotelo, José Antonio García Ramos,
Ariana Morales Flores and Brenda Rivas Herrea

Additional information is available at the end of the chapter

http://dx.doi.org/10.5772/intechopen.72188

Abstract

In this chapter, the methodology to determinate heat load is revised and presented. The main parameters must be fixed as function of climatization, internal thermic conditions (comfort, temperature, and humid) and the activities. According with literature, the roof structural requirements were checked. These are an important parameter because it represents the limits to the system such as load by devices (weight of equipment), orientation in solar systems (operating conditions), and building materials. The method of calculation of solar available is shown; the aim is to achieve the major collection of solar energy. Finally, the plate heat exchangers can be fabricated in gasketed, welded or module welded design characterized by the model in which the flow channels for the two heat exchanging media are sealed. The kind of exchanger is suitable depending on your requirements. The thermodynamic method of calculation of sizing the exchangers is reviewed. The aim of this section is to find the suitable devices for the operation of air-conditioning absorption system based on hydroxide.

Keywords: air-conditioning system, plate heat exchanger, roof structural conditions, life cycle assessment, sustainable cycle

1. Introduction

The world's main development is the energy because the technological advances and economic growth in countries rely on it. The energy demand is basically affected by three major factors, namely, population, economy, and the per capita energy consumption. The increase in energy demand leads to increased greenhouse gas emissions associated with the burning of fossil fuels and contributes to global warming. The energy demand associated with air-conditioning in most industrialized countries has been increasing in recent years. Traditional mechanical steam compression systems have been used for decades; nevertheless, it demands large amounts of electrical energy for the operation of the compressor; this energy demand not only affects the environment but also negatively impacts the user in economic terms associated with the cost of operation. Therefore, it has become crucial to design air-conditioning systems that are respectful to the environment and are capable of operating using waste or renewable energy sources. Commercially available absorption chillers for air-conditioning applications usually operate with LiBr/H_2O mixture and use steam or hot water as the heat source [1]. It has been testified that single-effect LiBr/H_2O absorption units using fossil fuels are not competitive from the energy, economic, and environmental points of view. They are only competitive when using waste or renewable heat as part of the driving energy [2]. Besides, according to the operating temperature range of driving thermal source, single-effect LiBr/H_2O absorption chillers have the advantage of being powered by ordinary flat-plate or evacuated tubular solar collectors. The main advantages of solar absorption cooling systems concern the reduction of peak loads for electricity utilities, the use of zero ozone depletion impact refrigerants, the reduction of primary energy consumption, and the reduction of global warming impact [3, 4]. Cold production through absorption cycles has been considered one of the most desirable applications for solar thermal energy.

2. Thermal capacity of the building

2.1. Determination of the working operation time of the absorption cooling system

An analysis of the environmental temperature was carried out in order to select the operation time of cooling absorption system. The TRNSYS software was used to simulate the building because it has implemented meteorological data such as radiation, environmental temperature, wind velocity, and so on for different cities around the world. **Figure 1** shows environmental temperature and global radiation profiles along a year (0–8760 h) at Temixco city, Mexico. The selected period was from March to May (1460-3560 h) to operate absorption system due to the high environmental temperature (**Figure 2**).

2.2. Determination of the cooling capacity of the building

The TRNSYS software has the advantage to simulate different kinds of processes (called types) such as pumps, photovoltaic modules, solar collectors, controllers, buildings, among others, and they can interact with each other with the environment in a dynamic way along time. The heat generation of the building considers four people in a rest position and three computers turned on from 8:00 to 18:00. Dimensions and main building characteristics are shown in **Table 1**.

http://dx.doi.org/10.5772/intechopen.72188

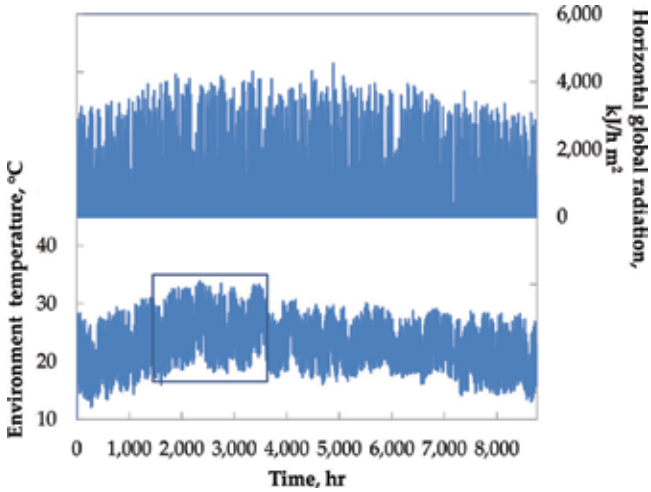

Figure 1. Environmental temperature data for an estimated year time in the TRNSYS software.

Figure 2. Photograph of the thermal and photovoltaic solar systems on the building roof.

Concept	Quantity
North and south wall	35 m^2
Ceiling and floor	75 m^2
West and east wall	12.5 m^2
Thickness of walls	0.12 m brick
Windows	4

Table 1. Home characteristics.

Figure 3 shows the behavior of environmental and building temperatures and relative humidity, as it can be seen 25°C was the set point temperature of the building. The relative humidity varied from 20 to 83%.

Figure 4 shows the behavior of cooling capacity of the building. The total energy consumed was 1.29×10^7 kJ from March to June. The maximum heat load capacity was 2.8×10^4 kJ/h (7.8 kW), and this value should be dissipated by the evaporator from absorption cooling system.

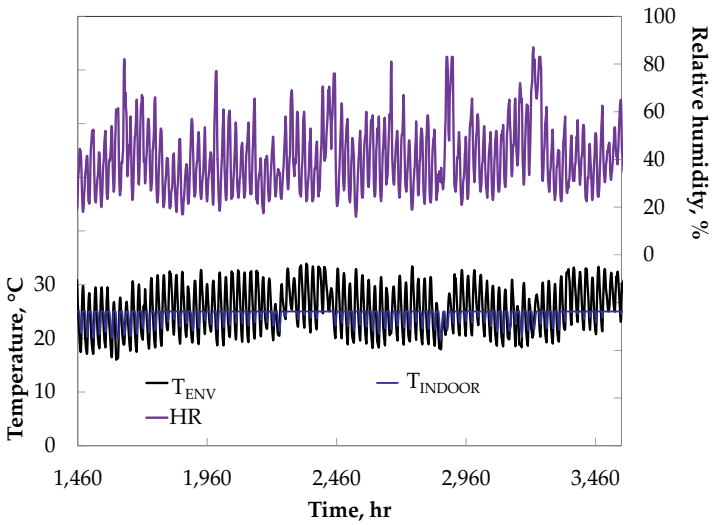

Figure 3. Indoor conditions of the building from 1417 to 2337 h (March).

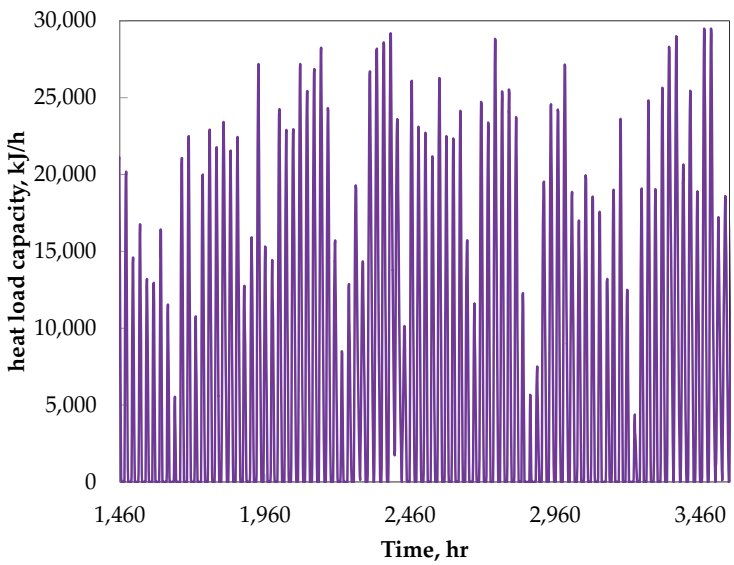

Figure 4. Cooling capacity profiles of the building from March to June.

http://dx.doi.org/10.5772/intechopen.72188

3. Structural conditions of construction

It is so important to consider structural conditions for the installation of absorption system, for example, loads or static, dynamic and cyclical forces, the mechanical properties that it must satisfy are resilience, tenacity, ductility, and resistance to the deformation. The structures of materials are considered to accomplish the requirements that are available in the market. The following structural materials were revised.

3.1. Structures of wood

The main advantages are di-electrical materials or natural insulation, seismic resistance, and they are cheap in comparison with the girders of reinforced concrete. Nevertheless, they can be attacked and destroyed by insects, by fungi, and by natural rot; in addition, they are not resistant to the fire. The weight capacity of structures of wood support, according to the position in floor or ceiling, is in a range from 3.5 to 4.2 kN/m^2; this means that they can support 2 kN/m^2 of useful load before suffering a deformation or fracture. Considered the wood type 2, the wood structures support from 1.5 to 2.2 kN/m2, before suffer deformation or fracture [5].

3.2. Structures of reinforced concrete

The characteristics of the reinforced concrete are as follows: it increases the rigidity and offers the possibility of completing the build later. The structure is formed per rigid knots and non-deformable edges. The disadvantages are low capacity acoustic and thermal insulation and high cost [6].

Structure	Wood	Metallic	Concrete
Advantages	- Thermal low - isolation cost to comparison with the girders of concrete and of steel	- Uniformity - Permanence - Ductility - Tenacity	- Rigid knots - rigid edges - major inflexibility - possibility of using the continuity of the element
Disadvantages	- Irresolute and destroyed for insects, for fungi, and for the rot. - It is not resistant to the fire - the weight that can load 2 kN/m^2 they are of the same structure to load 1.5–2.2 kN/m^2	- Corrosion - elastic bulge - Fatigues low - resistance to high temperatures	- Minor capacity of acoustic isolation - minor capacity thermal - high cost in comparison with armed with wood.
Loads	420 kN/m^2	>350 kN/m^2	>350 kN/m^2

Table 2. Comparison of structures.

3.3. Metallic structures

These structures are metallic and are characterized by their low cost in comparison with structures of reinforced concrete, high resistance of the metallic structures due to their properties of the steel such as useful long life, ductility, tenacity, and high electrical conductivity. Their advantages are as follows: rapidity of assembly, great capacity of laminated, resistance to the fatigue, armor with diverse types of shaped and possible structural reutilization after dismounting. The disadvantages are as follows: corrosion, elastic bulge, and high cost in comparison with the structures of wood.

Table 2 shows the advantages and disadvantages of the structural materials.

4. Air-conditioning absorption system

The use of solar energy to power an air-conditioning system is a convenient practice to replace conventional electricity [7]. This can be achieved by two methods: photovoltaic solar cooling and thermal driven sorption system [8]. However, thermal cooling technology is preferred because it can use more incident sunlight directly compared with the PV system [9]. Thermal cooling technologies include absorption, adsorption, desiccant systems, and ejector-compression systems; nevertheless, absorption cooling represents the most common globally technology due to the commercial availability [7, 10]. The process absorption is based on the absorption and desorption of a working fluid named refrigerant in an absorbent. Basic absorption cycle consists of four main components: generator, condenser, evaporator, and

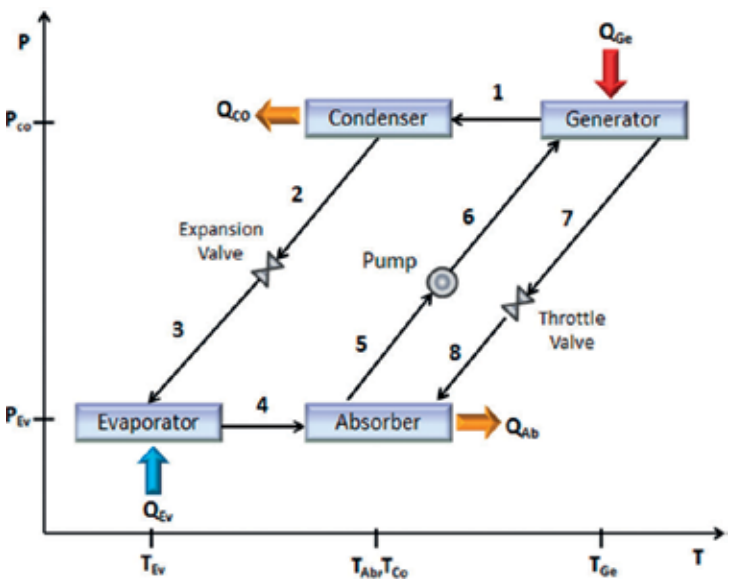

Figure 5. Schematic diagram of the absorption cooling cycle.

absorber; additionally, the system requires a solution pump and two valves, as shown in **Figure 5**. A quantity of heat (Q_{GE}) is added to the generator at a relatively high temperature (T_{GE}) to vaporize the working fluid from the solution. The vaporized working fluid (1) goes to the condenser, where it is condensed into a saturated liquid, and the heat released from this condensation process (Q_{CO}) is discharged to the atmosphere at an intermediate temperature (T_{CO}). The liquid leaving the condenser (2) passes through an expansion valve to reduce its pressure (3) and goes to the evaporator; as the saturation temperature of the refrigerant at lower pressure is much lower than room temperature (T_{EV}), the refrigerant absorbs the heat of the room (Q_{EV}), and it vaporizes, producing the cooling effect. Then, the vapor generated (4) moves to the absorber where it is absorbed by the strong solution of absorbent coming from generator (7, 8), delivering heat (Q_{AB}), which is dissipated to the ambient to keep the absorption process at a desirable temperature (T_{AB}). Finally, the mixture refrigerant/absorbent is pumped (5, 6) to the generator to restart the cycle.

The cycle can be mathematically described by the following equations derived from mass and energy balances:

$$Q_{GE} = m_6 H_6 - m_1 H_1 - m_7 H_7 \tag{1}$$

$$Q_{CO} = m_1 H_1 - m_2 H_2 \tag{2}$$

$$Q_{EV} = m_4 H_4 - m_3 H_3 \tag{3}$$

$$Q_{AB} = m_4 H_4 + m_8 H_8 - m_5 H_5 \tag{4}$$

$$COP = \frac{Q_{EV}}{Q_{GE} + W_p} \tag{5}$$

The coefficient of performance (COP) is a parameter that is defined as the ratio of available useful energy to the total power supplied to the system. As the work from the pump solution, W_p is relatively small (about 1%) with respect to the heat supplied in the generator, and it is usually negligible for analysis purposes.

These equations allow us to compute the system in order to simulate various operating conditions and determine which those that meet the requirements.

4.1. Working pair

The mixture refrigerant/absorbent is better known as working pair, and the performance of the cycle depends critically on it [11]. Generally, a suitable working pair should satisfy some requirements such as a high boiling point difference and a good miscibility between the components, chemically stable, nontoxic, environmental-friendly to mention a few [12, 13]. A wide variety of refrigerant/absorbent combinations have been suggested for absorption cooling systems [13], being the mixtures of water/LiBr and ammonia/water as the two most

Property	Sodium	Potassium
Vapor pressure	Olsson et al. [20], Balej [21]	Balej [21]
Density	Olsson et al. [20]	Akfcrlof et al. [22], Kelly et al. [25]
Enthalpy	Olsson et al. [20]	Biermann [23], Ginzburg et al. [24]
Viscosity	Olsson et al. [20]	Kelly et al. [25]

Table 3. Properties for sodium hydroxide and potassium hydroxide.

common working fluids [12]. However, both systems have their limitations, which make necessary to research different working pairs [14].

4.2. Hydroxides

According to research, the 2,497,819 and 4,151,721 U.S. patents proposed an arrangement for absorption of refrigeration systems based on aqueous solutions of hydroxides in order to present alternative mixtures with the aim to avoid the problems presented by the conventional working fluids. The patents propose soluble basic hydroxides such as sodium and potassium [15–17], and cesium hydroxide was considered later [15]. Subsequently, an aqueous mixture of ternary hydroxide was developed [18], and its performance was theoretically compared with the solution of lithium bromide showing promising results [19]. To calculate and optimize absorption processes, accurate data about the different properties of the mixtures are required. Unfortunately, the available information is scarce, and in most cases, it does not cover the full range of concentration and operating temperatures. However, **Table 3** presents different properties for sodium hydroxide and potassium hydroxide according to the analysis of authors.

Based on this lack, we can conclude that there is an area of knowledge yet to be explored.

5. Heat exchanger: selection and sizing

As it has been described previously, a conventional absorption heat pump includes, at least, four heat exchangers (generator, condenser, evaporator, and absorber), and the coefficient of performance (COP) is strongly affected by the heat and mass transfer efficiency of these components. The fact that the heat exchangers are widely used in many industrial applications allows that the new developments on heat transfer subject promote new designs on absorption heat pumps. Annex 33 of the International Energy Agency (IEA) Heat Pump Program, which was aimed at promoting use of compact heat exchangers in heat pump systems, included three main goals [26]:

1. Identify compact heat exchangers, either existing or under development, that may be applied in heat pumping equipment. This has the aims of decreasing the working fluid inventory, minimizing the environmental impact of system manufacture and disposal, and/or

increasing the system performance during the equipment life, thereby reducing the possible direct and indirect effects of the systems on the global and local environments.

2. Identify, where necessary propose, and document reasonably accurate methods of predicting heat transfer, pressure drop and void fractions in these types of heat exchangers, thereby promoting or simplifying their commercial use by heat pump manufacturers. Integral with these activities was an examination of manifolding/flow distribution in compact/microheat exchangers, in particular in evaporators.

3. Present listings of operating limits for different types of compact heat exchangers, for example, maximum pressures, maximum temperatures, material compatibility, minimum diameters, and so on and of estimated manufacturing costs or possible market prices in a large-scale production. It is intended within this context that opportunities for technology transfer from sectors where mass-produced CHEs are used (e.g., automotive) will be examined, and recommendations are made.

Plate heat exchanger (PHE) is a compact heat exchanger and has been used for absorption system applications [27–30]. Design, sizing, and selection of a PHE for absorption systems are restricted by the thermodynamic properties of the working mixture because they limit the heat transfer rate; consequently, the heat transfer area is in function of this. Other parameter to consider in heat exchanger selection is the operating conditions (temperature and pressure). Aqueous solutions such as LiBr, NaOH, CaCl, LiCl operate at vacuum pressure conditions (from 0.8 to 7 kPa) [31–35], but there are configurations that include a high-pressure generator (from 150 to 300 kPa) [30, 36, 37].

To the performance, a thermal or heat transfer analysis to heat exchanger is suitable to apply some of the methods such as LMTD, ε-Ntu, and P-Ntu. The methodologies have subtle variations but in essential are the same. P-Ntu method is often used for the calculation of the correlation factor F for the first method. LMDT and ε-Ntu methods have been widely applied in industrial practice [38]. A calculation procedure for plate heat exchanger and useful charts was developed as functions of the number of transfer units (Ntu) and the heat capacity ratio (R) for different heat exchanger configurations. Number of channels, number of passes of each fluids, and flow arrangement were the terms to classify the heat exchangers [39]. The ε-Ntu method avoids a rather cumbersome iteration through logarithmic terms, necessary in the LMTD method, and provides a very elegant method using dimensionless parameters that can be applied in easy way to new design and performance rating problems of heat exchangers.

The effectiveness (ε) is the ratio of heat transfer rate ($\dot{Q}$), to the maximum heat transfer potential rate ($\dot{Q}_{max}$),when the heat exchanger area is infinite:

$$\varepsilon = \frac{\dot{Q}}{\dot{Q}_{max}} \tag{6}$$

Heat capacity rates are obtained by multiplying the specific heat and mass flow rate of the fluid. The fluid with the higher heat capacity is designated C_{max} and the lower one C_{min}. If the cold fluid has the minimum heat capacity, then the effectiveness is defined as:

$$\varepsilon = \frac{C_{max}(T_{h,i} - T_{h,o})}{C_{min}(T_{h,i} - T_{c,i})} = \frac{C_{min}(T_{c,o} - T_{c,i})}{C_{min}(T_{h,i} - T_{c,i})} \tag{7}$$

where $T_{h,i}$ and $T_{h,o}$ are the inlet and outlet temperatures of the hot fluid and $T_{c,i}$ and $T_{c,o}$ are the inlet and outlet temperatures of the cold fluid. The ratio of capacities is defined by:

$$R = \frac{C_{min}}{C_{max}} \tag{8}$$

The dimensionless parameter Ntu (number of transfer units) expresses the size of the heat exchanger and is commonly used in heat exchanger analysis and is expressed as [40]:

$$Ntu = \frac{UA}{C_{min}} \tag{9}$$

Effectiveness correlations for different types of heat exchangers are summarized in **Table 4**.

If there is a phase change in a heat exchanger, the heat capacity of the fluid-changing phase becomes infinite, and Cr is zero, then effectiveness correlations reduce to:

$$\varepsilon = 1 - exp(-Ntu) \tag{10}$$

Regardless of the type of heat exchanger.

Heat exchanger type	Effectiveness (ε) relations
Parallel flow	$\varepsilon = \frac{1 - exp[-Ntu(1+R)]}{1+R}$
Counter flow	
R<1	$\varepsilon = \frac{1 - exp[-Ntu(1-R)]}{1 + R\,exp[-Ntu(1-R)]}$
R=1	$\varepsilon = \frac{Ntu}{1+Ntu}$
Cross flow both fluid unmixed	$\varepsilon = 1 - exp\left[\left(\frac{1}{R}\right) Ntu^{0.22}\left\{exp[-R(-Ntu^{0.78})] - 1\right\}\right]$
Cross flow	
C_{min} (unmixed)	$\varepsilon = \frac{1 - exp\left\{-R[1 - exp(-Ntu)]\right\}}{R}$
C_{max} (mixed)	
Cross flow	
C_{max} (unmixed)	$\varepsilon = 1 - exp\left\{-\frac{1}{R}[1 - exp(-Ntu * R)]\right\}$
C_{min} (mixed)	
Shell and tube one shell pas (2,4…tube passes)	$\varepsilon_1 = 2\left\{1 + R + (1+R^2)^{\frac{1}{2}} \frac{1 + exp\left[-Ntu\,(R^2)^{\frac{1}{2}}\right]}{1 - exp\left[-Ntu\,(1+R^2)^{\frac{1}{2}}\right]}\right\}$
n Shell passes (2n, 4n… tube passes)	$\varepsilon_n = \left[\left(\frac{1-\varepsilon_1 R}{1-\varepsilon_1}\right)^n - 1\right]\left[\left(\frac{1-\varepsilon_1 R}{1-\varepsilon_1}\right)^n - R\right]^{-1}$

Table 4. Effectiveness relations for different types of heat exchangers [41].

5.1. Condenser and evaporator

These devices for air-conditioning applications are designed considering the coil flooded with two-phase refrigerant and also a wall temperature equal to the refrigerant in general [42]. The outer side heat transfer coefficient and the physical properties are assumed constant. Thereby, the heat transfer rate is calculated according to [43]:

$$\dot{Q} = \dot{m}\, Cp(T_o - T_i) = \varepsilon\, \dot{m}\, Cp(T_s - T_i) \tag{11}$$

where $\dot{m}$ is the mass flow rate, T_i, T_o and T_s, are the inlet, outlet, and surface temperatures, respectively.

$$\dot{Q} = \varphi\, A_s(T_s - T_m) \tag{12}$$

The equation number 12 is the heat transfer rate, T_m is the mean flow temperature over the heat transfer area, and A_s and ε are the heat exchanger effectiveness.

6. Solar thermal technologies selection

Around the world are different types of sources of renewable energy. However, solar thermal energy is the most abundant, and the interest in their development has increased in recent years [44, 45]. This subsection describes the technologies used with solar thermal energy, advantages and disadvantages, and a guide to choose one of them depending on the project.

6.1. Solar radiation

The interest in solar energy has grown since the environmental problems caused by burning fossil fuels have become severe. One of the most important parameters for the use of solar energy is the estimate of solar radiation [46]. Solar radiation is compound of three elements: *direct radiation*, which is received direct from the sun without diffusion by the atmosphere and is used by the solar energy technologies; *diffuse radiation*, formed with sunlight diffused by atmosphere when in the sky, air molecules, dust and cloud interfere the natural path of the rays, "fragmenting" the sunlight; and *albedo*, which is the radiation reflected by the floor [43]. In order to reduce the greenhouse gases pollution, there exist technologies that transform the solar energy in thermal energy, which is called "solar thermal technologies".

6.2. Solar thermal technologies

Solar energy technologies are special kind of heat exchangers that transform solar radiation energy to thermal energy storing it in a fluid. The most important component of any solar technology is the solar collector, which is a device that absorbs the incoming solar radiation, converts it into heat, and transfers that heat to a fluid flowing through the collector [48].

These collectors can be divided into two types: nonconcentrating (NC) and concentrating (CC). Then, it describes their advantages and disadvantages [48, 49].

Advantages

- Heat transfer fluid (HTF) can achieve higher temperatures because the solar beam is focused on a point.
- The thermal efficiency is greater because of the small heat-loss area relative to the receiver area.
- With these systems, the HTF reduces exergetic losses through the STT; it means that the interchange between the fluid temperature and environment is less according to the smaller area of the receiver.
- For a CC, the cost per unit area of the solar collecting surface is cheaper than of a NC collector.

Disadvantages

- In a cloudy day, it may not work; it means, without solar radiation, these systems do not transform energy.
- Concentrator systems collect little diffuse radiation depending on the concentration ratio.
- Some form of tracking system is required to follow the Sun, generating more monetary and energetic costs.
- Solar reflecting surfaces may lose their reflectance with time and require periodic cleaning and refurbishing.

Even with these characteristics, not all solar collectors have the same design, depending on different concentrators and receivers; for that reason, they are divided into: linear fresnel reflector (LFR), parabolic trough collector (PTC), parabolic dish reflector (PDR) and central receiver (CR); finally, they are subdivided into solar tower (ST) and solar furnace (SF) [48, 49].

The **Figure 6(a)** shows the focus method to achieve the recollected energy of sun and increase the efficiency of collector; the PTC and PD are divided into mobile receivers; it means that the collector and the receiver need a tracking sun technology. On the other hand, LFR, SF, and ST are classified as fixed receivers because the receiver is static. In **Figure 6(b)**, a graph is shown comparing the concentration ratio with the temperature that can be achieved. LFR has a concentration ratio from 10 to 40 units, and a temperature ranges from 60 to 250°C. PTC increases its concentration compared with LFR, between 15 and 45 units; thus, the temperature range can reach from 60 to 300°C. On one hand, ST achieves a concentration ratio of 300–600 and can achieve a temperature above 800°C. On the other hand, PD has a concentration ratio between 100 and 1000 and a temperature range from 100 to 1600°C. Furthermore, SF has the highest concentration range of all STT, reaching 10,000 units; thus, this technology can arrive temperatures above 2000°C [48, 49].

6.2.1. Linear Fresnel reflector

LFR is a type of solar collector that collects sunlight by adapting long, narrow or slightly curved mirrors to reflect the Sun's ray into an absorber tube and concentrate that energy. They usually use water as HTF, which passes through the receiver and change to steam. Considering that the focal line in the LFR can be distorted by astigmatism of the mirror, usually a secondary mirror is placed above the receiver to refocus the Sun´s ray [6]. They have the advantages of easy manufacture and maintenance, and low cost comparing with other solar thermal technologies. However, these systems have the disadvantage of losing some portion of reflector aperture because the arrangement between each other blocks part of the sunlight and affecting their efficiency [50].

6.2.2. Parabolic trough collectors

PTCs have a parabolic shape and are covered by a bending sheet of reflective material. A metal black tube, covered with a glass tube to reduce heat losses, is placed along the focal line of the receiver. Then, parallel ray's incident on the reflective material and are reflected onto the receiver where a HTF absorbs the solar power [48]. Each collector is connected together in long lines, and a system tracks the Sun´s path throughout the day along a single axis, usually east to west [49]. These technologies have the following advantages: they are feasible commercial options to transform heat, and they are the most advanced of STT because of considerable experience and have several applications [51]. One of their principal disadvantages is the tracking mechanism because it must be reliable and able to follow the Sun with a certain degree of accuracy, returning the collector to its original position at the end of the day, increasing their cost and energy supply [48].

6.2.3. Parabolic dish (PD)

The parabolic dish (PD) is one of the most important methods in solar power generation. It is a point-focus collector that tracks the Sun in two axes, concentrating solar energy onto a receiver. The receiver absorbs solar radiation, transforming it into thermal energy. The thermal energy can either be transported through piped to a central power-conversion system or it can be transformed into electricity [48]. Solar dish presents some advantages such as high efficiency, hardness against deflection and wind load, modularity, versatility, durability against moisture and temperature changes, long-term low maintenance operation, and long lifetime. There are some disadvantages such as conversion of heat into electricity is needed in the system to have moving parts, increasing maintenance and cost, and is necessary for a great supply of energy to the tracking solar system [52].

6.2.4. Solar tower (ST)

This is a technology composed of multiple mirrors called heliostats distributed on a field, ordered and oriented automatically using a solar tracking system to reflect the direct radiation to a receiver situated a great height. Usually, each heliostat has 50–150 m^2 of reflective surface

transferring the thermal energy onto the receiver. The heat transportation system consists of pipelines, pumps, and valves, where the fluid flows in a closed circuit between receiver and storage tank. Some of the advantages of these are highly effective as much in the solar collection as in its transformation to electricity. Also, there is no necessity to flatten the field; therefore, this technology can be installed in a hill. One of the most important disadvantages is the higher cost of the solar tracking system compared with the same system installed in PTC because in ST, it is necessary to install in each heliostat one of these systems and in PTC, the tracking system can be installed by row [48, 53].

6.2.5. Solar furnace (SF)

These devices are used in tests, high-temperature processes, and other applications and are constituted by one or more heliostats, which track the Sun, reflecting the sunrays horizontal and parallel to an optical axis of the parabolic concentrator, which in turn concentrates the incoming rays into the focus of the parabola. This reflector can be composed of a parabolic mirror or a group of spherical mirrors. The furnace power can be attenuated by a shutter, which controls the amount of solar radiation. The concentrated radiation reaches the test area, which is located at the concentrator focus [44]. One of the most important advantages is that it can reach temperatures above 2000°C, allowing the scientific community to do specific researches. However, this technology is the most expensive between STT and needs high technical knowledge to operate them.

6.3. How to select one of the solar thermal technologies

There is no single criterion to make the selection of one of all STTs presented in this chapter; however, by looking applied examples of each technology, it is possible to facilitate the choice of the best technology for a project. Solar collectors have been used in a variety of applications. In **Table 5**, there are listed the most important solar thermal applications with the type of collector that can be used in each case. Other way to decide the best technology is to know first the temperature required for your process. As it is shown in **Figure 6(b)** depending on

Application	Collector
Solar water heating (temp range ≈ 90°C)	LFR PTC
Space heating and cooling (temp range ≈ 90°C)	LFR PTC PD
Solar refrigeration (temp range ≈ 150–200°C)	LFR PTC PD
Industrial process heat (temp range ≈ 80–240°C)	LFR PTC PD
Solar desalination (temp range ≈ 100°C)	LFR PTC PD
Solar thermal power systems (temp range ≈ 800–2000°C)	PD ST SF
High performance experiment like melting tungsten (temp range ≈ 3000°C)	PD SF

Table 5. Solar energy applications and type of collectors used [9].

http://dx.doi.org/10.5772/intechopen.72188

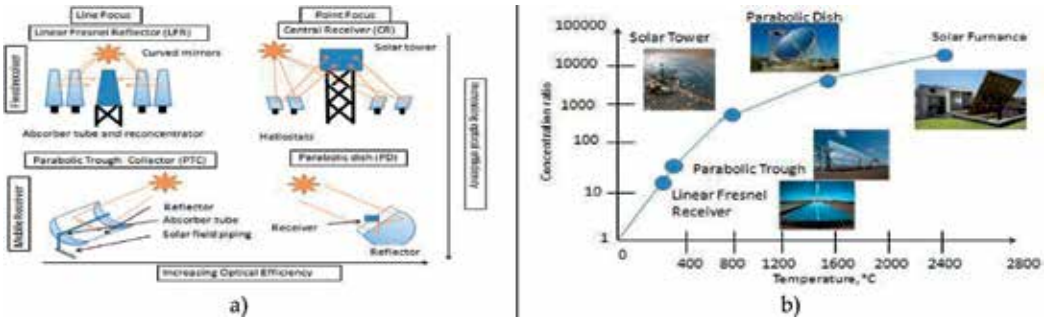

Figure 6. (a) Solar thermal energy technologies and (b) concentration ratio of STT [6].

your temperature range, it can be possible to select one of them. For example, if the project wants to transform solar energy into solar water heating with a range of 90°C, the possible technologies to use will be LFR and PTC.

The last aspect to take into account is the heat transfer fluid selection. This fluid is critical for storing and transferring thermal energy and can be used to directly drive a turbine to produce power or more commonly, be combined with a heat exchanger and secondary cycle to generate steam. Desired characteristics include [49]:

- Low melting point.
- High boiling point and thermal stability.
- Low vapor pressure (lower than 1 atm) at high temperature.
- Low corrosion with metal alloys used to contain *HTF*.
- Low viscosity.
- High thermal conductivity.
- High heat capacity for energy storage.
- Low cost

The HTFs can be divided into six main groups, according to the type of material [49]:

- *Air and other gases*. It is not common. However, the very low dynamic viscosity compared to the one of molten salts gives good flow that favors the heat transfer and may compensate its low thermal conductivity.
- *Water/steam*. They present corrosion problems and imply high operating pressures and complex controls for plant operation.
- *Thermal oils*. Mainly in PTC. There are three types: mineral oil, silicone oil, and synthetic oil and can be thermally stable only up to 400 °C. They have high cost.

- *Organics*. The most common are biphenyl/diphenyl oxide, which is a mixture of biphenyl ($C_{12}H_{10}$) and diphenyl oxide ($C_{12}H_{10}O$).
- *Molten salts*. They have stability at high temperature (greater than 500 °C); they also have properties comparable to water at high temperature, such as viscosity and low vapor pressure. Most of them are based on nitrates/nitrites, but salt production is restricted.
- *Liquid metals*. They have promising properties such as extensive operating temperature range, low viscosity, and efficient heat transfer characteristics. As a reference, liquid sodium has an operating temperature range between 98°C and 833°C.

7. Comparison of the environmental performance of a solar air-conditioning system vs a conventional electrical system, using LCA

Nowadays, the topic of global warming has become a top trending around the world. Life cycle assessment (LCA) was created in 1960. It is a tool to evaluate the environmental impacts and is an instrument to help take decisions, ecodesign, and comparative of alternatives. This section shows a comparasion of environmental performance of air-conditioning absorption system with conventional air-conditioning system by LCA according to international laws ISO 14040 and ISO 14044.

7.1. The solar system description

The air-conditioning absorption solar system (*ACASS*) considered for this study is installed as a prototype on the Research Center in Engineering and Applied Sciences (CIICAp) of the Autonomous University of the State of Morelos (UAEM), located in Cuernavaca, Mexico, with a warm subhumid climate. In this place, March, April, and May are the warmest months during the year, thus the required demand of air-conditioning increases, with an average per day solar radiation of 7.31, 6.85, and 6.16 kWh/m^2, respectively [54].

The capacity of *ACASS* installed is 17.6 kW such as providing air-conditioning for five offices. The design temperature average was proposed around 23°C, which is considered the comfort temperature. The system will be employed from Monday to Friday, during March to May, with a schedule from 11:00 to 16:00.

A plant of cylindrical-parabolic collectors that generate 26.44 kW was installed to drive the cycle, and 12 photovoltaic panels have been coupled to ACASS to generate 1.89 kW and supply electrical energy to the auxiliary devices that require it, covering 98.9% of the demand. Twenty-five years was considered as the useful period, according to the literature review [55].

7.2. Conventional air-conditioning system

This study considers a window-type conventional air conditioning (CAC) of 3.52 kW of capacity, and average energy demand is 1300 W. The operations conditions and useful life are considered for both systems; therefore, 12.5 units of 39.34 kg in average was evaluated. These units have a lifespan of 10 years according to the literature review [56].

http://dx.doi.org/10.5772/intechopen.72188

7.3. Life cycle assessment

According to the international standards ISO 14040 and 14044, LCA is defined as the assessment of the environmental impacts associated with a product, process, or service throughout their life cycle, tied in closely with the paradigm of "cradle to grave." This methodology consists of four phases, which can cross-interact at any point of the assessment, as shown in **Figure 7**.

7.3.1. Phase 1: objectives and scope definition

At this phase, it is important to fully understand the system under consideration and then be able to define the objectives and scope of the analysis. The functional unit and the system limitations are defined during this phase. The functional unit will allow to compare the two different systems based on a common function.

Therefore, the following aspects are defined at this phase for the case study:

- Objective: to compare the environmental performance between a ACASS system and a CAC system, in terms of CO_2 equivalent (CO_2eq).
- Scope: the stages of construction and operation are analyzed. The end-of-life stage is not considered in this study; however, it can be anticipated that this stage can lead to avoid impacts if a good final disposal scenario is proposed based on the recycling of the components, and this scenario would be a greater advantage for ACASS for ACS for the amount of material.
- System limitations: the construction stage will cover the material inputs, the energy consumption during the assembly of main components, and the transport of materials up to the construction site.

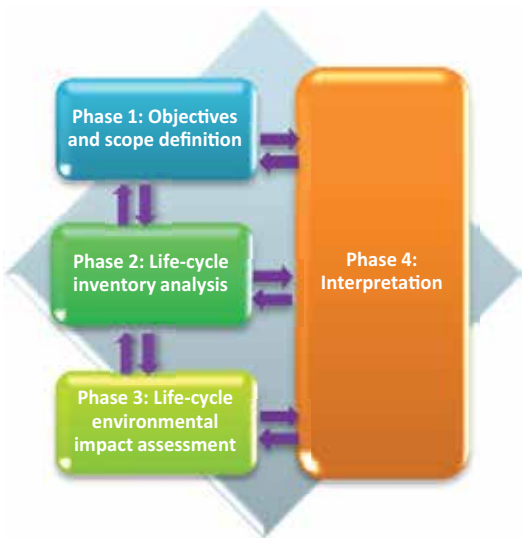

Figure 7. Life cycle Assessment phases.

- System function: to provide thermal comfort for five spaces of a ton of refrigeration each one.
- Functional unit: the total amount of refrigeration produced throughout the useful life of the system.

7.3.2. Phase 2: life cycle inventory analysis

During this phase, data are compiled for the inventory of the system at issue. For this analysis, the life cycle inventory (LCI) of the ACASS system is obtained from primary sources. The information was directly quantified on site, and some data are obtained from suppliers, some assumptions have also been made in the absence of some data, such as the type of transport used. For the LCI of the CAC system, the material content and percentages have been taken from the literature [57], suited to the requirements of the analysis. For the use stage, the equipment maintenance, part replacement, and electrical energy consumption are taken into consideration.

7.3.3. Phase 3: life cycle environmental impact assessment

LCA software is used at this phase for assessing the environmental impact of the systems. In this case, SimaPro™ PhD 8.3.0.3 is used for the case study. The assessment method considered in this analysis is the Intergovernmental Panel on Climate Change (IPCC) 2007 GWP 100 years, which only includes the impact category of global warming potential (GWP).

7.3.4. Phase 4: interpretation

A summary of the results and the corresponding discussion are carried out, and the final conclusions and recommendations are produced according to the results. In **Figure 8**, the ACASS system presents a reduction in CO_2e emissions of 77.34% compared with the CAC system, during the analyzed life cycle stages. In addition, employing the ACASS system also contributes to mitigate the environmental impacts due to the use of renewable solar energy. **Figure 9** shows the percentage of CO_2eq emissions at each life cycle stage for both

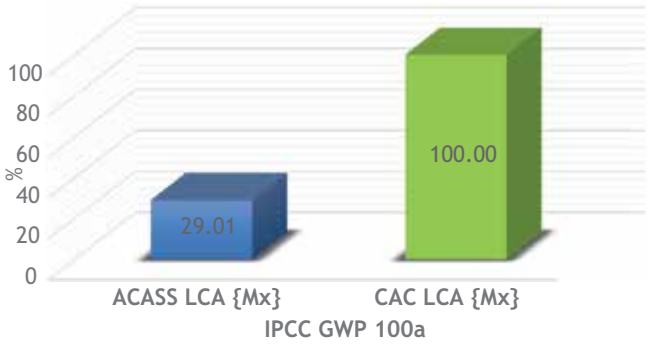

Figure 8. Total percentage of CO_2e emissions for the ACASS system compared against the CAS system at the stages of construction and operation.

http://dx.doi.org/10.5772/intechopen.72188

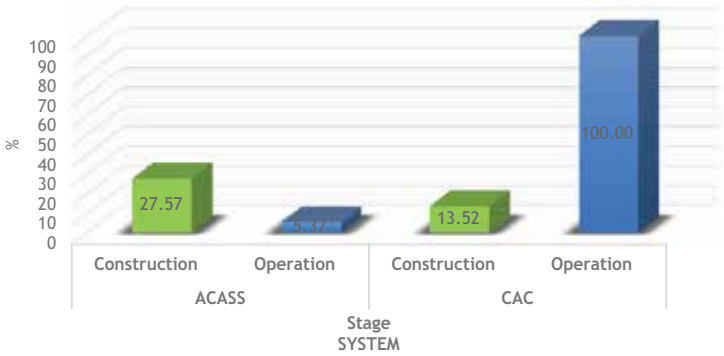

Figure 9. Percentage of CO_2eq emissions at each life cycle stage for both air-conditioning systems.

air-conditioning systems. The operation stage of the CAC system presents the highest CO_2eq emissions due to consumption of fossil fuel energy, while the ACASS system emits only 5.37% of the emissions at this stage.

During the construction stage, ACASS presents 14.05% higher CO_2eq emissions than the CAC system. This is attributed mainly to the difference in infrastructure demand for the construction of each system, and ACASS demands 79.20% more than CAC. It is important to note that the analysis is carried out considering 25 years of air-conditioning.

According to the results, it can be concluded that the ACASS system reduces greenhouse gas emissions due to lower consumption of fossil fuel energy. Therefore, for geographical regions where enough solar energy is available, the implementation of ACASS systems is a viable option for mitigating the environmental impacts related to global warming.

The high initial investment of the ACASS system might represent a barrier for its market, but it is necessary to continue working on the improvement of this type of systems, leading toward a massive production and aiming to reduce costs. As well, the intervention of decision makers is relevant to facilitate and incentivize the development of this kind of clean technologies.

8. Parameterized cost

Energy devices are expensive caused for the bin number of small parts to become a single product. In the air-conditioning systems, the parts for a roof device are based on three sections: solar concentrators, thermodynamic cycle part, and auxiliary system part.

Population in general has no money for investment for the energy consumption for the next 20 years to pay now. Then financial is the key for the installation for renewable energy systems.

A first approach to the cost of the entire air-conditioning system is based on the area of solar incident energy. The buildings have large area, but only the roof is useful for installation, but the thermal gain from wall and window is bigger than the size the roof solar-collected energy.

Then, the strategy for a quick viability evaluation is to evaluate the available solar roof in square meters and compare it with the value for required air-conditioning expressed in kW. If this value ratio is close to 1, then a detailed analysis for selection of the parts must be followed, if the value is lower than 0.5, then there is no opportunity for this roof technology because the solar loads and wall conduction are bigger than the total energy than a solar roof air conditional can exchange.

8.1. Solar concentrator system cost

There are some parts in the solar concentrator, which determines the total cost of this part. Installation is the biggest part [58], and it represents 38% of the investment, followed by storage thermal tank with a 24% of the total cost, and just a 14% from the solar thermal collector. The others are the cost from pipes with a 8%, thermal fluid with a 1%, pumping and controller 8% and fixing and mounting with a 7% (**Figure 10**).

8.2. Thermodynamic cycle cost

For the air-conditioning systems, there are just a few certified companies to build these devices. People have lack of information about the uncommercial devices. Considering than a conventional air-conditioning by compression is based on an evaporator, a condenser and a compressor, two of those heat exchangers are the same for an absorption cycle, but the metal is so different. In compression systems, aluminum and copper are used for the cycle. In an absorption cycle, the metal for the heat exchanger is stainless steel to avoid corrosion problems. This is a disadvantage for the cost because the cost of the stainless steel is higher than copper. Nowadays, the SS 304 has an average price about 1.62 USD by pound; aluminum has an almost constant price about 1.58 USD by pound, and copper has unstable price around 2.87 USD by pound.

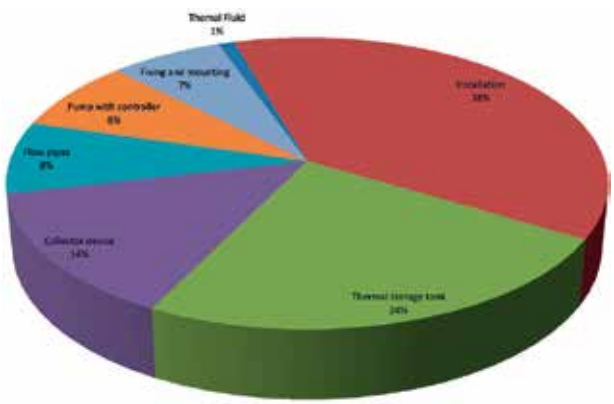

Figure 10. Cost for solar concentrator parts.

The heat exchanger areas are not the same for copper, aluminum or stainless steel because the thermal conductivity is quite different: copper is 386 W/mK, aluminum is 204 W/mK, and SS is 45 W/mK. This means that the thermal conductivity of the stainless steel is nine times lower than the copper.

Therefore, the four heat exchanger for the thermodynamic cycle must be costly, compared with a conventional compression air-conditioning, about 4.5 times the cost, based on the thermal conductivity and the cost today.

8.3. Auxiliary systems

The auxiliary systems are the installation and control between the solar concentrator and the thermodynamic cycle. The cost is based on the electronic device to control the pump as function of temperature, solar irradiation, and the instantaneous load into the building. The design is not commercial today, but it is not expensive because the energy for the operation has shown consumption about 1% of the total system by connection with inversed devices and solid-state circuits. The controller must be designed for the power of the pumps, those into the thermodynamic cycle and a circulator in the solar concentrator on the roof.

Electronic devices are really cheap based on Arduino © experiences, and these represent no more than 300 USD, and installation by a professional technician must be considered and the time for the installation by several hours may be expensive, as function of the building location, security conditions, roof access facilities. Then, in agree with the local cost by specialist cost hour, the auxiliary system may represent even a 30% of the installation device cost.

Finally, the total cost must be under a projected value for the lifetime of the roof air-conditioning system. This means that the cost must be compared with a cost for the actual technology and the total cost, for example, a storage tank of 243 L used by day into the roof air-conditioning system by the next 12 years [59] (**Figure 11**).

In the near future, the air-conditioning must be by solar, from the roof energy from thermal, photovoltaic, or a combination of those [60].

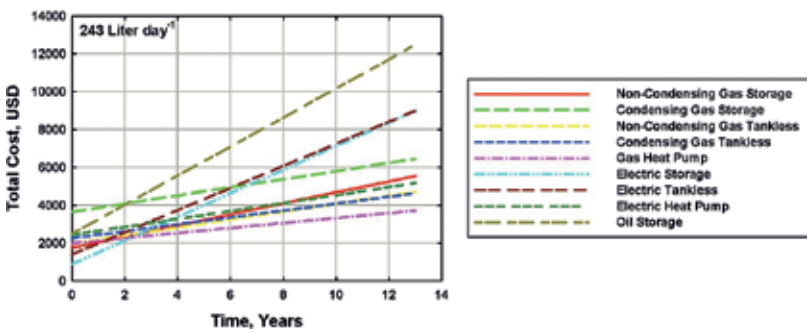

Figure 11. Total cost with actual technologies for air-conditioning [59].

9. Conclusions

This chapter shows a thermal load quantities based on physical values for a typical central Mexico location. The values for the home areas are common in the actual sizes for medium-prized houses for Temixco location. A conclusion for this scenario is that the medium-prized houses must have 4.2 kN/m^2 in weight capacity for a secure installation of solar roof facilities.

There are two aqueous solutions candidates to operate solar air-conditioning for roof applications: aqueous lithium bromide and aqueous hydroxides. Based on the working pair selection, the size for the heat exchanger must be defined by following the given methodology.

The solar devices are selected as function of the temperature and final use. These temperature values are higher than 90°C. The entire system (heat exchanger and solar devices) was evaluated just in operation phase and compared with a conventional air-conditioning system for 3.52 kW. The life cycle assessment concluded that in construction phase, the solar system is twice the emission in CO_2eq, but in operation phase, the CO_2eq is just 5.37% compared with the electrical device.

Acknowledgements

The authors are grateful to CEMIE-SOL-P09 for partial support. J. Ibarra-Bahena is thankful for the DGAPA-UNAM Postdoctoral Fellowship and Red Temática Sustentabilidad Energética Medioambiente y Sociedad.

Nomenclature

A	area, m^2
Cp	specific heat at constant pressure, kJ kg^{-1}K^{-1}
C	heat capacity flow rate, kJ s^{-1} K^{-1}
H	enthalpy, kJ kg^{-1}
m	mass flow rate, kg s^{-1}
Q	heat load, kW
R	heat capacity ratio, dimensionless
T	temperature, °C
U	overall heat transfer coefficient, kW m^{-2} K^{-1}
W	mechanical work, kW

http://dx.doi.org/10.5772/intechopen.72188

Subscripts

AB	absorber
CO	condenser
c	cold fluid
EV	evaporator
GE	generator
h	hot fluid
i	inlet condition
m	mean condition
min	minimum
max	maximum
o	outlet condition
p	pump
s	surface condition

Greek symbols

ε	effectiveness, dimensionless
φ	convective heat transfer coefficient, $Wm^{-2}°C^{-1}$

Author details

Yuridiana Rocio Galindo Luna[1], Rosenberg Javier Romero Domínguez[2]*, Jonathan Ibarra Bahena[3], Moises Montiel González[4], Jesús Cerezo Román[2], José Eduardo Jasso Almazán[1], Antonio Rodríguez Martínez[2], Karina Solano Olivares[1], Ana María Hernández Jasso[4], Sotsil Silva Sotelo[2], José Antonio García Ramos[4], Ariana Morales Flores[4] and Brenda Rivas Herrea[4]

*Address all correspondence to: rosenberg@uaem.mx

1 Posgrado en Ingeniería y Ciencias Aplicadas, Universidad Autónoma del Estado de Morelosdad, Cuernavaca, Morelos, México

2 Centro de Ingeniería y Ciencias Aplicadas, Universidad Autónoma del Estado de Morelos, Cuernavaca, Morelos, México

3 Instituto de Energías Renovables, Universidad Nacional Autónoma de México, Temixco, Morelos, México

4 Facultad de Ciencias Químicas e Ingeniería, Universidad Autónoma del Estado de Morelos, Cuernavaca, Morelos, México

References

[1] Gomri R. Investigation of the potential of application of single effect and multiple effect absorption cooling systems. Energy Conversion and Management. 2010;**51**(8):1629-1636. DOI: 10.1016/j.enconman.2009.12.039

[2] Rodriguez Hidalgo MC, Rodriguez AP, Izquierdo MM, Lecuona NA, Salgado MR. Energy and carbon emission savings in Spanish housing air-conditioning using solar driven absorption system. Applied Thermal Engineering. 2008;**28**(14-15):1734-1744. DOI: 10.1016/j.applthermaleng.2007.11.013

[3] Sozen A, Ozalp M, Arcaklioğlu E. Prospects for utilisation of solar driven ejector-absorption cooling system in Turkey. Applied Thermal Engineering. 2004;**24**(7):1019-1035. DOI: 10.1016/j.applthermaleng.2003.11.011

[4] Casals XG. Solar absorption cooling in Spain: Perspectives and outcomes from the simulation of recent installations. Renewable Energy. 2006;**31**(9):1371-1389. DOI: 10.1016/j.renene.2005.07.002

[5] Schmitt H. Enciclopedia de la construccion-2 techos o pisos, escaleras, balcones y terrasas, estructuras de las obras. Barcelona, España: Editorial Gustavo Gili, 1990

[6] Gonzalez C. Analisis estructural. Mexico, Mexico: Editorial Limusa; 2003

[7] Daut I, Adzriea M, Irwantoa M, Ibrahima P, Fitraa M. Solar powered air conditioning system. Energy Procedia. 2013;**36**:444-453. DOI: 10.1016/j.egypro.2013.07.050

[8] Kalkan N, Young EA, Celiktas A. Solar thermal air conditioning technology reducing the foot print of solar thermal air conditioning. Renewable and Sustainable Energy Reviews. 2012;**16**:6352-6383. DOI: 10.1016/j.rser.2012.07.014

[9] Otanicar T, Taylor RA, Phelan PE. Prospects for solar cooling—An economic and environmental assessment. Solar Energy. 2012;**86**:1287-1299. DOI: 10.1016/j.solener.2012.01.020

[10] Brumana G, Franchini G. Solar-powered air conditioning for buildings in hot climates: Desiccant evaporative cooling vs. absorption chiller-based systems. Energy Procedia. 2016;**101**:288-296. DOI: 10.1016/j.egypro.2016.11.037

[11] Perez- Blanco H. Absorption heat pump performance for different types of solutions. International Journal of Refrigeration. 1984;**7**(2):115-122. DOI: 10.1016/0140-7007(84)90024-0

[12] Srikhirin P, Aphornratana S, Chungpaibulpatana S. A review of absorption refrigeration technologies. Renewable and Sustainable Energy Reviews. 2001;**5**:343-372. DOI: 10.1016/S1364-0321(01)00003-X

[13] Sun J, Fu L, Zhang S. A review of working fluids of absorption cycles. Renewable and Sustainable Energy Reviews. 2012;**16**:1899-1906. DOI: 10.1016/j.rser.2012.01.011

[14] Abdelmessih AN, Abbas M, Al-Hashem A, Munson J. Ethylene glycol/water as working fluids for an experimental absorption cycle. Experimental Heat Transfer: A Journal of Thermal Energy Generation, Transport, Storage, and Conversion. 2007;**20**(2):87-102. DOI: 10.1080/08916150601091373

[15] Katzow A. Refrigerating system. U.S. Patent No. 2,497,819; 1950

[16] Kumm EL. Solar powered air conditioning system employing hydroxide water solution. U.S. Patent No. 4,151,721; 1979

[17] Erickson DC. Water vapor absorbent containing cesium hydroxide. U.S, Patent No. 4,614,605; 1986

[18] Herold KE, Radermacher R, Howe L, Erickson DC. Development of an absorption heat pump water heater using an aqueous ternary hydroxide working fluid. International Journal of Refrigeration. 1991;**14**:156. DOI: 10.1016/0140-7007(91)90070-W

[19] Romero RJ, Rivera W, Best R. Comparison of the theoretical performance of a solar air conditioning system operating with water/lithium bromide and an aqueous ternary hydroxide. Solar Energy Materials and Solar Cells. 2000;**63**:387-399

[20] Olsson J, Jernqvist A, Aly G. Thermophysical properties of aqueous NaOH-H_2O solutions at high concentrations. International Journal of Thermophysics. 1997;**18**(3):779-793

[21] Balej J. Water vapour partial pressures and water activities in potassium and sodium hydroxide solutions over wide concentration and temperature ranges. International Journal of Hydrogen Energy. 1985;**10**(4):233-243

[22] Akfcrlof G, Bender P. The density of aqueous solutions of potassium hydroxide. Journal of the American Chemical Society. 1941;**63**(4):1085-1088

[23] Biermann WJ. The relative enthalpies of concentrated potassium hydroxide solutions. Canadian Journal of Chemistry. 1960;**38**:57-60

[24] Ginzburg DM, Kochkalda VE, Guba NI. Enthalpies and heat capacities in the potassium hydroxide-water system. Russian Journal of Physical Chemistry. 1973;**47**:1214

[25] Kelly WR, Borza PF, Harriger RD. Densities and viscosities of potassium hydroxide solutions at low temperatures. Journal of Chemical & Engineering Data. 1965;**10**(3):233-234

[26] IEA Heat Pump Centre, Compact Heat Exchangers in Heat Pumping Equipment (2010). www.heatpumpcentre.org Report No. HPP-AN33-1, Borås, Sweden

[27] Marcos JD, Izquierdo M, Lizarte R, Palacios E, Infante Ferreira CA. Experimental boiling heat transfer coefficients in the high temperature generator of a double effect absorption machine for the lithium bromide/water mixture. International Journal of Refrigeration. 2009;**32**:627-637. DOI: 10.1016/j.ijrefrig.2009.02.003

[28] De Vega M, Almendros-Ibañez JA, Ruiz G. Performance of a LiBr–water absorption chiller operating with plate heat exchangers. Energy Conversion and Management. 2006;**47**:3393-3407. DOI: 10.1016/j.enconman.2006.01.005

[29] Cerezo J, Best R, Romero RJ. A study of a bubble absorber using a plate heat exchanger with NH_3-H_2O, NH_3-$LiNO_3$ and NH_3-NaSCN. Applied Thermal Engineering. 2011;**31**: 1869-1876. DOI: 10.1016/j.applthermaleng.2011.02.032

[30] Flamensbeck M, Summerer F, Riesch P, Ziegler F, Alefeld G. A cost effective absorption chiller with plate heat exchangers using H_2O and hydroxides. Applied Thermal Engineering. 1998;**18**:413-425. DOI: 10.1016/S1359-4311(97)00049-5

[31] Ochoa AAV, Dutra JCC, Henríquez JRG, Dos Santos CAC. Dynamic study of a single effect absorption chiller using the pair LiBr/H_2O. Energy Conversion and Management. 2019;**108**:30-42. DOI: 10.1016/j.enconman.2015.11.009

[32] She X, Yin Y, Xu M, Zhang X. A novel low-grade heat-driven absorption refrigeration system with LiCl-H_2O and LiBr-H_2O working pairs. International Journal of Refrigeration. 2015;**58**:219-234. DOI: 10.1016/j.ijrefrig.2015.06.016

[33] Gu Y, Wu Y, Ke X. Experimental research on a new solar pump-free lithium bromide absorption refrigeration system with a second generator. Solar Energy. 2008;**82**:33-42. DOI: 10.1016/j.solener.2007.05.001

[34] Xie G, Wu Q, Fa X, Zhang L, Bansal P. A novel lithium bromide absorption chiller with enhanced absorption pressure. Applied Thermal Engineering. 2012;**38**:1-6. DOI: 10.1016/j.applthermaleng.2011.12.047

[35] Saravanan R, Maiya MP. Thermodynamic comparison of water-based working fluid combinations for a vapour absorption refrigeration system. Applied Thermal Engineering. 1998;**18**:553-568. DOI: 10.1016/S1359-4311(97)00072-0

[36] Yilmaz IH, Saka K, Kaynakli O. A thermodynamic evaluation on high pressure condenser of double effect absorption refrigeration system. Energy. 2016;**113**:1031-1041. DOI: 10.1016/j.energy.2016.07.133

[37] Xu ZY, Wang RZ, Wang HB. Experimental evaluation of a variable effect LiBr–water absorption chiller designed for high-efficient solar cooling system. International Journal of Refrigeration. 2015;**58**:219-234. DOI: 10.1016/j.ijrefrig.2015.07.019

[38] Shah RK, Mueller AC. Heat exchangers. In: Rohsenow WM, Hartnett JP, Ganic EN, editors. Handbook of Heat Transfer Applications. New York: McGraw-Hill; 1989. pp. 1-32 (Chap. 4)

[39] Zaleski T, Klepacka K. Plate heat echangers-method of calculation, charts and guidelines for selecting plate heat exchanger configurations. Chemical Engineering and Processing: Process Intensification. 1992;**31**(1):49-56. DOI: 10.1016/0255-2701(92)80008-Q

[40] Ismail T, Özden A, Hakan D, Özgür Atayilmaz S. Zising, selection, and comparison of heat exchanger considering the lowest saving-investment ratio corresponding to the area at the tag and of the heat exchanger. Energy. 2014;**78**:114-121. DOI: 10.1016/j.energy.2014.08.035

[41] Incropera FP, Dewitt DP, Bergman TL, Lavine AS. Fundamentals of the Heat and Mass Transfer. John Wiley &Sons. Inc., New York;2007. pp. 670-70

[42] Abu-Khader MM. Plate heat exchanger: Recent advances. Renewable and Sustainable Energy Reviews. 2012;**16**:1883-1891. DOI: 10.1016/j.rser.2012.01.009

[43] Hermes JL. Thermodynamic design of condenser and evaporators: formulation and applications. International Journal of Refrigeration. 2013;**36**:633-640. DOI: 10.1016/j.ijrefrig.2012.10.032

[44] Thirugnanasambandam M, Iniyan S, Goic R. A review of solar thermal technologies. Renewable and Sustainable Energy Reviews. 2010;**14**:312-322. DOI: 10.1016/j.rser.2009.07.014

[45] Montagnino FM. Solar cooling technologies. Design, application and performance of existing proyects. Solar Energy. 2017;[S.V.]:[S.P.]. DOI: 10.1016/j.solener.2017.01.033

[46] Zhang J, Zhao L, Deng S, Xu W, Zhang Y. A critical review of the models used to estimate solar radiation. Renewable and Sustainable Energy Reviews. 2017;[S.V.]:[S.P.] DOI: 10.1016/j.rser.2016.11.124

[47] Labouret A, Villoz M. Energía solar fotovoltaíca "Manual práctico". España: Ed. A. Madridi Vicente y Mundi-Prensa; 2008. pp. 42-43

[48] Kalogirou SA. Solar thermal collectors and applications. Progress in Energy and Combustion Science. 2004;**30**:231-295. DOI: 10.1016/j.pecs.2004.02.001

[49] Roldán Serrano MI. Concentrating Solar Thermal Technologies, Analysis and Optimization by CFD Modeling. España: Springer; 2017. pp. 11-23 and 74-79

[50] Zhu Y, Shi J, Li Y, Wang L, Huang Q, Xu G. Design and thermal performance of a scalable linear Fresnel reflector solar system. Energy Conversion and Management. 2017;**146**: 174-181. DOI: 10.1016/j.enconman.2017.05.031

[51] Salgado Conrado L,Rodriguez-Pulido A, y Calderón G. Thermal performance of parabolic trough solar collectors. Renewable and Sustainable Energy Reviews. 2017;**67**: 1345-1359. DOI: 10.1016/j.rser.2016.09.071

[52] Hafez AZ, Soliman A, El-Metwally KA y Ismail IM. Solar parabolic dish Stirling engine system design, simulation and thermal analysis. Energy Conversion and Management. 2016;**126**:60-75. DOI: 10.1016/j.enconman.2016.07.067

[53] Lovegorve K, Stein W. Concentrating Solar Power Technology. Principles, Developments and Applications. USA: Elsevier; 2012. pp. 267-269

[54] Agencia Nacional de la Aeronáutica y del Espacio (NASA). Radiación incidente en la latitud N18.98 y longitud O99.23.[Estados unidos]. Recuperado el 18 de enero de 2017. https://eosweb.larc.nasa.gov/

[55] Beccali M, Cellura M, Longo S, Mugnier D. A simplified LCA tool for solar heating and cooling systems. Energy Procedia. 2016;**91**:317-324. DOI: 10.1016/j.egypro.2016.06.226

[56] Almutairi K, Thoma G, Burek J, Algarni S, Nutter D. Life cycle assessment and economic analysis of residential air conditioning in Saudi Arabia. Energy and Buildings. 2015;**102**:370-379. DOI: 10.1016/j.enbuild.2015.06.004

[57] Boustani A, Sahni S, Gutowski T, Graves S. Remanufacturing and energy savings. Environmental Science and Technology. 2011;**45**(10):4540-4547. DOI: 10.1021/es102598b

[58] Ramos Cabal A, Guarracino I, Mellor A, Alonso Álvarez D, Childs P, Ekins DN, Markides CN. Solar-thermal and hybrid photovoltaic-thermal systems for renewable heating. 2017:1-20. DOI: 10.13140/RG.2.2.10473.29280

[59] Keinath CM, Garimella S. An energy and cost comparison of residential water heating technologies. Energy. 2017;**128**:626-633. DOI: 10.1016/j.energy.2017.03.055

[60] Zhi Lim X. How heat from the Sun can keep us all cool. Nature. 2017;**542**:23-24. DOI: 10.1038/542023a

Chapter 4

Adsorption Refrigeration Technologies

Mahmoud B. Elsheniti, Osama A. Elsamni,
Raya K. Al-dadah, Saad Mahmoud,
Eman Elsayed and Khaled Saleh

Additional information is available at the end of the chapter

http://dx.doi.org/10.5772/intechopen.73167

Abstract

This chapter introduces a comprehensive overview about the principles, challenges and applications of adsorption refrigeration systems (ARSs), as a promising sustainable solution for many of cooling and heating applications. In addition to the features and the basics of ARSs, the following topics have been covered such as characteristics of working pairs, trends in improving the heat and mass transfer of the adsorber; advanced adsorption cycles and performance and operational data of some adsorption refrigeration applications. In some details, the operating range and the performance of ARSs are greatly affected by the employed working adsorbent/refrigerant pairs. Therefore, the study, development and optimum selection of adsorbent/refrigerant pairs, particularly the composite adsorbents, can lead to improving the performance and reliability of ARSs. Regarding the enhancement of heat and mass transfer in the adsorbent bed, two methods are commonly used: one is the development of adsorbents through different coating technologies or new materials such as metal-organic frameworks, and the second is the optimization of the adsorber geometrical parameters and cycle modes. Finally, a brief on some adsorption chillers applications have started to find their share in markets and driven by solar or waste heats.

Keywords: adsorption refrigeration, solar air conditioning, heat recovery, metal-organic frameworks, adsorbent bed

1. Introduction

Utilization of thermally driven refrigeration systems can reduce both direct and indirect emissions of the greenhouse gases and can contribute to a sustainable solution that meets

the escalating demand of the cooling equipment. The electrically driven refrigeration systems have high coefficients of performance (COP), low weights and small sizes compared to their current alternatives. However, they rely on a high-grade energy produced mostly from burning fossil fuels in thermal power plants and employ environmentally harmful refrigerants. Meanwhile, the increased demand of the electricity consumed by these refrigeration systems during the hot summer days leads to a considerable increase in the peak loads on the electricity grids causing increasing costs, blackouts and brownouts, and represents a great challenge in many of the developing countries. Thermally driven refrigeration technologies appear to be a promising alternative solution to limited energy resources and ecological problems. Such systems can utilize directly low-grade thermal energies or waste heat recovered from industrial processes, and use environmentally safe refrigerants as systems presented in [1]. The most interesting technologies are called 'sorption cooling systems' including desiccant, absorption and adsorption refrigeration systems (ARSs). Although the most cited drawbacks for sorption refrigeration systems are the high initial cost, heavy weight, large size, and the possible need for backup cooling systems, the benefits are nonetheless obvious [2]. They can employ natural substances as working fluids (water, ammonia, etc.), and use the available heat sources and clean energy more efficiently to produce refrigeration effect. For examples, burning fuels can be used directly to drive the sorption refrigeration systems; thereby the inefficiencies associated with the conversion of thermal energy to electricity and its transmission to the consumers can be eliminated. Solar refrigeration systems which offer the features of minimal operating cost, environmental preference, transforming solar energy directly into cooling power and maximum solar radiation are generally in phase with the peak demand of the cooling loads. Recovering the waste heats in industrial applications could improve the overall performance of such systems. Adsorption refrigeration systems (ARSs), one of these heat-driven systems, have a distinct advantage in their ability to be driven by relatively lower temperature heat sources as well as not involving any moving parts in the refrigerant cycle which means minimal maintenance and more durability. Nevertheless, there are two main drawbacks that limit their commercialization: the intermittently working principle (discontinuous cooling effect) and the low cycle COP. The latter is influenced by poor mass and heat transfer of the adsorbent bed, the heart of the cycle, which plays the role of compressor in conventional refrigeration cycles [3]. Historically, the earliest record of the adsorption phenomena for refrigeration purpose was introduced in 1848 by Faraday who found that the cooling capacity could be generated when silver chloride adsorbed ammonia. Compression refrigeration systems were developed starting from 1930s after Freon was developed. In the 1970s, the energy crisis took hold, and in the last four decades, the environmental impacts of conventional refrigeration systems had been recognized worldwide, which offered a great chance for the development of such ARSs. The objective of this chapter is to introduce a comprehensive overview about the principles, application and challenges of ARSs. In addition to the description of the basic adsorption system, the chapter covers the following topics such as characteristics and development of working pairs; trends in improving the heat and mass transfer of the adsorber; advanced adsorption cycles; and state of the art adsorption cooling applications.

http://dx.doi.org/10.5772/intechopen.73167

1.1. Basic adsorption refrigeration cycle

From the thermodynamics point of view, a basic adsorption refrigeration cycle can be considered as two separate cycles. One a heat engine and the other is a refrigerator (or heat pump), and operates with three temperature levels. It is assumed that the work produced by the heat engine is used to drive the refrigerator as illustrated in **Figure 1** [3].

$$COP_{ref} = \frac{Q_{eva}}{Q_{preheating} + Q_{des}} = \frac{1 - \left(\frac{T_I}{T_H}\right)}{\left(\frac{T_I}{T_L}\right) - 1} \quad (1)$$

The basic ARS consists of four main components: an adsorbent bed, which contains highly porous bodies called *adsorbent* with tremendously large internal surface (such as silica gel, activated carbon, zeolite, etc.) having strong adsorptive property to a specified gas or gases called *adsorbate/refrigerant* (such as water, ammonia, methanol, etc.). The adsorbent is normally packed on a metal surface which is required to conduct the heat transferred from/to a heat transfer fluid (HTF) (usually by heating and cooling water) that flows in the bed. The other 3 cycle components are: a condenser, an evaporator and an expansion valve. They are similar to those normally used in a simple conventional refrigeration cycle and play the same roles with an electrically driven compressor, so that the adsorbent bed is called a thermally driven compressor which circulates the refrigerant in an adsorption cycle by periodical switching between heating and cooling HTFs. The Carnot COP of a basic ARS can be expressed as Eq. (1) [4]:

A simple adsorption refrigerator produces cooling effect by subjecting the adsorbent bed to four sequential processes which are pre-heating, desorption, pre-cooling and adsorption as shown in **Figure 2**. Clapeyron diagram (LnP vs. −1/T) with respect to isosteres of adsorbent-adsorbate pair in **Figure 3** is typically used to illustrate the four ideal thermodynamic processes of an adsorbent bed and calculate the cycle COP theoretically. In this ideal cycle, the

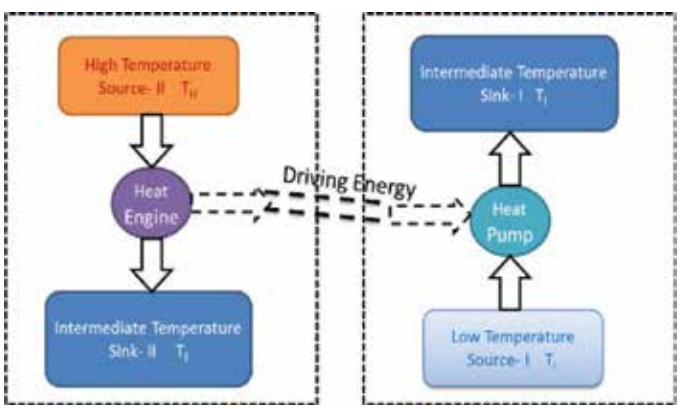

Figure 1. Representation of the thermodynamics cycle of ideal ARS.

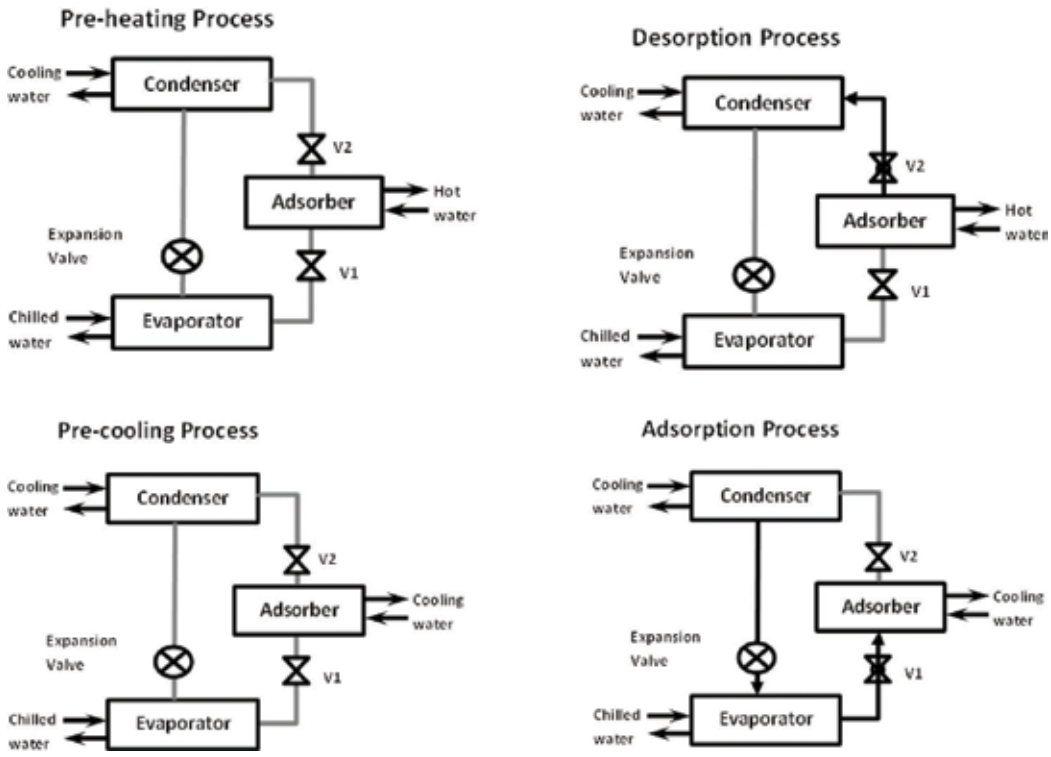

Figure 2. The flow diagrams of the basic adsorption cooling system under one complete cycle.

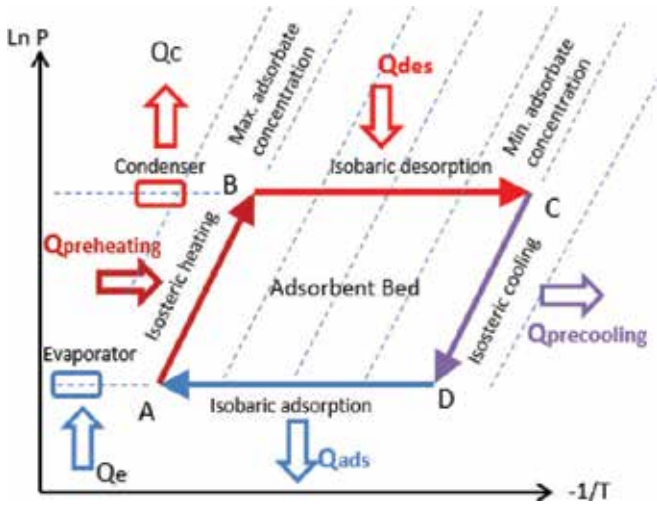

Figure 3. Clapeyron diagram of an ideal adsorption refrigeration cycle.

adsorber (adsorbent bed) operates between the two constant pressures, the condenser and evaporator pressures, and the two (minimum and maximum) adsorbate concentration levels. These four ideal processes can be described as follows:

Pre-heating process (A–B): In this heating and pressurization period, the valves between the adsorbent bed and both of the condenser and the evaporator (V1 and V2) are closed, and the adsorbent bed is operated as a closed system that is subjected to heat source at temperature of T_H by means of heating HTF. Meanwhile, the bed temperature increased sensibly which induces the vapor pressure inside the bed also to be increased. Whereas, the total amount of refrigerant in adsorbed phase remains constant at the maximum concentration. This process lasts until the vapor pressure reaches the condenser pressure at point B.

Desorption process (B–C): After the first process, the heating of the adsorbent bed is continued while the valve (V2) connecting the bed with the condenser is opened. The bed temperature is gradually increased, which induces a part of refrigerant which is in adsorbed phase to leave the solid surface of adsorbent to be in a vapor phase in a process called 'desorption process'. Then this desorbed vapor flows into the condenser and condenses there. The vapor pressure in the bed is considered equal to the condenser pressure during this period which is ended when the adsorbed amount reaches the minimum concentration level.

Pre-cooling process (C–D): After the bed reaches the maximum temperature in the cycle at point C, the cooling and depressurization period for the bed is stared, and the two valves (V1 and V2) are set closed. The temperature is then decreased which induces the pressure inside the adsorber to be reduced to the evaporator pressure level by the end of this process.

Adsorption process (D–A): In the last period in which only the effective cooling occurs, the valve between the adsorber and the evaporator is opened, and the adsorber is continuously subjected to cooling by means of cooling HTF which induces an adsorptive vapor to accumulate on the adsorbent surface and converted to a new phase called 'adsorbed phase' in a process named 'adsorption process'. Then, the vaporized vapor in the evaporator, which gives the cooling effect, is directed to the adsorber to take place in the adsorptive vapor. Cooling for the adsorbent bed is required in this process to release the associated heats from both the heating period and the adsorption process.

1.2. Performance indicators

The average cooling capacity Q_{eva}, heat added Q_{heat}, SCC and COP can be defined for an adsorption refrigeration chiller as follows:

$$Q_{eva} = \frac{1}{t_{cycle}} \int_0^{t_{cycle}} \dot{m}_{chw}\, c_{chw} \left(T_{chw,i} - T_{chw,o}\right) dt \tag{2}$$

$$Q_{heat} = \frac{1}{t_{cycle}} \int_0^{t_{cycle}} \dot{m}_{hw}\, c_{hw} \left(T_{hw,i} - T_{hw,o}\right) dt \tag{3}$$

$$SCC = \frac{Q_{eva}}{M_s} \tag{4}$$

$$COP = \frac{Q_{evap}}{Q_{heat}} \tag{5}$$

where M_s is the total amount of adsorbent packed in the adsorbers.

2. Working adsorbent/refrigerant pairs

The overall performance as well as the design and operating parameters for an ARS are greatly affected by the employed working adsorbent/refrigerant pairs. In general, good adsorbents should have wider range of adsorption capacity with temperature variation, higher heat and mass transfer properties, along with thermal stability and low susceptibility to contamination. In addition, distinctive properties of a refrigerant should be examined, and that include heat of vaporization, thermal conductivity, boiling point and working pressures, reactivity and stability, toxicity, environmental impact and freezing point. The adsorption capacity of an adsorbent-refrigerant pair is commonly determined from plots known as adsorption isotherms as shown in **Figure 4** [5]. These isotherms give the amount of adsorbed mass taken up by the adsorbent, after reaching the thermodynamic equilibrium, as a function of pressure at constant temperatures. Accordingly, adsorbent-adsorbate pairs and their developments can be compared based on their isotherms. However, when the adsorbent domain undergoes transient operating conditions, a kinetic model is required to define the mass transfer kinetics and gives the instantaneous amount of adsorbate through a relation with the equilibrium uptake that is given by the isotherms. Mass transfer kinetics is a catch-all term related to intraparticle mass transfer resistance. The increase in the adsorption capacity increases capability of an ARS to have a large cooling capacity, where it sets up the total amount of refrigerant that can be adsorbed in a cycle. However, faster mass transfer kinetics is required to insure higher cooling capacity as it controls the duration of the adsorption cycle.

The most commonly used adsorbent/refrigerant pairs are silica gel/water, zeolite/water, activated carbon/methanol, activated carbon/ammonia, calcium chloride/ammonia and composite adsorbent/ammonia. In general, according to the nature of the forces involved in the adsorption process, they are classified into three categories such as physical, chemical and composite adsorbent/adsorbate pair.

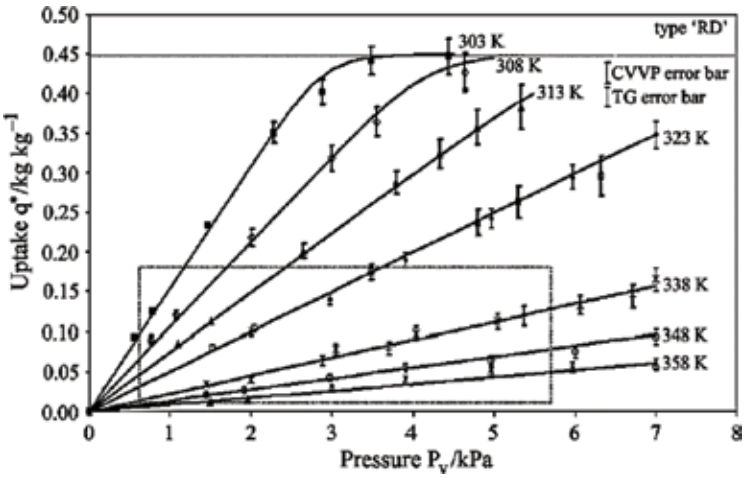

Figure 4. Isotherms for type RD silica gel-water pair [5].

2.1. Physical adsorbent-adsorbate pair

The physical adsorbents that are used in ARSs rely on van der Waal's forces to contain adsorbate. Three adsorbent-adsorbate pairs are generally considered to be the best available in applications:

2.1.1. Silica gel-water systems

Silica gel is an amorphous silicon dioxide, SiO_2, made synthetically from sodium silicate, and has a granular, vitreous and highly porous form. The high-density silica is the common type of silica gel used in adsorption systems such as Fuji Davison types 'A' and 'RD' silica gel, which have pore diameter in the range of 2.0–3.5 nm, the pore volume is 0.3–0.4 cm^3/g and the specific surface area is 400–700 m^2/g [6]. The other types of silica gel with relatively high pore sizes can be used as a host material in composite adsorbents. The thermodynamics characteristics of silica gel-water working pair were investigated experimentally by several researchers as in [5, 7], and the empirically determined parameters for the isotherm equations had been calculated from the experimental data. The performance of the two-bed silica gel-water was evaluated experimentally and analytically by several researchers [8–10].

In general, the main advantage of silica gel over other adsorbents is that the regeneration temperature is typically 85°C which makes such system to be suitable for solar energy use and low temperature waste heat sources. Moreover, it could be as low as 50°C when multi-stage configuration system is applied [11]. In such case, for non-regenerative cycle, the dynamic losses due to the heat capacities of the adsorber components will be reduced which lead to higher COPs since the adsorbent itself and the container vessel do not need to be heated to high temperatures. However, desorption temperature must not be too high. If it is higher than 120°C, silica gel will be destroyed. The adsorption heat is relatively higher than activated carbon pair between 2500–2800 kJ/kg. Also, silica gel porosity level is lower than activated carbon (100–1000 m^2/g). The maximum adsorption capacity at equilibrium could be between 0.35 and 0.4 kg/kg silica gel, while the net change in the instantaneous amount of adsorbate may not exceed 0.1 kg water/kg silica gel under typical operating conditions which is low. Another drawback is the limitation of evaporating temperature due to the freezing point of water and the uptake also is effected badly under a very low vacuum, that make silica gel-water refrigeration system be better to be applied in the air conditioning applications with large chilled water flow rates.

2.1.2. Zeolite-water systems

Zeolites are microporous, alumina silicate crystals composed of alkali or alkali soil. The zeolite-water working pair has a wide range of desorption temperature (70–250°C). Due to its stable performance at high temperatures, the adsorber can be directly heated by the exhaust gases from engines. Therefore, the zeolite-water system is simpler than that one driven by the hot water. However, the adsorption heat of zeolite-water is higher than that of silica gel-water, between about 3300 and 4200 kJ/kg [12], which will lead to low COPs, in addition to the drawbacks associated with using the water as a refrigerant. Several studies had been

presented experimentally and theoretically to investigate and improve the performance of zeolite-water adsorption system particularly for vehicle air conditioning.

2.1.3. Activated carbon (ammonia/methanol) systems

Activated carbon is a form of carbon that has a large specific area available for adsorption approximately between 800 and 1500 m^2/g for most used carbon. Initially, raw materials such as coal, lignite, wood, nut shells and synthetic polymers undergo number of special pyrolysis or chemical treatment at high temperatures (700–800°C) to produce activated carbons. They can be produced in many forms including powders, microporous, granulated, molecular sieves and carbon fibers. Activated carbon has advantages of that: a relatively low adsorption heat among the other types of physical adsorbent pairs (1800–2000 kJ/kg), low adsorption heat is beneficial to the system's COP because the majority of heat consumption in the regeneration phase is the adsorption heat [12], higher surface reactivity, suitable pore size [13] and large surface area. However, the thermal conductivity of activated carbon is poor and is near to the insulation material. For example, ACF-methanol system with a higher specific adsorption reaches up to 0.55 kg/kg_{ads}, and good mass transfer characteristics where void fraction of ACF layer is more than 0.90%, but the measured thermal conductivity is as low as 0.0893 W/(mK) [14]. The carbon physical characteristics could be optimized to obtain the best performance of ARSs.

a. Activated carbon-ammonia

While most of adsorbent-adsorbate pairs operate under high vacuum, an activated carbon-ammonia pair system has a high working pressure (about 1600 kPa when the condensing temperature is 40°C). So, permeability of sorbent is not critical and it can be easier and more applicable than sub-atmospheric systems. It is also more suitable than the activated carbon/methanol pair for heat sources of 200°C or higher. The drawbacks of this working pair are the toxicity and pungent smell of ammonia.

b. Activated carbon-methanol

Large adsorption capacity of activated carbon-methanol pair has adsorption capacity of about 0.45 kg/kg_{ads}. Low regeneration temperature can be used to drive ARS employing activated carbon-methanol pair (about 100°C). On the other hand, it should not be used with regeneration temperature higher than 120°C, where activated carbon will catalyze methanol to decompose into dimethyl ether at a temperature more than 150°C, and operating pressure of the system will be sub-atmospheric and that requires assistant vacuum system.

2.2. Chemical adsorbents-adsorbate pair

Chemical adsorbents sorb the refrigerants differently than physical adsorbents where the strong chemical bond between the adsorbent and the refrigerant takes place in chemical adsorption. The uptake in the chemical adsorbents is not limited by the surface area of the material, which generally leads to higher mass transfer kinetics when compared to physical adsorbents. The metal chlorides are commonly used as chemical adsorbents due to their high

adsorption capacity, and they involve calcium chloride ($CaCl_2$), strontium chloride ($SrCl_2$), magnesium chloride ($MgCl_2$), barium chloride ($BaCl_2$), manganese chloride ($MnCl_2$) and cobalt chloride ($CoCl_2$), among others. For example, in $CaCl_2$/ammonia pair, 1 mole calcium chloride can adsorb 8 moles ammonia [15].

Generally, chemical adsorbents have very large uptakes with specific adsorptions approaching 1 kg/kg_{ads} in some cases, and desorption temperatures varying from 40 to 80°C which are very promising. However, chemical adsorption systems stability is lower than that for physical adsorption systems due to agglomeration and swelling phenomena, which are common in chemical adsorbent beds. This instability reduces heat and mass transfer which limits the cooling capacities of chemical adsorbents. Consequently, heat-driven chillers utilizing these adsorbents have been less common than those using physical adsorbents. To overcome this problem, the porous heat transfer matrixes were put forward for the improvement of mass transfer as well as the heat transfer by using composite adsorbents.

2.3. Composite adsorbents-adsorbate pair

Composite adsorbents, also called "Salt in Porous Matrix (CSPM)" represent the promising solution of aforementioned drawbacks associated with pure physical and chemical adsorbents. Thus, many of these composites, which are typically made of porous media and chemical adsorbents, have been developed synthetically to be applied in adsorption refrigeration systems as in Refs. [16–18]. In such composites, porous media work on improving the heat and mass transfer properties of the chemical adsorbents along with limiting the swelling characteristics of the chemical adsorbents, while the chemical adsorbents increase the refrigerant uptake of the adsorbent pair. The common examples of these composites are combinations of metal chlorides and AC, ACF, expanded graphite, silica gel or zeolite. For example, silica gel and chlorides/water which are known as selective water sorbents (SWSs) which are tested and studied by Aristov et al. [6]. Composite adsorbents of silica gel and chloride are usually produced using the impregnation method. The silica gel is immersed in a chloride salt solution and is then dried to remove the water. There are also four types of porous media were used with chlorides to produce composite adsorbents/ammonia: activated carbon, activated carbon fiber, expanded graphite or vermiculite.

2.4. Novel adsorbent materials: metal-organic frameworks (MOFs)

Metal-organic frameworks (MOFs) are highly crystalline porous material that are widely regarded as promising materials for various applications such as catalysis [19], gas separation [20] and gas storage [21]. The high crystallinity of MOFs can be highlighted through the description of MOF-5 structure which was once described as "The zinc carboxylate cluster with the six carboxylate carbons forming a regular octahedron but with tetrahedral symmetry was elegantly beautiful especially when linked in such regular arrays like terracotta warriors" [22]. Usually, the approach of assembling new frameworks out of molecular building blocks or secondary building blocks held together by strong bonding has been considerably used in designing new materials even though it is a challenge to control the assembly of the basic building blocks in the solid state and thus predicting of the resulting structure. Based

on the same concept or what is called the reticular synthesis, MOFs are designed based on the assembly of organic units and metal clusters as secondary building units (SBUs) to build the robust complex structures (**Figure 5**) [23]. Compared to conventional microporous inorganic materials such as zeolites and silica gel, MOFs were found to be flexible regarding controlling their architecture and functionalization of the pores [24]. Such tunable properties have given the lead to MOFs over conventional adsorbents as they offer high stability and porosity as shown in **Figure 6** . As mentioned above, these exceptional properties made this class of materials very interesting in a number of applications. Adsorption heat pumping for cooling applications has attracted a massive research over the past few years. For decades, the adsorption cooling application was mainly based on silica gel, activated carbon and zeolites which suffer from the limited adsorption capacity. The next section will discuss the different MOF materials with different refrigerants for cooling applications.

2.4.1. MOFs-water pair

Water is an environment friendly refrigerant with high latent heat of evaporation and high heat and mass transfer properties. Water-based adsorption systems use adsorbents like silica gel and zeolites which have limited water uptake capabilities (up to 0.3 g_w/g_{ads}) leading to low specific cooling power. The introduction of metal-organic frameworks (MOFs) material for adsorption cooling application allowed an improvement in the performance of the systems due to the high-water uptake that can reach up to 1 g_w/g_{ads} and the potential of using low temperature waste heat or solar collectors as primary energy sources. Shi et al. [25] showed that using CPO-27(Ni) MOF material (a max water uptake of 0.45 g_w/g_{ads}) for automotive air conditioning can outperform SAPO 34 zeolite material in terms of specific cooling power. They showed that CPO-27(Ni) produced specific cooling power of 440 W kg^{-1} at a desorption temperature of 130°C and a cycle time of 900 s compared to 310 W kg^{-1} for SAPO-34 at the same operating conditions. Numerous metal-organic framework materials have been studied to investigate their water adsorption capacity, **Figure 7** shows maximum water uptake of a number of MOFs that were investigated for adsorption cooling applications at 25°C.

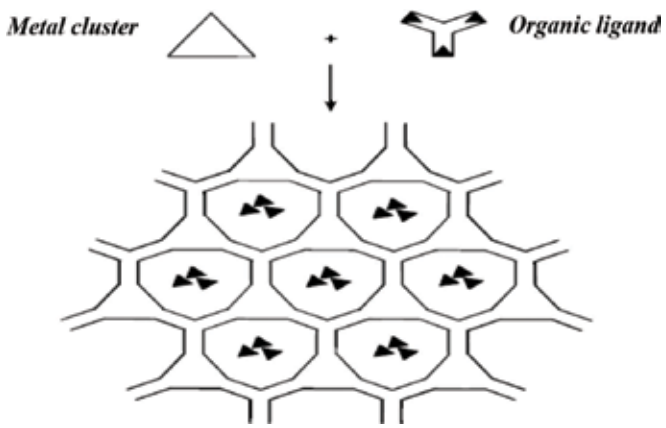

Figure 5. Schematic representation of how the framework is formed [47].

http://dx.doi.org/10.5772/intechopen.73167

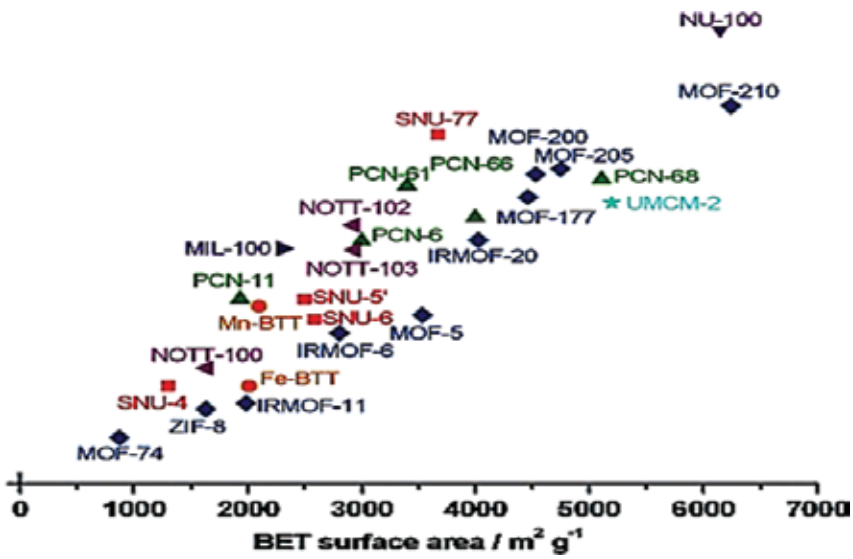

Figure 6. BET surface area comparison between some reported MOFs and zeolite [48, 49].

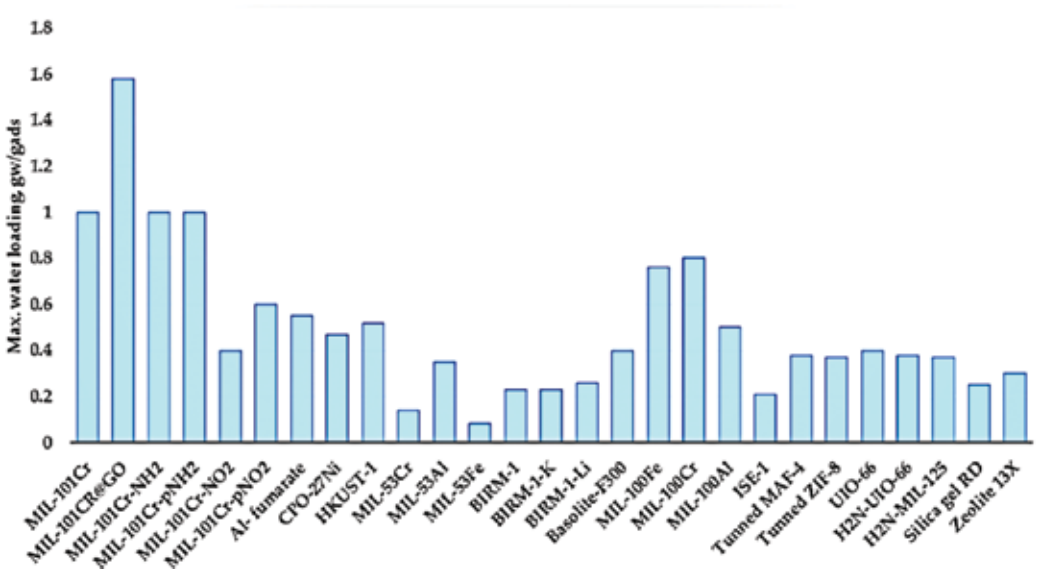

Figure 7. Maximum water uptake comparison between some reported MOFs, silica gel and zeolite.

Ehrenmann et al. [26] showed that MIL-101Cr can adsorb up to 1 g_w/g_{ads} with high performance stability, also the heat of adsorption value was near the evaporation enthalpy of water, meaning that the interaction energy with the framework was believed to be very low compared to other materials used so far, like zeolites and hence the material do not require high regeneration temperature. A further modification was investigated by Khutia et al. [27] as

the water loading capacity of four nitro or amino-functionalized MIL-101Cr materials (fully and partially functionalized) was assessed for heat transformation applications. The fully aminated MIL-101Cr-NH_2, and partially aminated MIL-101Cr-pNH_2, showed the best water loadings (about 1.0 g_w/g_{ads}) and proving the weak host-guest interactions and hence a lower regeneration temperature is required. Elsayed et al. [25] further improved the thermal conductivity and the water vapor capacity of MIL-101(Cr) to be used in adsorption heat pump application through using hydrophilic graphene oxide. Two methods have been used to develop MIL-101(Cr)/GrO composites. It was shown that introducing low amounts of GrO (2%) to the neat MIL-101(Cr) enhanced the water adsorption characteristics at high relative pressure but enhanced the heat transfer properties by 20–30% while using more than 2% of GrO reduced the water adsorption uptake but significantly enhanced the thermal conductivity by more than 2.5 times. Yan et al. [28] managed to improve the performance of the material through developing another composite (MIL-101@GO) of MIL-101(Cr) and graphite oxide (GO) with high-water vapor capacity for adsorption heat pumps (AHPs). It showed that MIL-101@GO possessed a super-high adsorption capacity for water vapor up to 1.58 g_w/g_{ads}. This superior water vapor adsorption/desorption performance make MIL-101@GO a promising candidate as the water vapor adsorbent for adsorption heat pumps (AHPs) process. Another factor that was studied was the effect molding on the water adsorption properties of MIL-101(Cr) after pressing the prepared powder into a desired shape which was investigated by Rui et al. [29] . It showed that the forming pressure has a large influence on pore structure of shaped MIL-101, as the forming pressure increases from 3 to 5 MPa, the equilibrium adsorption capacity of water is up to 0.95 g_w/g_{ads} at the forming pressure of 3 MPa. Other types of MOFs such as Al fumarate was investigated by Jeremias et al. [30] in the form of coating on a metal substrate via the thermal gradient approach. It was concluded that Al fumarate is a promising adsorbent for heat pumping applications as it can be regenerated at low temperature as low as 60°C with a water loading difference higher than 0.5 g_w/g_{ads}. Fadhel et al. [31–33], generated cooling effect from using aluminum fumarate and MIL-101(Cr) in different multi-bed water adsorption systems. The performance was compared to other adsorbent materials such as AQSOA-Z02 and conventional silica gel. The isostructural CPO-27(Ni) was compared to aluminum fumarate by Elsayed et al. [34]. It was highlighted that the CPO-27(Ni) outperformed the aluminum fumarate at low evaporation temperatures, while the aluminum fumarate was more suitable for applications requiring high evaporation temperature. It was also mentioned that CPO-27(Ni) is suitable for systems operated with high desorption temperature while on the contrary aluminum fumarate can be regenerated at low desorption temperatures.

The performance of a number of MOFs such as HKUST-1 and MIL-100(Fe) was investigated and compared to silica gel RD-2060 by Rezk et al. [35]. They showed that HKUST-1 performed better than silica gel RD-2060 with an increase of water uptake of 93.2%, which could lead to a considerable increase in refrigerant flow rate, cooling capacity and/or reducing the size of the adsorption system. However, MIL-100(Fe) MOF showed reduced water uptake comparable to silica gel RD-2060 for water chilling applications with evaporation at 5°C. These results highlight the potential of using MOF materials to improve the efficiency of water adsorption cooling systems. Other MOFs such as MIL-53(Cr), MIL-53(Fe), Birm-1,

Birm-1(K) and Birm-1(Li) showed water uptake of 0.14–0.35 g_w/g_{ads} which is lower than the water adsorption capacity of HKUST-1, proving that HKUST-1 regarding to the water capacity outperform conventional porous materials such as silica gel and other MOF materials [36], comparing HKUST-1 with other zeolite materials like SAPO-34 and AlPO-18 showed that the best SAPO-34 samples had a water uptake of 0.253 g_w/g_{ads} which is a factor of 4.9 larger compared to the reference silica gel. Those results were only exceeded by the best AlPO-18 sample with a measured water uptake of 0.254 g_w/g_{ads} for the low driving temperatures. This equaled an improvement by a factor of 6.2. For driving temperature of 140°C, the highest water uptake was found for the metal-organic framework HKUST-1 [37].Other MOFs such as MIL-100 (Fe and Al) with a water uptake of 0.76 and 0.5 g_w/g_{ads} were found to be also very interesting candidates for thermally driven, sorption-based chilling or heat pump systems [38, 39]. A 3D MOF material (ISE-1) was found to have water loading of 0.210 g_w/g_{ads} which was found to be larger than other five zeolites in that study and of the reference silica gel demonstrating the potential of MOF materials for use in adsorption heat pumping processes [40]. MIL-53(Al), MIL-100(Fe) and ZIF-8 were compared with the previous materials and were found to have a water uptake higher than 0.3 g_w/g_{ads} proving that MOFs are a very promising class of materials for the use in adsorption heat pumping/cooling processes [41, 42]. The amino-functionalized MOFs UiO-66 and MIL-125 (H_2N-UiO-66 and H_2N-MIL-125) featured also very promising H_2O adsorption isotherms due to their enhanced hydrophilicity with a water load of ≈0.4 g_w/g_{ads} and were considered to be especially beneficial for the intended heat pump application [43].

2.4.2. MOFs-ethanol pair

Saha et al. [44] presented experimental and theoretical investigations of adsorption characteristics of ethanol onto metal-organic framework namely MIL-101(Cr). The experiments have been conducted within relative pressures between 0.1 and 0.9 and adsorption temperatures ranging from 30 to 70°C, which are suitable for adsorption cooling applications. Adsorption isotherm data exhibit that 1 g of MIL-101(Cr) can adsorb as high as 1.1 g of ethanol at adsorption temperature of 30°C. The experimental results showed that the studied pair would be a promising candidate for developing high performance cooling device. Rezk et al. [45] experimentally investigated the ethanol adsorption characteristics of six MOF materials namely CPO-27(Ni), MIL-101(Cr), HKUST-1, MIL-100(Fe), MIL-53(Cr) and MIL-100(Cr) compared to that of silica gel as a conventional adsorbent material that is widely used in commercial adsorption systems. The results revealed that MIL-101(Cr) have shown superior performance with uptake value of 1.2 g_w/g_{ads}. Also, MIL-101(Cr) proved to be stable through 20 successive cycles at 25°C. The results from theoretical modeling of a two-bed adsorption system with heat and mass recovery have shown that using MIL-101(Cr)/ethanol pair has remarkable potential in low temperature cooling applications.

2.4.3. MOFs-methanol pair

Jeremias et al. [46] showed that the use of alcohols (methanol) as working fluids turned be a good prospect for the application of otherwise promising, but hydrothermally unstable or

not sufficiently hydrophilic materials like HKUST-1 or MIL-101(Cr), respectively, or for low temperature applications, where the vapor pressure of H_2O is not sufficient for acceptable kinetics and that heat and mass transfer could be optimized by various shaping procedures.

3. Heat and mass transfer enhancements

Enhancing the heat and mass transfer (HMT) of the adsorber is the most crucial part in developing ARSs. For a given cooling capacity, higher specific cooling capacity (SCC) means smaller amount of adsorbent to be used, and that can be a direct result of improving the heat and mass transfer performance of the adsorber. Besides, a lighter weight and smaller volume are existed in such case. As the adsorption system consumes less heat during regeneration modes, the COP is increased. Two methods are commonly used to increase the HMT: one is the development of adsorbents and the second is the optimization of the adsorber designs and cycle modes.

3.1. Adsorbent developments

Intensifying the heat transfer of an adsorbent depends mainly on increasing its thermal conductivity where the conduction is the major way to transfer the heat through the adsorbent. Consolidating the adsorbent or using additives with good thermal conductivity into the adsorbent are the common approaches used to enhance the heat transfer in the adsorbent [50, 51]. However, such approaches always decrease the permeability of the adsorbent leading to a decrease in inter-particle mass transfer. The overall performance of the bed will be affected by this contradiction between *heat transfer* and *mass transfer* in the adsorbent. Thus, it should be considered that the increase in thermal conductivity 20-fold, for example, does not mean a similar great enhancement in the overall performance due to the reduction in mass transfer. On microscopic level, the distribution of micro layers inside the samples of an adsorbent affects both the thermal conductivity and permeability, and then investigation can be applied for enhancing both of them as made in Ref. [52]. Therefore, sample preparation and filling techniques can be optimized to enhance both heat and mass transfer. Testing adsorbents in various forms and sizes is also an effective way to investigate the best HMT performance of the adsorber. Developments of the composite adsorbents are another active area used to enhance refrigerant uptake of the pure adsorbents and their stability. More recently, there are two trends: coating the adsorbent over the heat transfer metal surfaces of adsorbers, aiming at the elimination both of thermal contact resistances and large inter-particle voids, or using the new metal-organic frameworks (MOFs) materials which provide attractive adsorption characteristics compared to common adsorbents.

3.1.1. Adsorbent coatings

From the standpoint that loose grains and consolidated adsorbent beds have poor heat transfer and mass transfer properties, respectively, the concept of coated adsorber has been developed

to introduce adsorbers with efficient heat and mass transfer. Applying direct synthesis, or using a binder for deposition a layer of adsorbent over walls of the metal heat exchangers are two common technologies of adsorbent coatings. Different approaches have been reported and discussed in Ref.s [53, 54] as for illustrated in **Figure 8** [55].

3.2. Optimization of the adsorber design and cycle modes

Optimized parameters and sophisticated designs of adsorber configurations can help in enhancing the inter-particle mass transfer in the adsorbent domain, along with facilitating the heat transfer between the adsorbent and heat transfer fluid HTF. Extended metal surfaces 'fins' are commonly used to intensify the heat transfer and overcome the low thermal conductivity of the adsorbent materials. However, the COP of an adsorption system is strongly affected by the metal-adsorbent mass ratio [56]. Therefore, the net effects of the fins parameters such as fin spacing, height and thickness should be investigated carefully to optimize the overall system performance [57–60].

In the same context, operational control parameters, such as adsorber modes' durations and fluid flow rates, influence considerably the ARSs' performance and need to be also optimized. Basically, in view of the fact that the diffusion of mass within the adsorbent particles is better with higher temperatures, therefore, the desorption process is carried out faster than the adsorption process. That explains why the differences between equilibrium and instantaneous amount of adsorbate (W_{eq}–w) in desorption and adsorption modes are not identical during the cyclic steady state. A larger difference is required during an adsorption mode to adsorb the same total amount desorbed during a desorption mode for making cyclic steady state. Increasing the cooling water velocity and/or adsorption duration over heating water velocity and/or desorption mode are the common ways to reach steady state cycle. And that increases need to be optimized for maximizing the adsorption system performance, as by adsorption/desorption times reallocation, [61]. Operating under low pressures is another challenge as in the case of water and methanol as refrigerants. In this case, the poor mass transfer in adsorbers can lessen greatly the difference in the refrigerant uptakes during the cycle. That requires more developed designs for such adsorbers to improve their performances. It is important to mention that studying the net effect of any operating parameter on the adsorption kinetic during only one mode (adsorption or desorption) based on given initial conditions may lead to inaccurate predictions for the overall performance.

Figure 8. Adsorbers' manufacturing procedure [55].

4. Advanced adsorption cycles

In view of the fact that the basic adsorption cycle produces intermediated cooling output and its COP is low, many advanced adsorption refrigeration cycles have been proposed and developed to help in overcoming these main drawbacks such as the heat recovery cycle, mass recovery cycle, thermal wave cycle, cascade cycle and multi-stage cycle. However, the basic cycle is mostly used in the solar powered adsorption system for its simplicity.

4.1. Two-bed adsorption cycles

The flow diagrams of a conventional two-bed cycle representing one complete cycle are illustrated in **Figure 9**. Each adsorber undergoes four operating modes: pre-heating, heating (desorption), pre-cooling and cooling (adsorption) processes in repeating cycles and according to the sequence shown in **Table 1**. The system consists of two adsorbent beds, a condenser, an evaporator and an expansion valve, in addition to the four connecting valves and connecting pipes. The working principle of the basic cycle is discussed in detail in Section 1.1 for one-bed ARS. In a two-bed ARS, while hot water is used to heat up Bed-A during the first two processes: cooling water is used to cool down Bed-B. The hot water is switched to Bed-B in the last two processes, as Bed-A is subjected to cooling water. The four valves are completely closed during the two switching modes. Circulating the cooling water and chilled water in the condenser and evaporator, respectively, are supposed to be continuous during the whole cycle.

In a system of two or more adsorbers work between an evaporator and a condenser, there is a hot adsorber under cooling process and a cold one under heating process which offers the availability to recovery the heat inside the system. The experimental results show that the COP of the system will increase by up to 25% with the heat recovery cycle [62]. In a

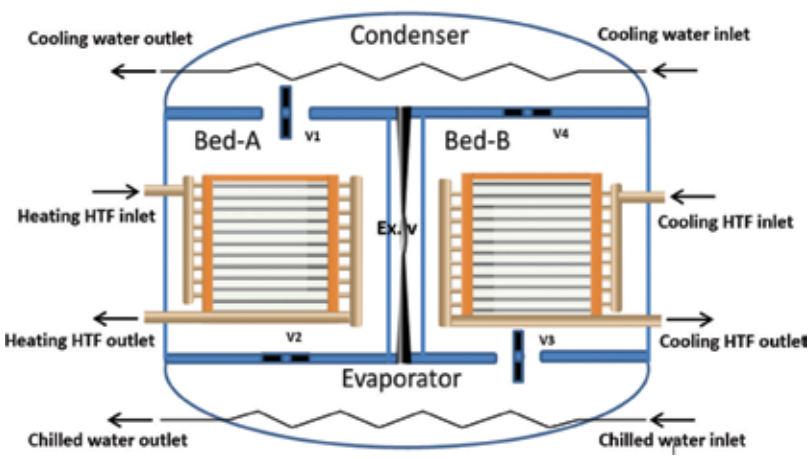

Figure 9. Schematic diagram of a conventional two-bed adsorption chiller, as Bed-A in desorption mode, Bed-B in adsorption mode.

http://dx.doi.org/10.5772/intechopen.73167

Mode	Component					
	Bed-A	**Bed-B**	**V1**	**V2**	**V3**	**V4**
Mode-A switching	Pre-heating	Pre-cooling	X	X	X	X
Mode-B Des/Ads	Heating/Des	Cooling/Ads	O	X	O	X
Mode-C switching	Pre-cooling	Pre-heating	X	X	X	X
Mode-D Ads/Des	Cooling/Ads	Heating/Des	X	O	X	O

Table 1. Cycle modes and valve positioning.

typical two-bed cycle equipped with mass recovery system, while one bed at the end of desorption mode at higher pressure and temperature, the other bed at the end of adsorption mode at lower pressure and temperature. Internal mass recovery process is started via connecting the high-pressure adsorber to the low-pressure one typically by means of a valve. The process ends when the two pressures become equal. The combined heat and mass recovery procedures may increase COP more than 10% [62], compared to heat recovery cycle. Thermal wave cycle is another way to recovery the heat inside the cycle. A typical thermal wave cycle is composed of two adsorbers, an evaporator, a condenser, a cooler and a heater as shown in **Figure 10** [63]. Experimental results showed that the COP of a two-bed adsorption air conditioner (zeolite-water) with thermal wave cycle was approximately 1.0 in cooling season [12].

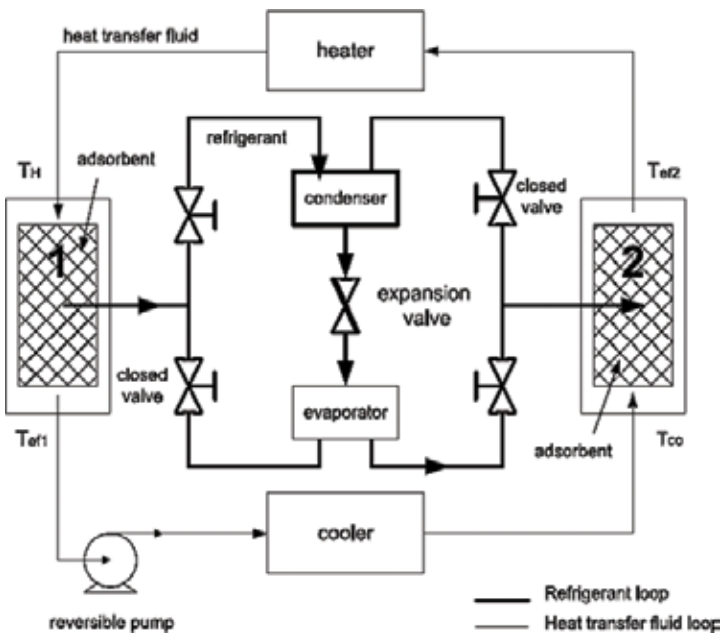

Figure 10. Schematic representation of the thermal wave adsorption heat pump during the first half of the cycle [63].

An adsorption chiller installed in the University hospital in Freiburg [64]	
Working pair: silica gel-water CC(kW): 70 and COP – Backup: thermally driven by steam network of the hospital Daily solar radiation: temperate, central European climate Solar collector type: evacuated tube Area: 170 (m^2) Main features: solar system is working on assisting the main driving heat system and can deliver about 90% of the heating required in mid-day hours (4 hours)	 Adsorption chiller installed in the University hospital in Freiburg
Two-bed adsorption chiller developed by SorTech [65]	
Working pair: silica gel-water CC (kW): 7.5 and COP: 0.55 (system) Electricity consumption: 9 W. Heat supply circuit: 72/67°C at 1.6 m^3/h. Heat rejection circuit 27/32°C at 3.7 m^3/h. Chilled water circuit 18/15°C at 2.0 m^3/h. Daily solar radiation: temperate, central European climate Solar collector type: flat plate Area: 3.5–4.5 (m^2/kW) Main features: developed by SorTech AG, and it enables to paste the heat exchanger surface with silica gel pellets with the aid of epoxy resin without blocking the entrance pores of the pellets	 The Fraunhofer ISE institute building and SorTech adsorption chiller in the technical room (sources: Fraunhofer ISE) [34]
Silica gel-water adsorption chiller developed in SJTU [66]	
Working pair: silica gel-water CC(kW): 15 COP: 0.35 (system) 0.15 (solar) Regeneration temp. (°C): 85 Solar collector type and area: 90 m^2 of U-type evacuated tube and 60 m^2 of heat pipe evacuated tubular Main features: the adsorber is a compact finned-tube heat exchanger, the condenser is a shell and tube heat exchanger, and the evaporator cooling is output through a methanol chamber, which acts as a gravity heat pipe. Power consumption for pumps was 1.87 kW	 Photo of the adsorption chiller

Table 2. Summary of some adsorption prototypes.

4.2. Other advanced cycles

There are many of advanced and novel cycles proposed in literature for ARSs. The advanced cycles such as multi-bed cycle, multi-stage cycle and dual-mode cycle are originally developed to make utilize of lower temperature heat sources applicable and more efficient. Another trend in advanced cycles is eliminating the vacuum valves by putting the adsorber, condenser and evaporator in a single chamber to increase the reliability of the system, particularly under the vacuum operating conditions. **Table 2** summarizes data about some applied or prototype adsorption chillers.

5. Conclusions

Adsorption refrigeration systems have a lot of advantages making them more and more competitive when compared to conventional vapor compression refrigeration systems. Apparently, the environmental regulations and local safety considerations, the expensive and limited petrol energy resources, solar driven possibility and the increasing of industrial waste heat availability are all in favor of thermally driven refrigeration systems, particularly adsorption systems. The adsorption refrigeration technology has not been carrying out in mass production level yet. That justifies its higher initial cost compared to the conventional technology. On the other side, there is a serious need to consider together all aspects of energy, exergy, environment and economy in the future comparative studies. Also, it should be noticed that the thermal COPs of ARSs are around 0.6 which is low. However, the electrical COP values of ARSs can reach up to 10 which is high compared to that values of conventional systems typically between 3 and 5. In order to find out new direction of adsorption refrigeration systems developments, previous related researches are reviewed and classified in this chapter.

Acknowledgements

This work is funded by the Science and Technology Development Fund (STDF) program in Egypt under the UK-Newton Institutional Links Grants, project ID 26148, in collaboration with University of Birmingham, Birmingham in UK.

Nomenclatures

ARSs	adsorption refrigeration systems
COP	coefficient of performance
HEX	heat exchangers

MOFs	metal-organic frameworks
SCC	specific cooling capacity
W_{eq}	equilibrium amount of adsorbate

Author details

Mahmoud B. Elsheniti[1]*, Osama A. Elsamni[1], Raya K. Al-dadah[2], Saad Mahmoud[2], Eman Elsayed[2] and Khaled Saleh[1]

*Address all correspondence to: melsheniti@gmail.com

1 Mechanical Engineering Department, Alexandria University, Alexandria, Egypt

2 School of Mechanical Engineering, University of Birmingham, Birmingham, UK

References

[1] Wang RZ, Xu ZY, Pan QW, Du S, Xia ZZ. Solar driven air conditioning and refrigeration systems corresponding to various heating source temperatures. Applied Energy. 2016;**169**:846-856

[2] Deng J, Wang RZ, Han GY. A review of thermally activated cooling technologies for combined cooling, heating and power systems. Progress in Energy and Combustion Science. 2011;**37**:172-203

[3] Demir H, Mobedi M, Ülkü S. A review on adsorption heat pump: Problems and solutions. Renewable and Sustainable Energy Reviews. 2008;**12**:2381-2403

[4] Pons AKM. Entropic analysis of adsorption open cycles for air conditioning part1: First and second law analyses. 2000;**24**:251-262

[5] Wang X, Zimmermann W, Ng K, Chakraboty A, Keller J. Investigation on the isotherm of silica gel+water systems. Journal of Thermal Analysis and Calorimetry. 2004;**76**:659-669

[6] Aristov YI. New family of solid sorbents for adsorptive cooling: Material scientist approach. Journal of Engineering Thermophysics. 2007;**16**:63-72

[7] Wang XL, Chua HT, Gao LZ. A thermogravimetric analyzer for condensable gas adsorption under subatmospheric conditions. Journal of Thermal Analysis and Calorimetry. 2007;**90**:935-940

[8] Chua HT, Ng KC, Malek A, Kashiwagi T, Akisawa A, Saha BB. Modeling the performance of two-bed, sillica gel-water adsorption chillers. International Journal of Refrigeration. 1999;**22**(5):194-204

[9] Chua HT, Ng KC, Wang W, Yap C, Wang XL. Transient modeling of a two-bed silica gel–water adsorption chiller. International Journal of Heat and Mass Transfer. 2004;**47**: 659-669

[10] Wang X, Chua HT. Two bed silica gel–water adsorption chillers: An effectual lumped parameter model. International Journal of Refrigeration. 2007;**30**:1417-1426

[11] Saha BB, Akisawa A, Kashiwagi T. Solar/waste heat driven two-stage adsorption chiller: The prototype. Renewable Energy. 2001;**23**:93-101

[12] EAV Kai, Wang PE, "New opportunities for solar adsorption refrigeration," ASHRAE Journal. September 2011:2011

[13] Ullah KR, Saidur R, Ping HW, Akikur RK, Shuvo NH. A review of solar thermal refrigeration and cooling methods. Renewable and Sustainable Energy Reviews. 2013;**24**: 499-513

[14] Hamamoto Y, Alam KCA, Saha BB, Koyama S, Akisawa A, Kashiwagi T. Study on adsorption refrigeration cycle utilizing activated carbon fibers. Part 1. Adsorption characteristics. International Journal of Refrigeration. 2006;**29**:305-314

[15] Wang DC, Li YH, Li D, Xia YZ, Zhang JP. A review on adsorption refrigeration technology and adsorption deterioration in physical adsorption systems. Renewable and Sustainable Energy Reviews. 2010;**14**:344-353

[16] Saha BB, Chakraborty A, Koyama S, Aristov YI. A new generation cooling device employing $CaCl_2$-in-silica gel-water system. International Journal of Heat and Mass Transfer. 2009;**52**:516-524

[17] Gordeeva L, Grekova A, Krieger T, Aristov Y. Composites "binary salts in porous matrix" for adsorption heat transformation. Applied Thermal Engineering. 2013;**50**:1633-1638

[18] Ahn KW, Jang SY, Hwang MH, Kim S-G. $CaCl_2$-in-Mesoporous silica grown on superabsorbent polymer to enhance water uptake. Kona Powder and Particle Journal. 2015; **32**:207-216

[19] Ranocchiari M, van Bokhoven JA. Catalysis by metal-organic frameworks: Fundamentals and opportunities. Physical Chemistry Chemical Physics. 2011;**13**:6388-6396

[20] Zhao ZX, Ma XL, Kasik A, Li Z, Lin YS. Gas separation properties of metal organic framework (MOF-5) membranes. Industrial & Engineering Chemistry Research. Jan 2013;**52**: 1102-1108

[21] Li B, Wen HM, Zhou W, Chen BL. Porous metal-organic frameworks for gas storage and separation: What, how, and why? Journal of Physical Chemistry Letters. Oct 2014;**5**: 3468-3479

[22] O'Keeffe M. Design of MOFs and intellectual content in reticular chemistry: A personal view. Chemical Society Reviews. 2009;**38**:1215-1217

[23] Kim J, Chen BL, Reineke TM, Li HL, Eddaoudi M, Moler DB, et al. Assembly of metal-organic frameworks from large organic and inorganic secondary building units: New examples and simplifying principles for complex structures. Journal of the American Chemical Society. Aug 2001;**123**:8239-8247

[24] Li H, Eddaoudi M, O'Keeffe M, Yaghi OM. Design and synthesis of an exceptionally stable and highly porous metal-organic framework. Nature. Nov 1999;**402**:276-279

[25] Shi B, Raya A-D, Mahmoud S, Elsayed A, Elsayed E. CPO-27 (Ni) metal-organic framework based adsorption system for automotive air conditioning. Applied Thermal Engineering. 2016;**106**:325-333

[26] Ehrenmann J, Henninger SK, Janiak C. Water adsorption characteristics of MIL-101 for heat-transformation applications of MOFs. European Journal of Inorganic Chemistry. 2011;**2011**:471-474

[27] Khutia A, Rammelberg HU, Schmidt T, Henninger S, Janiak C. Water sorption cycle measurements on functionalized MIL-101Cr for heat transformation application. Chemistry of Materials. 2013;**25**:790-798

[28] Yan J, Yu Y, Ma C, Xiao J, Xia Q, Li Y, et al. Adsorption isotherms and kinetics of water vapor on novel adsorbents MIL-101 (Cr)@ GO with super-high capacity. Applied Thermal Engineering. 2015;**84**:118-125

[29] Zhengqiu R, Quanguo L, Qun C, Haiyan W, Haijun C, Huqing Y. Adsorption refrigeration performance of shaped MIL-101-water working pair. Chinese Journal of Chemical Engineering. 2014;**22**:570-575

[30] Jeremias F, Fröhlich D, Janiak C, Henninger SK. Advancement of sorption-based heat transformation by a metal coating of highly-stable, hydrophilic aluminium fumarate MOF. RSC Advances. 2014;**4**:24073-24082

[31] Al-Mousawi FN, Al-Dadah R, Mahmoud S. Different bed configurations and time ratios: Performance analysis of low-grade heat driven adsorption system for cooling and electricity. Energy Conversion and Management. 2017;**148**:1028-1040

[32] Al-Mousawi FN, Al-Dadah R, Mahmoud S. Low grade heat driven adsorption system for cooling and power generation with small-scale radial inflow turbine. Applied Energy. 2016;**183**:1302-1316

[33] Al-Mousawi FN, Al-Dadah R, Mahmoud S. Low grade heat driven adsorption system for cooling and power generation using advanced adsorbent materials. Energy Conversion and Management. 2016;**126**:373-384

[34] Elsayed E, Raya A-D, Mahmoud S, Elsayed A, Anderson PA. Aluminium fumarate and CPO-27 (Ni) MOFs: Characterization and thermodynamic analysis for adsorption heat pump applications. Applied Thermal Engineering. 2016;**99**:802-812

[35] Rezk A, Al-Dadah R, Mahmoud S, Elsayed A. Characterisation of metal organic frameworks for adsorption cooling. International Journal of Heat and Mass Transfer. 2012;**55**: 7366-7374

[36] Rezk A, Al-Dadah R, Mahmoud S, Elsayed A. Experimental investigation of metal organic frameworks characteristics for water adsorption chillers. Proceedings of the Institution of Mechanical Engineers, Part C: Journal of Mechanical Engineering Science. 2013;**227**:992-1005

[37] Henninger S, Schmidt F, Henning H-M. Water adsorption characteristics of novel materials for heat transformation applications. Applied Thermal Engineering. 2010;**30**:1692-1702

[38] Jeremias F, Khutia A, Henninger SK, Janiak C. MIL-100 (Al, Fe) as water adsorbents for heat transformation purposes—A promising application. Journal of Materials Chemistry. 2012;**22**:10148-10151

[39] Henninger SK, Jeremias F, Kummer H, Janiak C. MOFs for use in adsorption heat pump processes. European Journal of Inorganic Chemistry. 2012;**2012**:2625-2634

[40] Henninger SK, Habib HA, Janiak C. MOFs as adsorbents for low temperature heating and cooling applications. Journal of the American Chemical Society. 2009;**131**:2776-2777

[41] Henninger SK, Jeremias F, Kummer H, Schossig P, Henning H-M. Novel sorption materials for solar heating and cooling. Energy Procedia. 2012;**30**:279-288

[42] Janiak C, Henninger SK. Porous coordination polymers as novel sorption materials for heat transformation processes. Chimia International Journal for Chemistry. 2013;**67**: 419-424

[43] Jeremias F, Lozan V, Henninger SK, Janiak C. Programming MOFs for water sorption: Amino-functionalized MIL-125 and UiO-66 for heat transformation and heat storage applications. Dalton Transactions. 2013;**42**:15967-15973

[44] Saha BB, El-Sharkawy II, Miyazaki T, Koyama S, Henninger SK, Herbst A, et al. Ethanol adsorption onto metal organic framework: Theory and experiments. Energy. 2015;**79**: 363-370

[45] Rezk A, Raya A-D, Mahmoud S, Elsayed A. Investigation of ethanol/metal organic frameworks for low temperature adsorption cooling applications. Applied Energy. 2013;**112**: 1025-1031

[46] Jeremias F, Fröhlich D, Janiak C, Henninger SK. Water and methanol adsorption on MOFs for cycling heat transformation processes. New Journal of Chemistry. 2014;**38**:1846-1852

[47] Yaghi OM, Li HL, Davis C, Richardson D, Groy TL. Synthetic strategies, structure patterns, and emerging properties in the chemistry of modular porous solids. Accounts of Chemical Research. Aug 1998;**31**:474-484

[48] Basdogan Y, Keskin S. Simulation and modelling of MOFs for hydrogen storage. CrystEngComm. 2015;**17**:261-275

[49] Huong TTT, Thanh PN, Son DN. Metal–organic frameworks: State-of-the-art material for gas capture and storage. VNU Journal of Science: Mathematics-Physics. 2016;**32**

[50] Tamainot-Telto Z, Critoph RE. Monolithic carbon for sorption refrigeration and heat pump applications. Applied Thermal Engineering. 2001;**21**:37-52

[51] Askalany AA, Henninger SK, Ghazy M, Saha BB. Effect of improving thermal conductivity of the adsorbent on performance of adsorption cooling system. Applied Thermal Engineering; 2016

[52] Wang LW, Tamainot-Telto Z, Metcalf SJ, Critoph RE, Wang RZ. Anisotropic thermal conductivity and permeability of compacted expanded natural graphite. Applied Thermal Engineering. 2010;**30**(9):1805-1811

[53] Freni A, Dawoud B, Bonaccorsi L, Chmielewski S, Frazzica A, Calabrese L, et al. Characterization of Zeolite-Based Coatings for Adsorption Heat Pumps. Springer Cham Heidelberg New York Dordrecht London: SpringerBriefs in Applied Sciences and Technology; 2015

[54] Tatlier M. Performances of MOF vs. zeolite coatings in adsorption cooling applications. Applied Thermal Engineering. 2017;**113**:290-297

[55] Gullì G, Calabrese L, Palomba V, Frazzica A, Brancato V, La Rosa D, et al. An innovative adsorptive chiller prototype based on 3 hybrid coated/granular adsorbers. Applied Energy. 2016;**179**:929-938

[56] Sharafian A, Nemati Mehr SM, Thimmaiah PC, Huttema W, Bahrami M. Effects of adsorbent mass and number of adsorber beds on the performance of a waste heat-driven adsorption cooling system for vehicle air conditioning applications. Energy. 2016;**112**: 481-493

[57] Niazmand H, Talebian H, Mahdavikhah M. Bed geometrical specifications effects on the performance of silica/water adsorption chillers. International Journal of Refrigeration. 2012;**35**:2261-2274

[58] Çağlar A. The effect of fin design parameters on the heat transfer enhancement in the adsorbent bed of a thermal wave cycle. Applied Thermal Engineering. 2016;**104**:386-393

[59] Jribi S, Miyazaki T, Saha BB, Koyama S, Maeda S, Maruyama T. CFD simulation and experimental validation of ethanol adsorption onto activated carbon packed heat exchanger. International Journal of Refrigeration. 2017;**74**:345-353

[60] Rogala Z. Adsorption chiller using flat-tube adsorbers – Performance assessment and optimization. Applied Thermal Engineering. 2017;**121**:431-442

[61] El-Sharkawy II, AbdelMeguid H, Saha BB. Towards an optimal performance of adsorption chillers: Reallocation of adsorption/desorption cycle times. International Journal of Heat and Mass Transfer. 2013;**63**:171-182

[62] Wang RZ. Performance improvement of adsorption cooling by heat and mass recovery operation. International Journal of Refrigeration. 2001;**24**:10

[63] Chahbani MH, Labidi J, Paris J. Modeling of adsorption heat pumps with heat regeneration. Applied Thermal Engineering. 2004;**24**:431-447

[64] Henning H-M. Solar assisted air conditioning of buildings – An overview. Applied Thermal Engineering. 2007;**27**:1734-1749

[65] Jakob U, Mittelbach W. Development and investigation of a compact silica gel/water adsorption chiller integrated in solar cooling systems. In: VII Minsk International Seminar "Heat Pipes, Heat Pumps, Refrigerators, Power Sources". Minsk, Belarus; 2008. pp. 8-11

[66] Zhai XQ, Wang RZ, Wu JY, Dai YJ, Ma Q. Design and performance of a solar-powered air-conditioning system in a green building. Applied Energy. 2008;**85**:297-311

Section 3

Low Carbon Air Conditioning Systems

Chapter 5

Introduction of Low-Carbon Community Energy Systems by Combining Information Networks and Cogeneration-Type District Heating and Cooling Systems

Yujiro Hirano, Shogo Nakamura, Kei Gomi,
Takuya Togawa, Tsuyoshi Fujita and Makoto Ooba

Additional information is available at the end of the chapter

http://dx.doi.org/10.5772/intechopen.75129

Abstract

Achievement of a low-carbon society is becoming extremely important. In this report, we introduce an example of carbon dioxide (CO_2) emission reductions and energy savings, using a local energy-control system. Our research is focused on the town of Shinchi in the Fukushima Prefecture, Japan. Shinchi is pursuing initiatives to create a low-carbon, energy-efficient society and a disaster-resilient community. The National Institute for Environmental Studies provides academic support for the design and planning of low-carbon community energy systems by the local government of Shinchi, based on the Basic Cooperation Agreement. For the redevelopment of the Japan Railway (JR) Shinchi Station district that is being carried out, construction of a cogeneration-type district heating and cooling system is currently in progress. CO_2 reductions of about 20% can be expected by introducing this community energy system. To support these initiatives, we have developed an information and communication technology (ICT) system that shares a wide range of local information to support energy conservation. By analyzing electricity consumption data from the ICT, we evaluated the pattern of residential power consumption and confirmed that the project supports energy-saving behavior within the community. Additionally, the community energy project in the JR Shinchi Station district enables adjustment of the supply and demand balance.

Keywords: cogeneration, community energy management system, district heating and cooling, information and communication technology, waste heat recovery absorption chiller-heaters (genelink)

1. Introduction

As global warming becomes more serious, development of a low-carbon society has become an urgent task [1–3]. In particular, reduction of the energy used to cool and heat buildings, which is a large portion of energy usage during summer and winter, is an important issue [4, 5]. However, CO_2 emission due to heating and cooling-related energy consumption is still increasing. Thus, practical measures are needed to reduce CO_2 emissions.

As shown by recent examples, such as locally implemented plans to counteract global warming, formulation of new regional energy conservation visions, and proposals for environmental model/future cities, there are many opportunities for local governments to employ energy-efficient measures and CO_2 emission reduction plans [6]. Energy consumption for cooling and heating is strongly influenced by local factors such as climate, land use, and building-related aspects [7, 8]. The potential for energy and CO_2 reductions from both non-structural and structural measures is high [9], and there are proposals for such measures that incorporate various regional efforts.

In Japan, energy usage has changed greatly since the 2011 Great East Japan Earthquake [10–12]. Before the earthquake, during the period between the United Nations Framework Convention on Climate Change and the first commitment period prescribed by the Kyoto Protocol, reduction of CO_2 emissions was an important policy issue for mid-term to long-term global warming countermeasures. Since the earthquake, there have been many global warming countermeasures and energy policies such as government-imposed power-saving measures to mitigate power peak loading, various programs associated with nuclear power generation, a renewable energy feed-in tariff, and liberalization of power retailers.

There are three reasons that the Great East Japan Earthquake caused changes to energy-related matters. First, the vulnerability of Japan's large-scale energy supply network was exposed. The supply network for power and gas was disrupted during the earthquake, and the energy supply was discontinued over wide areas, even in areas that suffered only minor earthquake damage. In some cases, people survived the earthquake and tsunami but ultimately died due to the absence of power, which resulted in a lack of heating and a shortage of dry clothes. This situation led to a focus on renewable energy as an emergency power source during disasters. Through the introduction of a distributed power supply and construction of an autonomous energy network, energy supply and demand are becoming more efficient at the local scale [13].

Second, the earthquake-related accident at the Fukushima Daiichi Nuclear Power Plant increased the public's awareness of energy supply issues [14–16]. To mitigate peak power loading as the nuclear power plant ceased to function, rolling blackouts and legally binding power usage restrictions were implemented. Additionally, radioactive contamination led to a large-scale evacuation order for residents. During post-disaster reconstruction, many citizens cooperated with energy-saving measures during periods of peak energy demand in summer. As a result, a large number of citizens became aware of energy supply issues.

Third, the Great East Japan Earthquake intensified the problems of depopulation, declining birthrate and the aging population in Japan. For municipalities in disaster-affected areas, these issues are pressing. Population decline along with decentralization of residential areas

leads to an increase in CO_2 emissions per capita. By making cities compact, travel becomes more efficient, and the air conditioning load of housing complexes is reduced, thus increasing energy efficiency [17]. The decrease in energy consumption related to cooling and heating results in reduced CO_2 emission. As such, during the reconstruction process following the earthquake, many disaster-affected municipalities aimed to build compact, energy-efficient cities, with improved energy supply and demand balance [18, 19].

This paper examines the advanced case of Shinchi, which is a town located on the northern edge of the Fukushima Prefecture. In Shinchi, after major damage from the Great East Japan Earthquake, a community heat supply system was introduced to link an information and communication technology (ICT) system with a cogeneration system (CGS). The National Institute for Environmental Studies provides academic support for the design and planning of such systems, as well as assessing the feasibility, energy conservation, and CO_2 emission reductions [20, 21]. As a social demonstration experiment, we introduced smart meters and tablet-type display terminals to sample households. Coupled with smart meters, the household display terminals show a variety of information such as real-time energy consumption, comparison with the previous day or year, and electricity-saving messages. Thus, Shinchi is not simply a case of disaster reconstruction but also successful realization of a low-carbon society to benefit future generations.

2. Case community

2.1. Outline of the town of Shinchi

Shinchi is a small municipality with a population of about 8000 and a total area of 46.53 km^2, located about 300 km north of Tokyo, near the border between the Miyagi and Fukushima Prefectures, in the northernmost part of the Fukushima Prefecture on the Pacific Ocean side of Japan (**Figure 1**). The population peaked in 1995 and has since declined, with an aging population and a diminished birthrate. The temperature of Shinchi is low compared to Tokyo, with especially cold winters (**Figure 2**). However, the summer temperatures tend to be high; thus, air conditioning is typically required on summer days.

In Shinchi, approximately 120 people died as a result of the Great East Japan Earthquake and subsequent tsunami that occurred on March 11, 2011. The tsunami inundated a large area of land 10 m above sea level, with flooding encompassing about 20% of the town. The tsunami destroyed 516 houses; including damage from the earthquake, 630 houses were totally or partially destroyed. The JR Joban Line Shinchi Station was destroyed, and 40% of agricultural land, 420 ha, was inundated. Furthermore, radioactive contamination due to the Fukushima Daiichi Nuclear Power Plant accident resulted in a mean air radiation dose of 0.2–0.6 μSv/h for the town in 2011, which has been declining ever since.

Before the earthquake, the main railway was the JR Joban Line, but it was closed immediately after the tsunami disaster. The JR Joban Line was reopened in December 2016, allowing access to Sendai, located north of Shinchi. Redevelopment of the district around the JR Shinchi Station, which was damaged by the tsunami, is currently being carried out.

Figure 1. Location of Shinchi.

2.2. The smart hybrid town concept

In the process of disaster reconstruction, Shinchi proposed "the smart hybrid town" concept, which benefits the environment, economy, and society (**Figure 3**). The aim of this concept is to reconstruct the area by combining ICT with a social mechanism that supports the community. Specifically, community residents are linked with the municipality, research facilities, and businesses through a bidirectional information network. In this manner, a prototype for a new community information infrastructure, which shares information on the local environment and community lifestyle, is constructed. With this local information infrastructure, energy consumption monitoring systems are installed in homes, public facilities, and commercial facilities. The aim is to create a "community energy support network" that promotes energy conservation on the energy demand side, an "aging community support network" that accommodates an aging society, and a "community traffic support network" that improves the operation of public transportation, based on vehicle location information from global positioning systems (GPSs) and information supplied by users. With this concept, as a disaster-affected site, Shinchi was selected as a "future city" by Japan's Cabinet Office in December 2011.

Now the focus is on developing an energy management system based on a community energy support network to adjust supply/demand and to increase efficient use of renewable energy. On the supply side, the system forecasts electricity output and CO_2 emissions from the combination of thermal power generation, natural energy, and waste heat utilization and utilizes the forecast as control information. On the demand side, smart meters are provided to every household. These smart meters are not only display monitors but also interactive information

http://dx.doi.org/10.5772/intechopen.75129

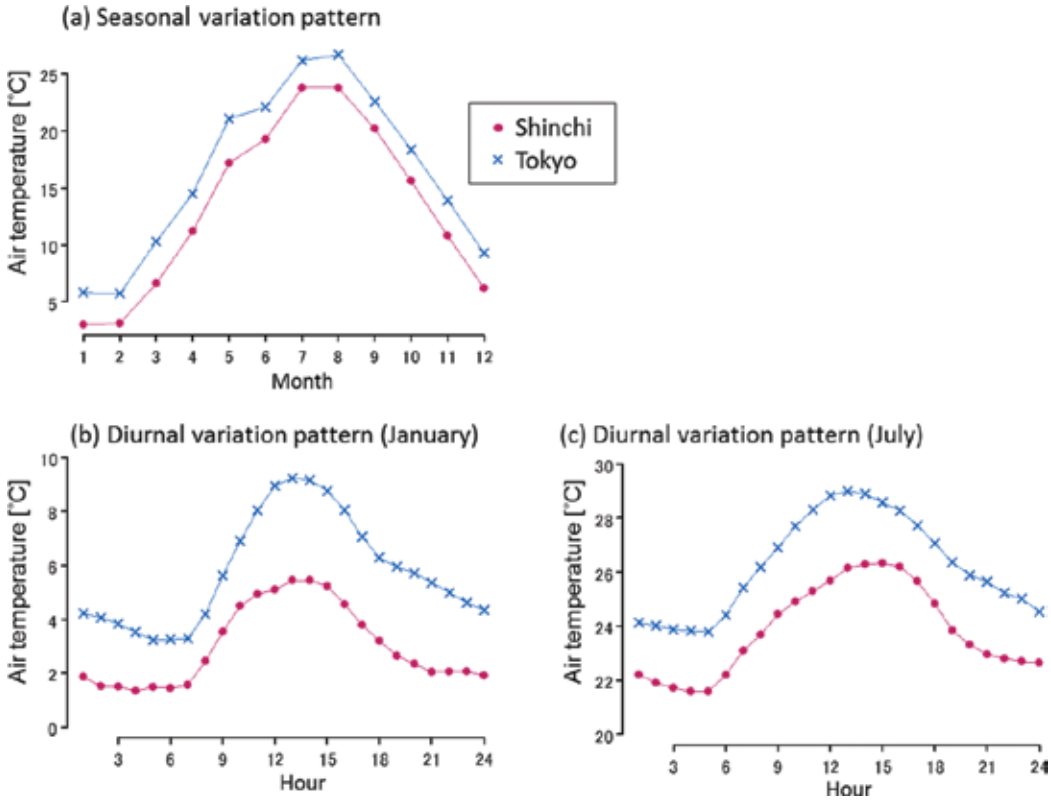

Figure 2. Air temperature variation pattern of Shinchi and Tokyo.

terminals. The information from both the supply and demand sides is gathered and managed at the smart hybrid center to improve energy efficiency. For example, messages are generated and sent to the demand side, asking for electricity savings based on the supply and demand situation. The system can "visualize" electricity-saving behavior and provide information such as energy-saving rankings within the community.

The next step will be the introduction of an automatic demand response control, which is realized by the combination of dynamic pricing and remote control of electrical appliances. Dynamic pricing continuously varies the price of electricity, which can provide economic benefits to consumers who proactively save electricity during power shortages and use electrical appliances such as washing machines when electricity is in surplus. By adjusting supply and demand with automatic dynamic pricing, it also becomes possible to introduce renewable energy sources on a large scale. For example, solar and wind power generation systems should be proactively introduced, as they have significant potential for reducing CO_2 emissions and can be used as emergency energy sources during natural disasters. However, renewable energy sources have drawbacks. For example, their output depends on factors such as the weather, and long-term energy storage is difficult. We are therefore developing a system to balance energy supply and demand by linking the supply and demand sides with the information network.

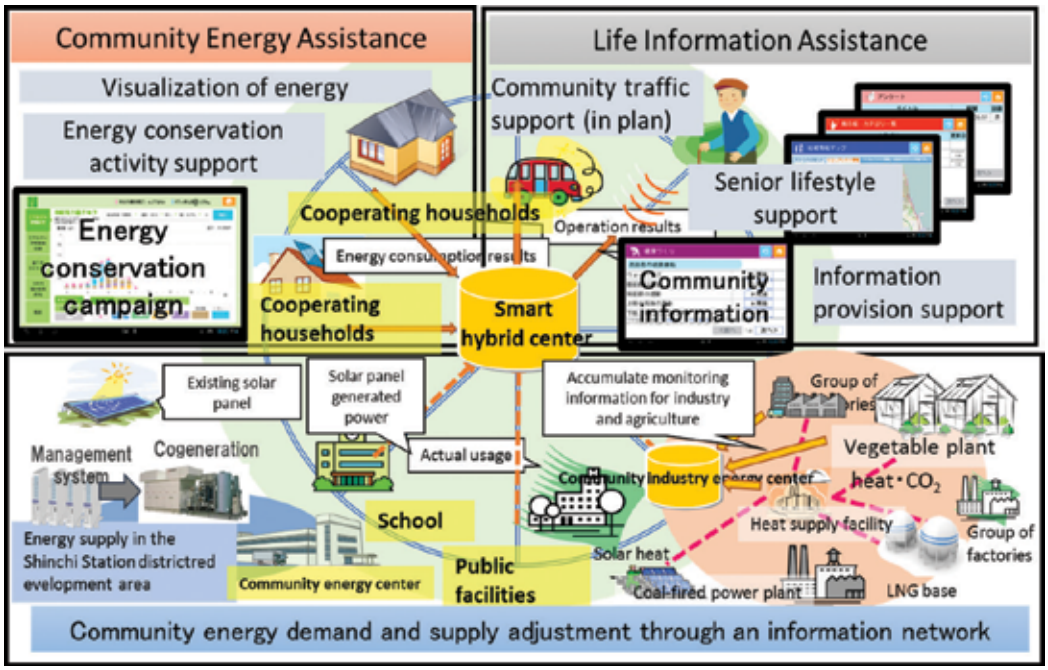

Figure 3. Schematic diagram of the smart hybrid town concept in Shinchi.

With Shinchi's selection as a "future city," discussion regarding reconstruction began, and in March 2013, a Basic Cooperation Agreement was drawn up between Shinchi and the National Institute for Environmental Studies. The National Institute for Environmental Studies has been supporting construction of future visions, maintenance of the ICT base, and comprehensive town reconstruction, based on academic knowledge such as social communication [20, 21].

3. Introduction of the JR Shinchi Station district community energy project system

3.1. Outline of the community energy project

In Shinchi, in addition to reconstruction of infrastructure, the aim is to implement a future city "smart hybrid town" concept, which promotes town reconstruction with a view to benefiting the environment and society. Thus, the reconstruction plan for the area around the JR Shinchi Station, where there was major damage from the tsunami, promotes the introduction of a community energy management system (CEMS) that utilizes natural gas and other clean sources (The Smart Community Project [22, 23]).

In the Smart Community Project, natural gas from a pipeline connected to the soma liquefied natural gas base (currently under construction) will be utilized, and combined heat and power will be supplied from the natural gas CGS to facilities around Shinchi Station. The Smart Community Project involves construction of a community energy center, local heat

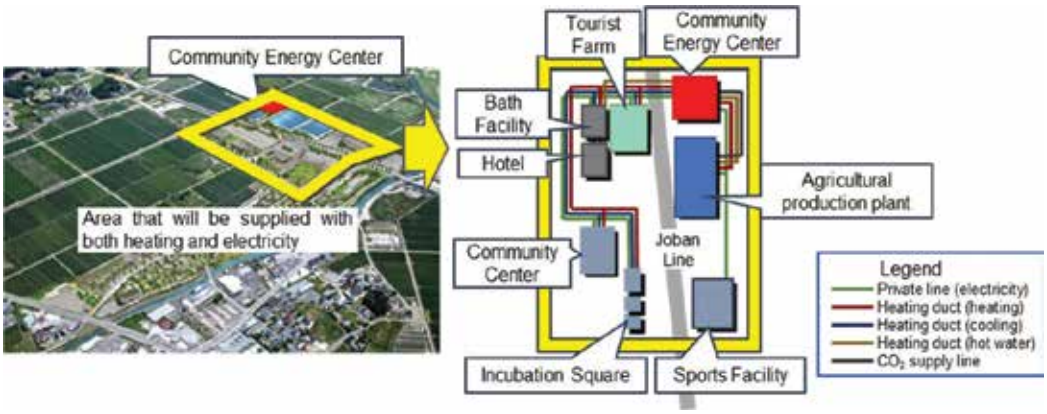

Figure 4. Locations of energy demand facilities in the area surrounding Shinchi Station (revised by authors based on reference [23]).

conduits, a community power grid, and CO_2 supply pipes. In addition, solar power facilities and batteries will be introduced to public facilities. To manage these facilities integrally, CEMS will be utilized.

3.2. Estimating facility energy demand

In this investigation, projections were made regarding the energy demands of facilities in the Shinchi Station area to be served by the distributed energy system. These estimates were based on two sources of data. The first source is an existing study, the 2016 smart community adoption promotion project titled "Master Plan Formulation Project for Revitalization Community Building Centered Around the Use of Energy Produced and Consumed in Shinchi City." The second source is responses obtained during a consultation with people in Shinchi's hotel industry regarding the progress of community reconstruction. These projections are shown in **Figure 4** and **Table 1**.

Facility	Use	Total floor area [m^2]	Supplied energy
Agricultural production plant	Agricultural facility	9000	Electricity, heat (heating/hot water) (CO_2)
Tourist farm	Office	1200	Electricity, heat (cooling/heating)
Sports facility	Futsal court	3000	Electricity
Hotel	Hotel	4770	Electricity, heat (cooling/heating/hot water)
Bath facility	Welfare facility	1400	Electricity, heat (cooling/heating/hot water)
Community center	Cultural facility	1800	Electricity, heat (cooling/heating)
Incubation square	Office	610	Electricity, heat (cooling/heating)

Table 1. Demand facilities in the area surrounding Shinchi Station that are considered in this investigation.

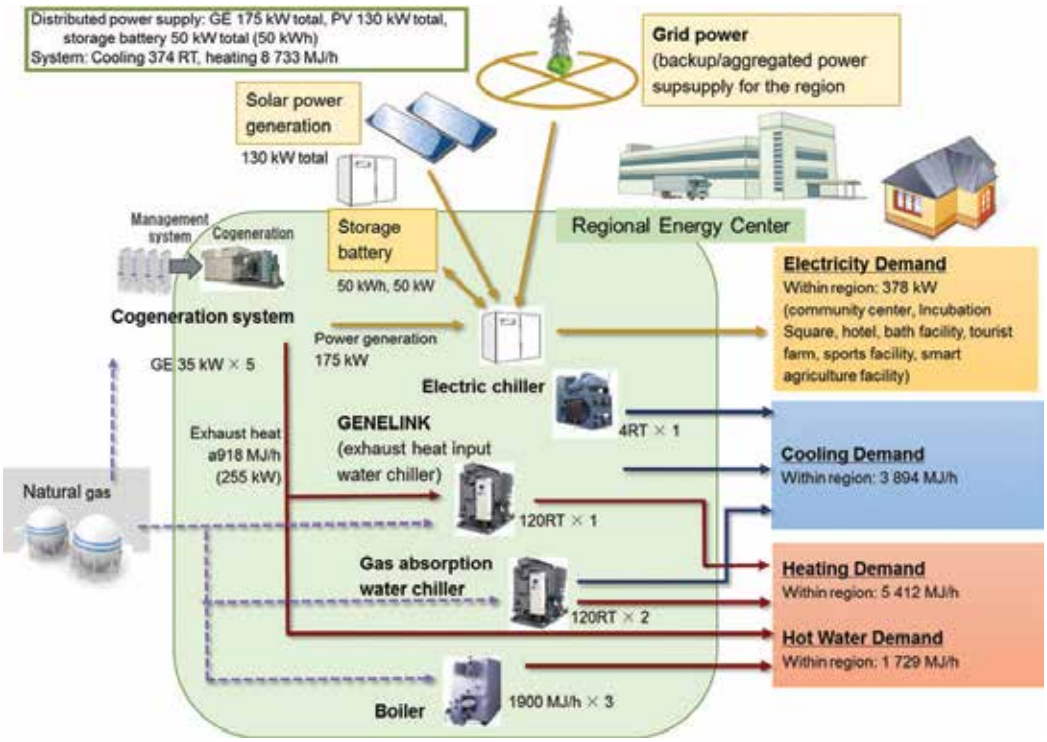

Figure 5. Components of the regional energy center equipment (revised by authors based on reference [23]).

3.3. Energy system overview

An overview of the energy system being planned for this project is shown in **Figure 5**. The system composition follows the plans that were developed during the design of the master plan. The capacity of the solar panels was changed to approximately 75 kW to address actual conditions.

4. Environmental features

4.1. Cogeneration facilities

In this project, we introduce a district heating and cooling system for the Shinchi Station area that utilizes natural gas supplied by pipelines. Additionally, the total energy efficiency is increased by introducing a CGS that utilizes waste heat from power generation.

This project involves cogeneration for cooling requirements during the summer. In Japan, power peaks occur during the summer when air conditioning is being used; thus, to reduce peak loads, the use of absorption chiller-heaters has become widespread. Absorption chiller-heaters produce cold and hot water using waste heat from power generation. These waste heat recovery absorption chiller-heaters are known as “genelink” systems in Japan. Some of

these CGSs obtain steam using gas turbines. However, due to the small scale of this project, the CGSs in this case utilize gas engines, and the waste heat only provides hot water. In this project, cooling and heating requirements are satisfied using genelink systems to produce hot wastewater from power generation. Compared with conventional facilities, genelink systems provide a 10 to 15% increase in energy conservation. Therefore, genelink technology has the potential to be very useful, especially in Asia, where the climate is hot and humid.

4.2. Community energy management system

A CEMS is used to manage the energy consumption for the whole system and to increase the efficiency of energy use. Multiple autonomous power supplies are managed to conserve energy and to reduce CO_2 emissions.

One of the functions of the CEMS is to provide the necessary information for management of the community energy center. Cogeneration equipment is combined with multiple auxiliary heat sources and power purchased from existing power companies (grid power), thus reducing excess heat while avoiding production of unnecessary excess power. With this system, prediction of energy demands and power generation via renewable sources such as solar power becomes essential. Under such complex conditions, the information necessary for energy management personnel to make appropriate decisions is provided by the CEMS, which improves efficient operation of the community energy center.

The second function of the CEMS is demand response control during periods of insufficient power. Demand response control is performed in three steps. The first step is battery storage control at the community energy center. The CEMS controls the charge and discharge of batteries installed at the community energy center. Batteries are charged at night, and when the power procured from the grid exceeds a threshold, it is automatically released. The second step is automatic control of the lighting in public facilities. A control signal from the CEMS is sent to lighting control devices installed in the public facilities. These devices control lighting in areas with minimal impact to users. The third step is transmission of an energy-saving request to facility staff. Facility staff control power usage through predetermined energy-saving activities such as turning off lighting and air conditioning in unoccupied rooms.

4.3. The use of CO_2 by agricultural facilities

It is well known that increased CO_2 concentration improves crop production in greenhouses. Therefore, by sending gas engine exhaust with a high CO_2 concentration into greenhouses, crop growth can be promoted.

The city of Tomakomai in the Hokkaido Prefecture of Japan has been using a trigeneration system (a system involving heat, power, and CO_2) since 2015. Presently, the project is at the stage of recruiting companies that operate agricultural facilities and preparing these facilities so that a supply of CO_2 can be started immediately upon completion of the company recruitment process.

5. Residential interface for the community energy project

5.1. Outline of the community information system

In the Shinchi community energy project, heat is supplied to the Shinchi Station area through cogeneration, while power is supplied to surrounding residences. In addition, the plan includes construction of residences such as company dorms for community companies and permanent residence housing in the area around the station.

Based on this plan, the National Institute for Environmental Studies has developed an information system that will be used as the residential interface for the community energy project. This information system is presently in the social demonstration and implementation phase. It was developed as part of the future city "smart hybrid town" concept discussed above. With this information system, a central control server system "smart hybrid center" is constructed on the cloud server, and users utilize a tablet terminal called the "Shinchi Life Assist Tablet" to receive information. In this manner, a bilateral community ICT base is actualized.

Figure 6 shows a schematic of the energy in the system that is currently being developed. At its most basic, the supply is power procured from existing power companies, but in the future, it will be power supplied from the community energy project in Shinchi. At that time, cogeneration

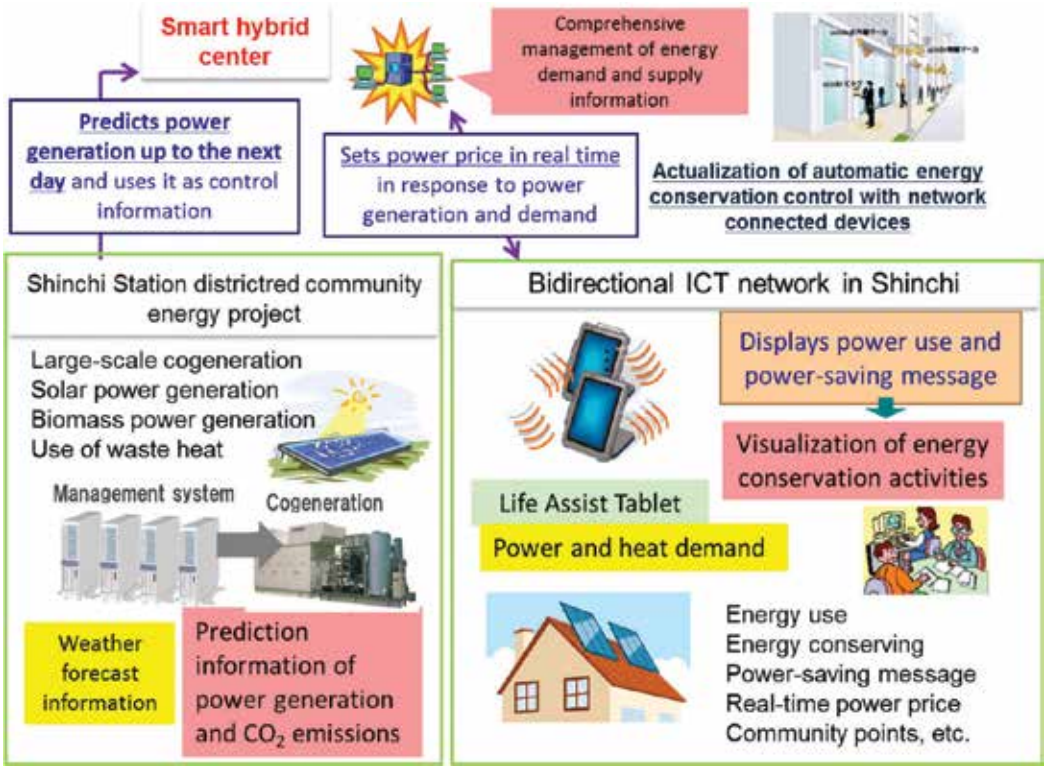

Figure 6. A control flow chart of the community information system.

and renewable energy will be combined to predict power generation and CO_2 emissions, and this prediction information will be used as the control information. On the demand side, a power measurement device was installed at each home with the system introduced (**Figure 7**), and each home will use a "Shinchi Life Assist Tablet" as the display terminal.

The power measurement device analyzes the main power line and the branch lines using a current transformer (CT). This device measures the purchased power from the electric power system at the distribution board. The purchasing and selling of power are also measured by a CT for photovoltaic (PV) power generation systems.

A connection with the CEMS that comprehensively manages supplier information in the Shinchi Station area still needs to be developed, but various other functions of the system, such as visualization of energy use on the demand side, are already available. At the present phase of social demonstration and implementation, tablet terminals have been distributed to 75 households in Shinchi. Briefing sessions, individual visits, seminars, and opinion exchange meetings are often held. Operation is stable and communication with residents is maintained. The electricity consumption data obtained by this system have been already utilized for energy consumption modeling in Shinchi [24]. In 2016, the system was opened to allow for use with typical personal computers and smartphones in addition to the distributed tablet terminal. In this manner, information can be remotely obtained and viewed in real time.

Figure 8 shows the display on a tablet terminal. Power consumption can be viewed in real time with the "Shinchi Life Assist Tablet," which displays a comparison with the previous day or year, the energy conservation ranking compared to other households, power uses within the community, and power-saving messages. Through this process, the system encourages

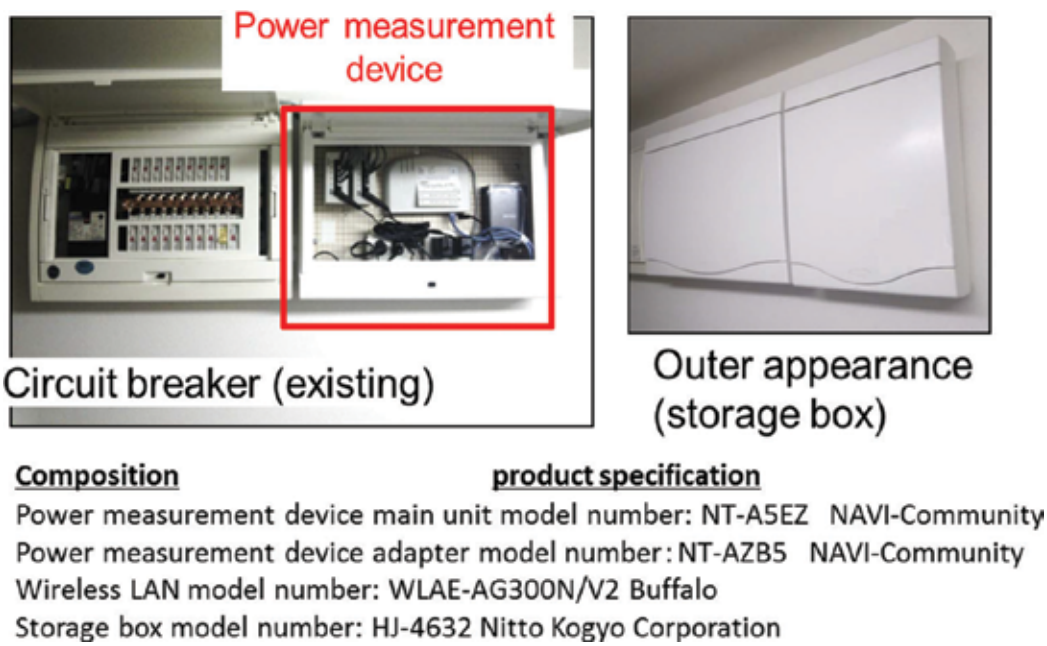

Figure 7. Power measurement device installed in each home.

Figure 8. Example of the energy display on a Shinchi Life Assist Tablet.

people to save electricity proactively during power shortages, thereby voluntarily adjusting the supply and demand balance and reducing or shifting power peaks. Furthermore, through incentives such as community energy conservation campaigns and provision of information regarding power usage for each household, community energy supply and demand can be improved, and actual energy conservation activity can be measured.

A community energy conservation campaign has already been implemented using this information system, contributing to improved awareness of energy conservation and a more engaged community. This energy conservation campaign also demonstrates implementation of energy conservation activities; effective results were obtained regarding the provision of energy conservation information and added economic incentives for residents [25].

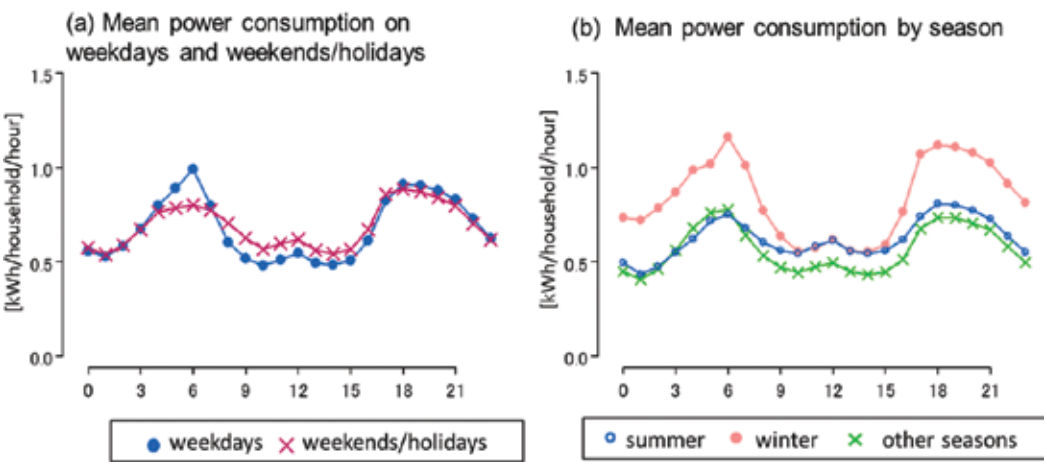

Figure 9. Example of power monitoring results.

5.2. An example of power monitoring results

Figure 9 shows an example of a data summary obtained from power monitoring. Because there is a large variation among individual data, we have presented diurnal patterns averaged for weekdays, weekends/holidays, and seasons. Results show a diurnal pattern of typical domestic energy consumption, with peaks in the morning and evening. When weekdays and weekends/holidays were compared in **Figure 9(a)**, a large peak was observed around 6 a.m. on weekdays, which rapidly decreased by around 9 a.m. In contrast, this trend was much weaker on weekends/holidays, and power usage was higher during the day on weekends/holidays. Seasonal comparison based on **Figure 9(b)** shows a large peak in the morning during winter, but summer usage is similar to spring and fall usage, indicating that a large heating load occurs as people turn their heaters on upon waking. Subsequently, power usage during the day before bedtime was higher for summer and winter than the other seasons, showing that increased cooling and heating loads occur in the summer and winter months.

5.3. Connection with the Shinchi Station district CEMS and future outlook

Introduction of automatic demand response control is being evaluated for the community energy project in the JR Shinchi Station district redevelopment area. Automatic demand response control involves a bidirectional information network that connects the demand and supply sides and automatic control of cooling, heating, and lighting based on the demand. In this manner, reductions can be made to peak loads and excess power at existing power plants, the heat and power balance at cogeneration plants can be adjusted, and the demand and supply balance can be controlled when introducing unstable power, such as natural energy.

6. Energy simulations

Energy simulations were used to calculate electricity and gas consumption, which is the core component of fuel costs in energy service businesses. The input conditions for the energy simulation are summarized below.

6.1. Simulation model and energy demand data

In this simulation, input data were provided, and we calculated the load allotment of various heat sources based on input data and the setting of the driving order. Next, we calculated city gas and electricity consumption based on the coefficient of performance (COP) of the heat source equipment, efficiency data, and so on. Based on this result, we calculated the energy savings, CO_2 reductions, and running costs for this system. The calculation for the flow of energy simulation is shown in **Figure 10**.

The estimate for energy demand was based on the consumption rates that were selected during the master plan investigation (**Tables 2** and **3**). In turn, these calculated consumption rates were based on reference materials from past studies, hearings, and estimates made for existing similar facilities (please refer to the master plan report for details).

6.2. Estimation of energy demand

The energy demand in each period is different because the expected opening date for each facility varies. The energy demand for each operating period is summarized below.

6.2.1. Standard: after all facilities are in operation

Values shown below are estimates of the demand in the standard scenario. The construction of the energy system and evaluation of the net profit are based on these values (**Table 4**).

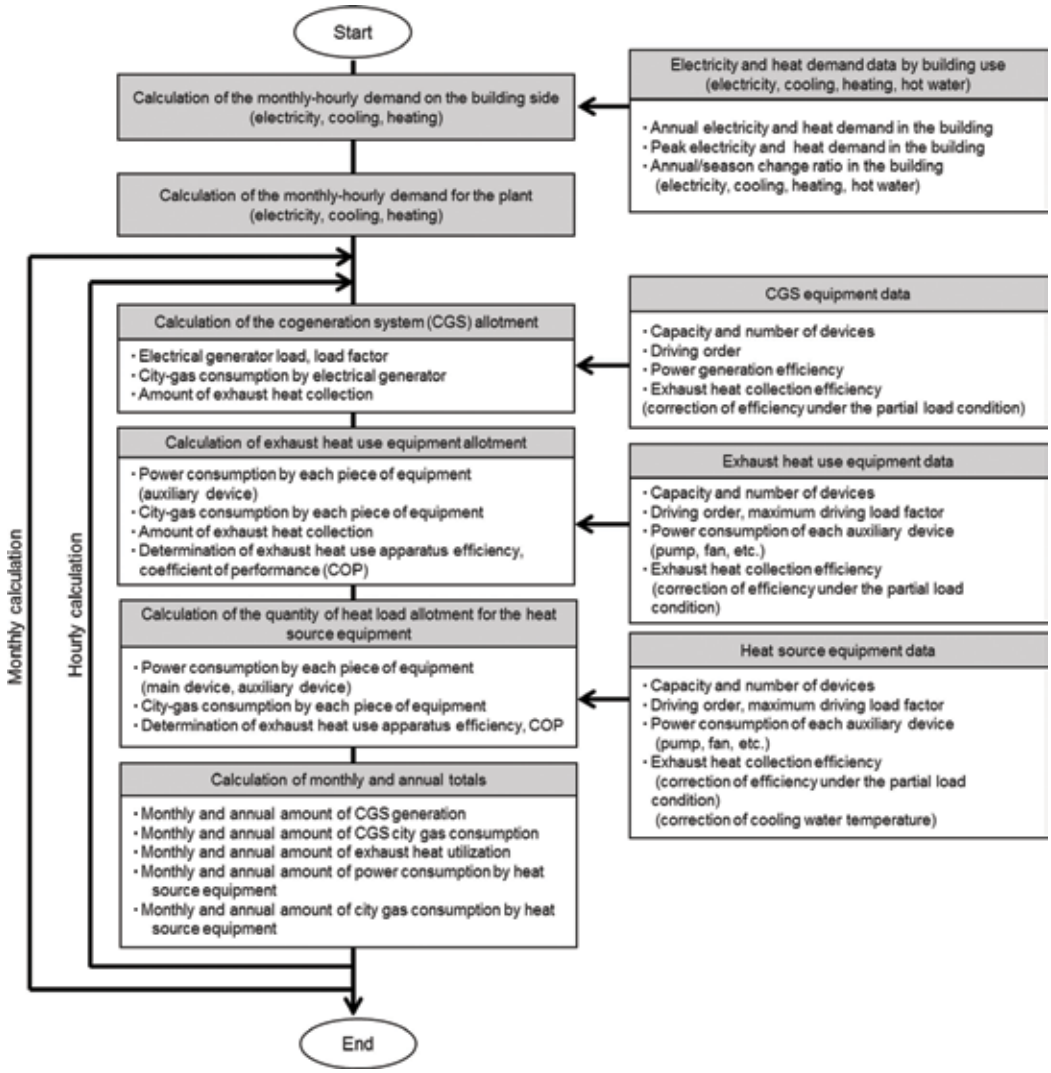

Figure 10. Calculation for the flow of energy simulation.

Facility	Electricity	Cooling	Heating	Hot water
	[W/m²]	[kJ/m²·h]		
Agricultural plant	5	—	249	—
Tourist farm	37	357	268	—
Sports facility	11	—	—	—
Hotel	31	472	369	300
Hot bath facility	35	174	247	213
Community center	20	418	322	—
Incubation square	37	357	268	—

Table 2. Maximum energy demand consumption rate.

6.2.2. Early phase 1: early phase of project start

The energy demand in the early phases of the project, when only the hotel and bath facility are in operation, was calculated as shown in **Table 5**.

6.2.3. Early phase 2: public facilities open

The energy demand, when the public facilities (community center, incubation square, and sports facility) were open, 3 months after the beginning of the project, was estimated and tabulated (**Table 6**).

6.3. Estimation of energy consumption and CO_2 emissions

The energy consumption (including electricity, natural gas, and water and sewage requirements) of the system was calculated through an energy simulation for each of the operation periods described above.

Facility	Electricity	Cooling	Heating	Hot water
	[kWh/m²]	[MJ/m²·year]		
Agricultural plant	9	—	320	—
Tourist farm	115	295	56	—
Sports facility	26.5	—	—	—
Hotel	183	366	200	420
Hot bath facility	120	232	238	638
Community center	63	385	260	—
Incubation square	115	295	56	—

Table 3. Annual energy demand consumption rate.

Facility	Total floor area [m²]	Electricity	Cooling	Heating	Hot water
		[MWh/year]	[GJ/year]		
Agricultural plant	9000	81	—	2880	—
Tourist farm	1200	138	354	67	—
Sports facility	3000	80	—	—	—
Hotel	4770	873	1746	954	2003
Hot bath facility	1400	168	325	333	893
Community center	1800	113	693	468	—
Incubation square	610	70	180	34	—
Total	21,780	1523	3298	4737	2896

Table 4. Annual energy demand (standard).

The calculated results are shown in **Figure 11**.

CO_2 emissions were calculated based on the simulated energy consumption under standard conditions after all facilities are operational. For comparison, CO_2 emissions were calculated for a case in which conventional systems were introduced in the individual buildings. The results show that a CO_2 reduction of about 20% can be expected by introducing the community energy system (**Figure 12**).

6.4. Project cost calculations and investigation of the business plan

Various quantities, such as expenses and revenues related to the commercialization of this system, were included in the calculations. Because most of the initial costs were covered by a subsidy, the investigation focused on the operational costs. The two scenarios that were considered in the calculation of business income and expenditures are as shown in **Figure 13**.

Facility	Total floor area [m²]	Electricity	Cooling	Heating	Hot water
		[MWh/year]	[GJ/year]		
Agricultural plant					
Tourist farm					
Sports facility					
Hotel	4770	873	1746	954	2003
Hot bath facility	1400	168	325	333	893
Community center					
Incubation square					
Total	6170	1041	2071	1287	2896

Table 5. Annual energy demand (early phase 1).

Facility	Total floor area [m²]	Electricity	Cooling	Heating	Hot water
		[MWh/year]	[GJ/year]		
Agricultural plant					
Tourist farm					
Sports facility	3000	80	—	—	—
Hotel	4770	873	1746	954	2003
Hot bath facility	1400	168	325	333	893
Community center	1800	113	693	468	—
Incubation square	610	70	180	34	—
Total	11,580	1304	2944	1789	2896

Table 6. Annual energy demand (early phase 2).

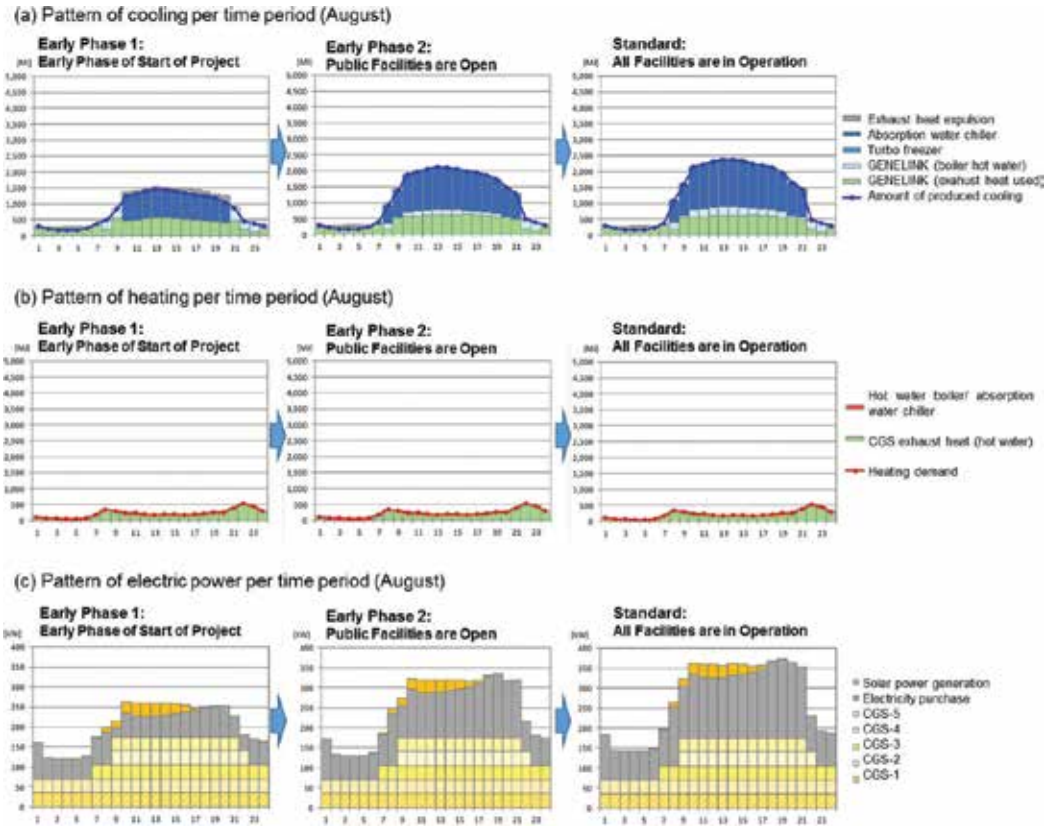

Figure 11. Results of the energy simulation (operation status in the summer season for each standard scenario).

We have performed a detailed cost evaluation to support the local government. However, as an energy company is now going to be established, the business income and expenditure are not openly available as official information from the local government. Therefore, the quantitative

evaluation result shown here is not official information but is our individual research result. In this evaluation, although the costs are set realistically, the introduction scenario is given hypothetically. The costs of sales, such as electricity costs, natural gas costs, water and sewage

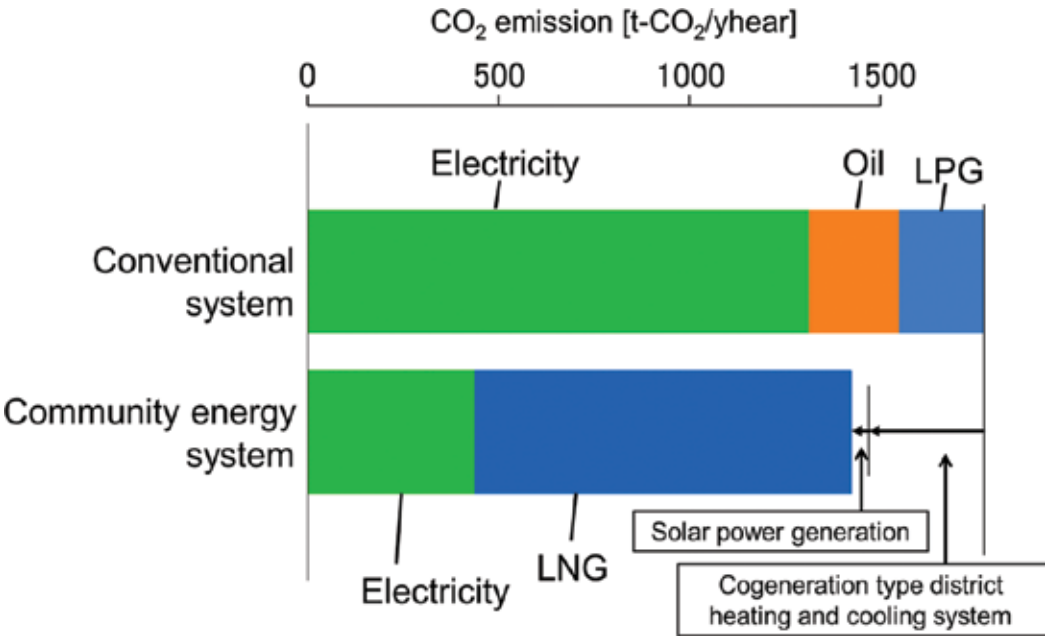

Figure 12. Estimation of the CO_2 emissions for each system.

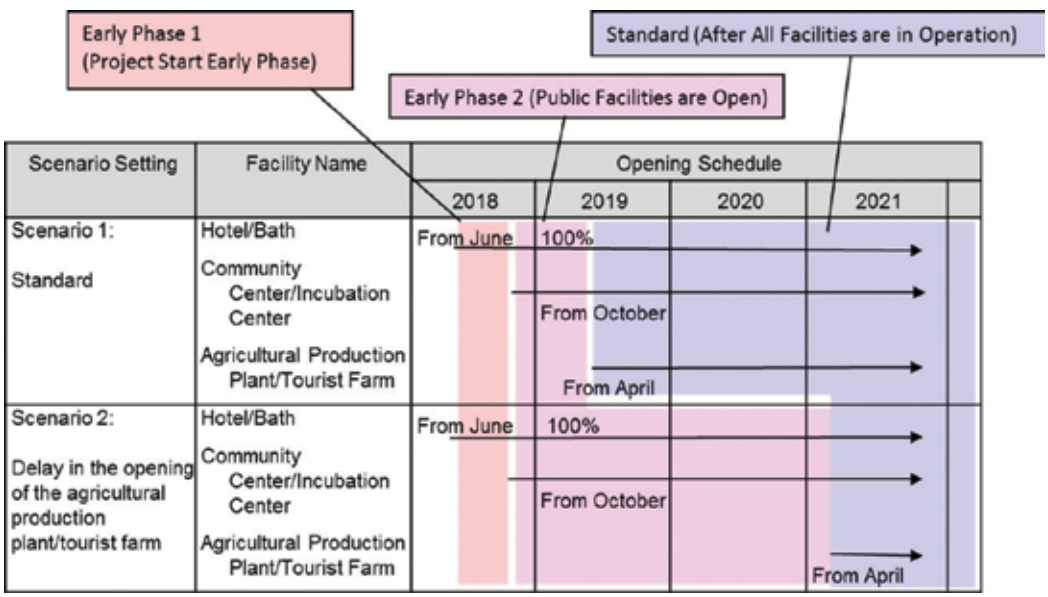

Figure 13. Investigated scenario settings and considerations regarding estimations of operation periods.

http://dx.doi.org/10.5772/intechopen.75129

costs, CGS/heat source maintenance costs, consumable part costs, equipment repair costs, CEMS/home energy management system (HEMS) operation costs, personnel costs, and business operation costs, were calculated based on the scenarios.

The result of the evaluation is shown in **Figure 14**. Based on the above scenarios, it can be concluded that the viability of this business depends on whether the opening of the agricultural production facility/tourist farm is delayed or not. In addition, since around 60% of the sales revenue comes from the hotel/bath facilities, it can be deduced that stable operation of these facilities is crucial. At this stage, it is essential to hold meetings with the managers of the hotel and bath facilities to examine their demands and obtain appropriate estimates of future requirements.

As shown by the results, in the standard scenario (Scenario 1), the business is expected to yield an operating profit after the second year, and the business is stable and performing well. In the scenario in which the opening of the agricultural production facility and tourist farm is delayed (Scenario 2), the business will post a loss for the first several years but will yield a profit after the agricultural production facilities open. The business is expected to recover the losses in the seventh year, in 2024. Therefore, it is necessary to obtain additional information from the city regarding the opening of the agricultural facility and tourist farm, including business details and the energy demand of the hotel and bath facility. The impact of such information on

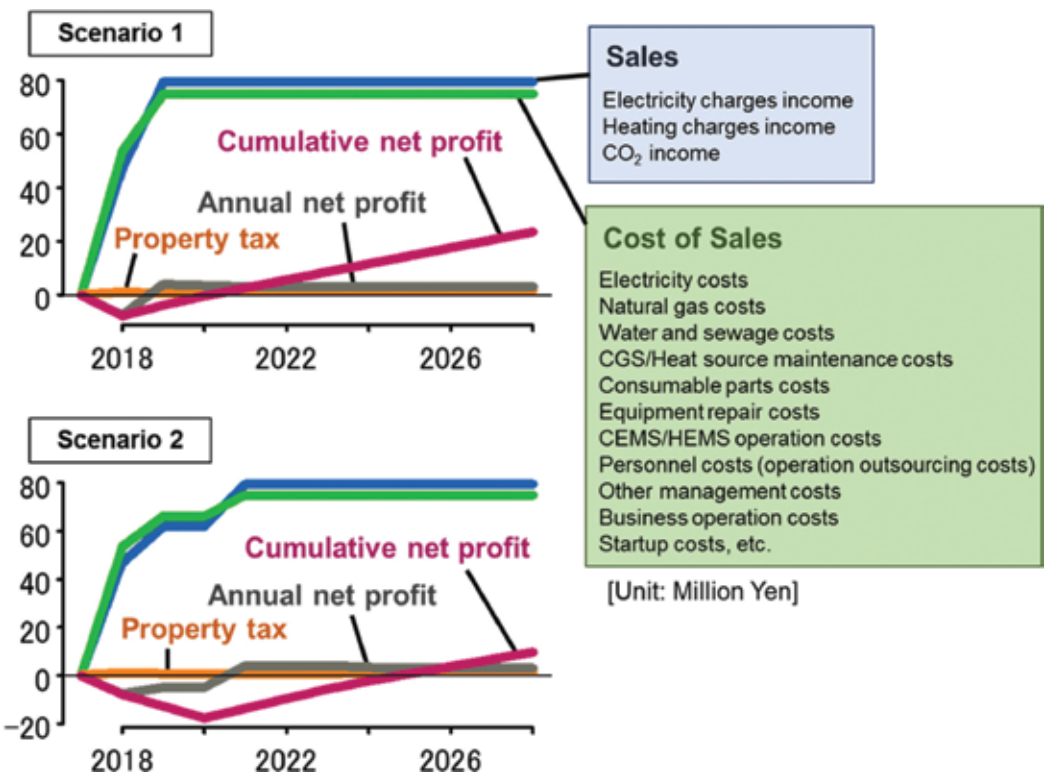

Figure 14. Estimation of business earnings and expenses.

businesses, which is the subject of the city's call for submissions, will have to be investigated. It is also necessary to consider adjusting the heating and electricity charges as needed.

7. Conclusions

In this paper, we introduced an example of a community energy project that is in progress in the town of Shinchi. For the redevelopment of the JR Shinchi Station district being carried out by the local government of Shinchi, construction of the cogeneration-type district heat and cooling system and community energy system is currently in progress.

In this case, the key to improving environmental performance is effective energy management that combines heat and power. In other words, multiple autonomous energy management systems must work together to optimize demand and supply through energy demand predictions and power consumption reductions during peak energy demand, ultimately improving energy conservation and achieving a low-carbon society. The heat and power supply system introduced in this paper is a useful and advanced example. This technology can be developed in other communities as a model of local production and consumption of heat and power, which promotes locally produced energy and vitalizes the community.

We developed a central control server system known as the "smart hybrid center" and a user information terminal, the "Shinchi Life Assist Tablet," for which demonstration experiments involving local residents have already begun. With this information network, continuous power monitoring in households has been implemented, providing energy consumption data for the present community. In addition, by examining individual household energy consumption, power-saving activities were proposed to suit each household, heightening power-saving awareness in the community and optimizing power demand. Utilizing an existing base of 75 households and adding residences being constructed around Shinchi Station to this base, energy demand information from typical households can be collected. By sharing information on CO_2 emission reduction efforts in the area among residents, new communities around the station can be planned. As community-linked energy conservation measures develop, the new smart community can progress smoothly. Residents can gain energy-related knowledge and can be expected to approve of the system. Furthermore, through an integrated supply and demand energy management system that is linked via the CEMS, automatic demand response control can be introduced, and further improvements in energy efficiency and CO_2 emission reductions can be expected.

Acknowledgements

The project introduced in this paper is being conducted by the Smart Community Adoption Promotion Project, with the National Institute for Environmental Studies acting as the academic advisor and supervisor, based on the Basic Cooperation Agreement, with cooperation of related companies. Many companies, such as Japan Petroleum Exploration Co., Ltd., Keiyo Plant Engineering Co. Ltd., Japan Environment Systems Co. Ltd., and NEC Global, are participating as business entities.

Author details

Yujiro Hirano*, Shogo Nakamura, Kei Gomi, Takuya Togawa, Tsuyoshi Fujita and Makoto Ooba

*Address all correspondence to: yhirano@nies.go.jp

National Institute for Environmental Studies, Tsukuba, Japan

References

[1] National Institute for Environmental Studies. 2050 Low-Carbon Society Scenario [Internet]. Available from: http://2050.nies.go.jp/LCS/eng/japan.html [Accessed: July 30, 2017]

[2] "2050 Japan Low-Carbon Society" scenario team. Japan Scenarios and Actions towards Low-Carbon Societies (LCSs) [Internet]. Available from: http://2050.nies.go.jp/report/file/lcs_japan/2050_LCS_Scenarios_Actions_English_080715.pdf [Accessed: August 12, 2017]

[3] "2050 Japan Low-Carbon Society" Scenario Team. Japan Roadmaps towards Low-Carbon Societies (LCSs) [Internet]. Available from: http://2050.nies.go.jp/report/file/lcs_japan/20090814_japanroadmap_e.pdf [Accessed: August 12, 2017]

[4] Murakami S, Levine M D, Yoshino H, Inoue T, Ikaga T, Shimoda Y, Miura Y, Sera T, Nishio M. Sakamoto Y, Fujisaki W. Energy Consumption, Efficiency, Conservation, and Greenhouse Gas Mitigation in Japan's Building Sector. Institute for Building Environment and Energy Conservation (IBEC); 2006. 84 p

[5] Murakami S, Levine MD, Yoshino H, Inoue T, Ikaga T, Shimoda Y, Miura S, Sera T, Nishio M, Sakamoto Y, Fujisaki W. Overview of energy consumption and GHG mitigation technologies in the building sector of Japan. Energy Efficiency. 2009;**2**:179-194

[6] Hirano Y, Fujita T, Bunya S, Inoue T. Examination of how various measures in urban districts affect the development of low carbon cities - a case study of cooling energy savings in the city of Kawasaki. Environmental Science (in Japanese). 2011;**24**(4):255-268

[7] Hirano Y, Gomi K, Nakamura S, Yoshida Y, Narumi D, Fujita T. Analysis of the impact of regional temperature pattern on the energy consumption in the commercial sector in Japan. Energy and Buildings. 2017;**149**:160-170. DOI: 10.1016/j.enbuild.2017.05.054

[8] Hirano Y, Fujita T. Analysis of effects of climatic conditions on energy consumption in office buildings. Journal of Japan Society of Civil Engineers, Ser.G(Environmental Research) (in Japanese). 2011;**67**(5):I_103-I_111

[9] Hirano Y, Fujita T. Simulating the CO_2 reduction caused by decreasing the air conditioning load in an urban area. Energy and Buildings. 2016;**114**:87-95. DOI: 10.1016/j.enbuild.2015.06.033

[10] Komiyama R, Fujii Y. Analysis of Japan's long-term energy outlook considering massive deployment of variable renewable energy under nuclear energy scenario. Electrical Engineering in Japan. 2012;**132-B**(9):780-792

[11] Zhang Q, Mclellan BC. Review of Japan's power generation scenarios in light of the Fukushima nuclear accident. International Journal of Energy Research. 2014;**38**:539-550. DOI: 10.1002/er.3158

[12] Benjamin DL. Evaluation of post-Fukushima Japanese electricity strategies: A stochastic simulation model. International Journal of Energy Research. 2014;**38**:1578-1598. DOI: 10.1002/er.3181

[13] Iwamura K. Smarter social infrastructure and its operation and management. Environmental information science (in Japanese). 2015;**44**(3):12-18

[14] Hall HL. Fukushima Daiichi: Implications for carbon-free energy, nuclear nonproliferation, and community resilience. Integrated Environmental Assessment and Management. 2011;**7**(3):406-408. DOI: 10.1002/ieam.225

[15] Suzuki A. Managing the Fukushima challenge. Risk Analysis. 2014;**34**(7):1240-1256. DOI: 10.1111/risa.12240

[16] Yamane F, Ohgaki H, Asano K. The immediate impact of the Fukushima Daiichi accident on local property values. Risk Analysis. 2013;**33**(11):2023-2040. DOI: 10.1111/risa.12045

[17] Hirano Y, Fujita T, Takahashi T. Examination and formulation of household CO_2 emissions and energy uses in major cities in Japan. Environmental Systems Research (in Japanese). 2010;**38**:309-316

[18] Kitakaze R. Power retail business managed by local governments in electricity deregulation era: Current states, challenges, potentialities. Environmental Information Science (in Japanese). 2016;**45**(1):32-38

[19] Hayashi Y. Japanese energy management in smart grid after the great East Japan earthquake. Electrical Engineering in Japan. 2014;**189**(2):20-25

[20] Fujita T, Hirano Y. New town planning from Fukushima - Regional innovation in Shinchi-machi. Japan Society of Civil Engineers (JSCE) Magazine (in Japanese). 2016; **101**(12):60-63

[21] Hirano Y, Gomi K, Togawa T, Nakamura S, Ooba M, Fujita T. Multidisciplinary reconstruction support to evolve from disaster recovery to environmental creation. Environmental Information Science (in Japanese). 2017;**46**(1):47-52

[22] Shinchi town, UR Linkage, NTT Facilities, Keiyo plant engineering co. ltd., NEC global. Master plan formulation project for revitalization community building centered around the use of energy produced and consumed in Shinchi town. The 2016 smart community adoption promotion project (in Japanese); 2016. 138 p

[23] Keiyo Plant Engineering Co. Ltd. The report on analysis and evaluation of the commercialization of the distributed energy system (in Japanese). The National Institute for Environmental Studies. 2017:43

[24] Shiraki H, Nakamura S, Ashina S, Honjo K. Estimating the hourly electricity profile of Japanese households-coupling of engineering and statistical methods. Energy. 2016;**114**: 478-491

[25] Shiraki H, Tanaka H, Nakamura S. Effect of energy saving campaign in Fukushima. Booklet series of environmental emergency research, The National Institute for Environmental Studies. 2016;**3**:6-10

Chapter 6

Renewable and Sustainable Air Conditioning

Muhammad Mujahid Rafique and Shafiqur Rehman

Additional information is available at the end of the chapter

http://dx.doi.org/10.5772/intechopen.73166

Abstract

The simultaneous control of air temperature and humidity are the main functions of an air conditioner in order to provide human thermal comfort conditions. The conventional vapor compression air conditioning system cools the air below its dew point temperature to remove the moisture from the air. In hot and humid regions, considerable amount of energy is used for moisture removal using these systems. Because of the high energy cost of conventional systems and poor control of latent load, need arises for some alternative cooling devices. In this chapter alternative and renewable based air conditioning systems are described to overcome the increasing use of primary energy by conventional air conditional systems. Desiccant cooling is found to be a suitable alternative to these cooling systems. The configurations of desiccant cooling systems to achieve better performance are described. Furthermore, a comparative analysis of desiccant cooling system operating on ventilation and recirculation cycle has been presented. The results showed the system operating under the ventilation cycle has a better coefficient of performance as compared to the recirculation cycle because of the less input/regeneration heat required. The desiccant cooling technology is both cost-effective and environmental friendly as no refrigerant is used in these systems.

Keywords: renewable based cooling, sustainability, energy efficient, desiccants, evaporative cooler

1. Introduction

The increasing population, technological advancements, and materialistic living standards have significantly increased the energy demand for cooling devices in last few decades. Almost 15% of world's total energy is consumed by air conditioning systems. The human thermal comfort conditions are described in terms of efficient control of sensible and latent load. The basic function of an air conditioner is to simultaneously control temperature,

humidity, and quality of supply air as shown in **Figure 1**. Generally, in order to provide thermal comfort conditions to the occupants, an air conditioning system should maintain indoor air temperature of 18–26°C and relative humidity of 40–70%. The accurate and effective control of humidity becomes more crucial for applications where less moist environment is required.

The term sensible heat ratio is used to determine the performance of an air conditioner in terms of its ability to control sensible and latent load. Smaller the value of sensible heat ratio larger is the value of latent cooling loads. The value of sensible heat ratio is about 0.75 for the commonly used conventional vapor compression air conditioning system. The vapor compression air conditioning system controls the latent load by condensation process. The air is cooled below its dew point temperature to remove the moisture and then reheated again to desired supply temperature. A considerable amount of energy is wasted during this process of overcooling and reheating which lowers the system overall coefficient of performance. Moreover process of condensation creates an environment for the growth of harmful fungi and bacteria. Because of the high energy cost of these conventional systems and poor control of latent load, need arises for some alternative cooling devices.

To avoid the excessive waste of energy, an alternative way to achieve desired moisture reduction is the use of desiccant dehumidification system in which a desiccant material absorbs moisture from the humid air. Thermal energy is used to regenerate the desiccant material and cycle continues. The system is both cost-effective as well as environmental friendly. Since no refrigerant is used in these systems so depletion of ozone layer is minimized. Low-temperature heat sources, like waste heat from engine or solar heat, can be used to operate the system.

A good desiccant should have better moisture absorption capability and lower temperature of regeneration. Different types of new desiccant materials with high dehumidification performance have been proposed in past few years. These materials have the potential to improve

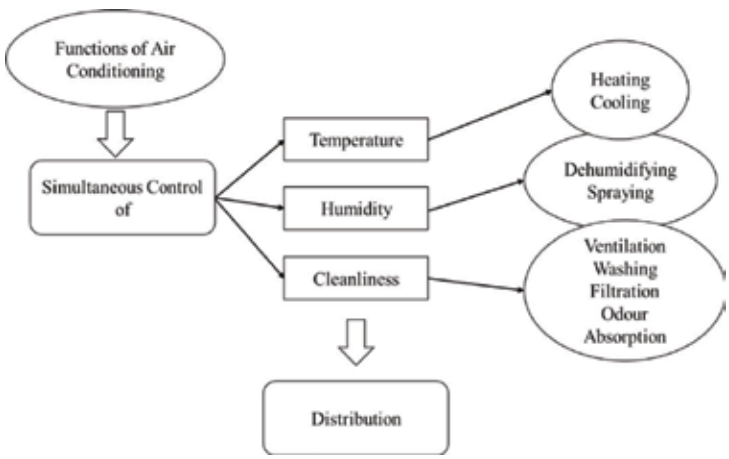

Figure 1. The basic functions of an air conditioner.

http://dx.doi.org/10.5772/intechopen.73166

the performance of liquid desiccant cooling systems because of lower heat input required for its regeneration. The desiccant cooling system can either be solid or liquid depending upon the type of desiccant material used. Liquid desiccants have advantage over the solid desiccants that these only requires low-temperature heat source to drive the system. The available configurations of the desiccant cooling system are shown in **Figure 2** [1].

The development of desiccant-based cooling technology is a topic of interest now a day and has been widely investigated. Most recently, Rafique et al. [2] investigated the thermal and exergetic performance of a newly developed absorption type desiccant dehumidifier. The aim of this study was to lower the required regeneration temperature by employing liquid desiccant instead of solid desiccant materials. The computed results show that better supply air conditions can be obtained to provide human comfort in the hot and humid climate with effectiveness of the system largely dependent on air flow rate, wheel width, and humidity ratio of the process air. The annual average value of dehumidification performance is found to be 0.55 which shows that system can control the latent load efficiently throughout the year. In another study, Rafique et al. [3] studied the performance of desiccant assisted cooling system for five different sites in Saudi Arabia. The coefficient of performance (COP) of the system was observed to vary from 0.275 to 0.476 for different locations. Kabeel et al. [4] the performances of a solar energy assisted desiccant air conditioning system with different types of storage materials are numerically investigated.

In other studies the development of new configurations [4, 5], parametric and statistical analysis [6, 7], second law and anergy analysis [7, 8], exergoeconomy [9] and different other advancements [10] for desiccant cooling systems have been studied. The desiccant-based technology is on path of development but still a lot of work needs to be done in order to

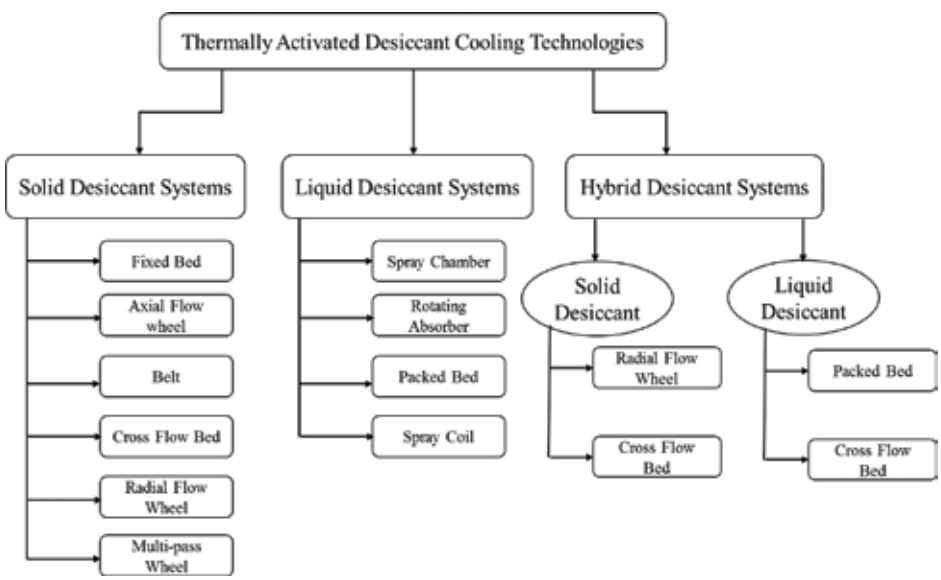

Figure 2. Different configurations for various desiccant systems [1].

make this technology with market friendly. In this regard, the major aim of this chapter is to introduce with the concept of alternative cooling technology, its need and recent developments. Different cooling cycles which can be employed for better performance of the system have been described in this chapter. Based on the developed mathematical model, a comparison has been made between two different configurations of desiccant cooling system.

2. Need of renewable based technology

The use of renewable energy is gaining attention and lot of work still need to be done for different technologies. The overall world energy consumption is presented in **Figure 3**. The increasing use of fossil fuels not only causing fast depletion of energy sources but also causes emitting harmful gases which directly affects the human life. A summary of direct and indirect effects of climatic changes due to burning of these fossil fuels are illustrated in **Figure 4** [11]. Understanding the above mentioned hidden impacts of fossil fuels is critical for evaluating the true cost of fossil fuels—and for promoting our choices for future energy production. These hidden costs must be considered while comparing feasibility of clean energy sources.

Furthermore, major part of the primary energy consumed in the building is accounted for cooling or heating. With regard to the use of energy consumption for HVAC technology, its demand is increasing rapidly, as shown in **Figure 5** [1]. This increasing use of HVAC technology encourages developing alternative cooling technologies which can efficiently utilize renewable energy for its operation.

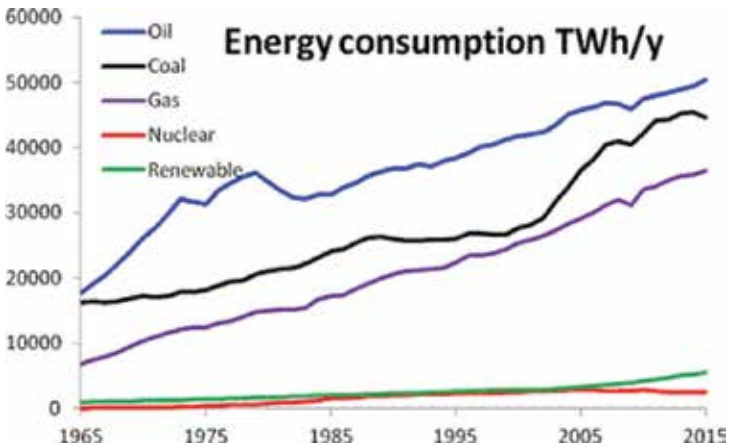

Figure 3. The world's energy consumption according to data of 2015. Source: BP statistical review of world energy 2016.

http://dx.doi.org/10.5772/intechopen.73166

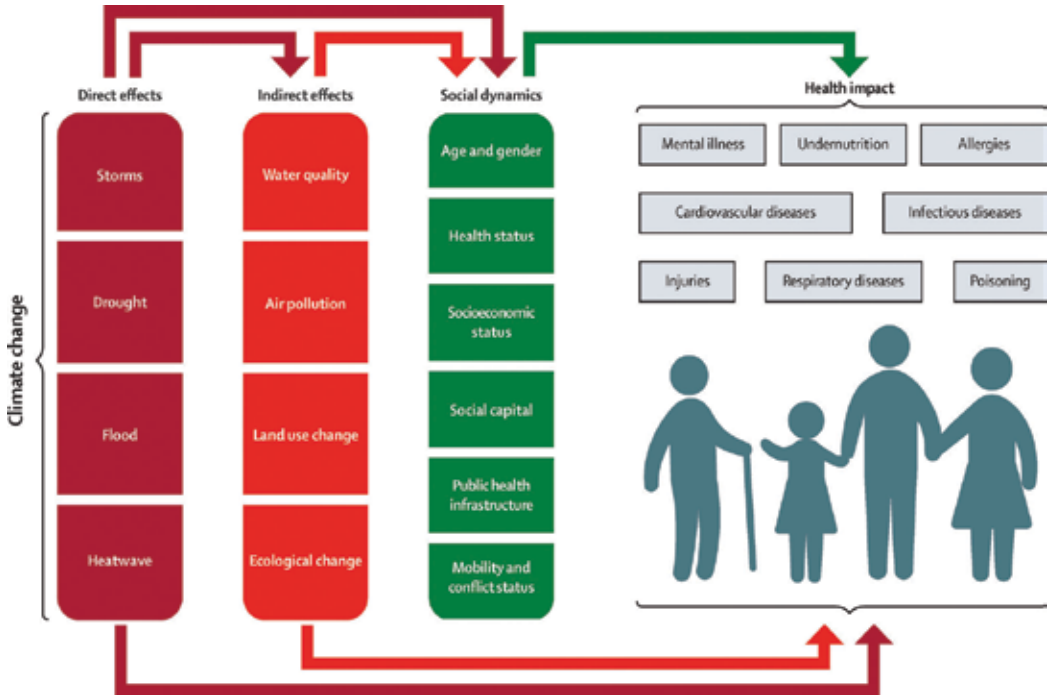

Figure 4. Direct and indirect effects of climate change on public health [11].

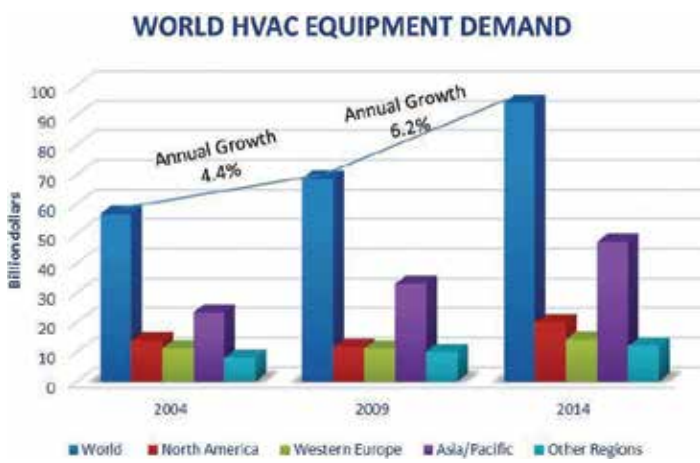

Figure 5. HVAC equipment demand and annual growth. Source: The Freedonia group, Inc. world HVAC equipment demand, Cleveland, OH, USA.

3. System description

The cooling needs for thermal comfort and sunshine timings follow the same pattern. The demand of air conditioning is higher in summer when the sun shines with higher intensity. What if this intensity of sun can be used as an input energy source for the cooling devices?

The issues related to conventional air conditioning technology can be addressed using a new technology called desiccant-based evaporative cooling. This technology is a combination of a desiccant dehumidifier and an evaporative cooler. The schematic representation of desiccant cooling system is shown in **Figure 6** [1]. In such systems, the energy is required to drive the fans, operate the water pump, and to regenerate the desiccant dehumidifier. The required energy can be provided using solar thermal collector for desiccant dehumidifier and photovoltaic modules to drive the fans and the water pump according to the load requirements. The desiccant dehumidifier controls the latent load whereas; evaporative cooler controls the sensible load. Heat recovery medium is used to make the system more energy efficient. For the continuous operation of the system, the regeneration air is heated up to the required regeneration temperature using a solar thermal collector to regenerate the desiccant dehumidifier. The load demand and sunshine follows the same profile which makes this system an effective alternative to conventional air conditioning system. The energy demands for continuous operation of this system can be fulfilled using solar heat according to the load profile.

The use of desiccant cooling technology reduces the energy consumption substantially because of no overcooling and reheating of supply air for moisture removal. More research

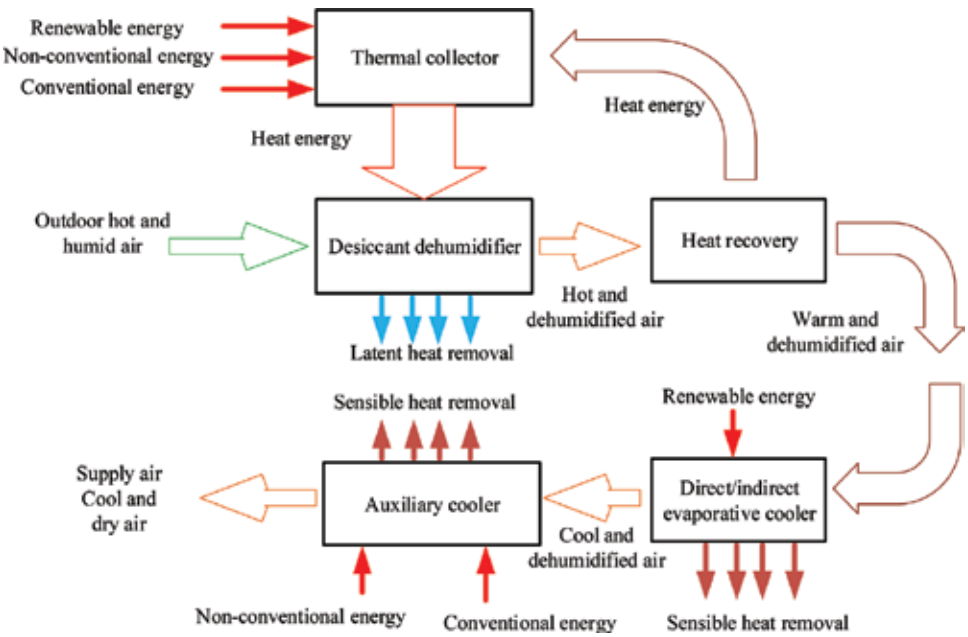

Figure 6. Principle of desiccant-based evaporative cooling technology [1].

http://dx.doi.org/10.5772/intechopen.73166

should be conducted on innovative design of this technology taking into consideration the associated investment costs. The development of technology is in progress and it is attaining stability in the market. It appears to be reliable, safe, and environmental friendly system according to the needs of our society. This technology needs to be developed and more attention is required for its implementation and promotion.

4. Desiccant cooling cycles

Desiccant cooling is used as an alternative to conventional cooling system. These systems operate without the use of any refrigerant and control the latent as well as sensible load independently which helps in better control of moisture and improve air quality. Thermal energy required for regeneration of these units can be supplied from different heat sources such as solar, biomass, waste heat, etc.

Desiccant technology is a cooling technology which removes moisture from air by a process known as sorption (adsorption or absorption). Different desiccant materials are used for this process. Due to vapor pressure difference, adsorption material absorbs the water vapors from the air. To repeat the cycle continuously, moisture from the desiccant wheel is removed using thermal energy. Basic operating cycles of solid and liquid desiccant cooling are illustrated in **Figure 7** [12] and **Figure 8** [13], respectively. In both cooling systems, desiccant dehumidifier is the major component which controls the latent load followed by an addition cooing system i.e. evaporative cooler. Input heat is provided through some thermal energy medium

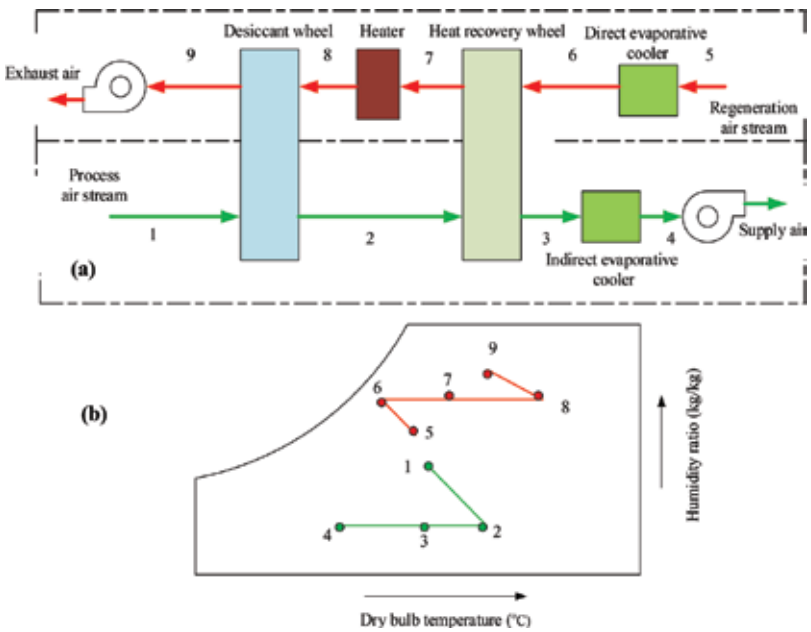

Figure 7. (a) Systematic solid desiccant cooling system with evaporative cooler (b) psychometric processes [12].

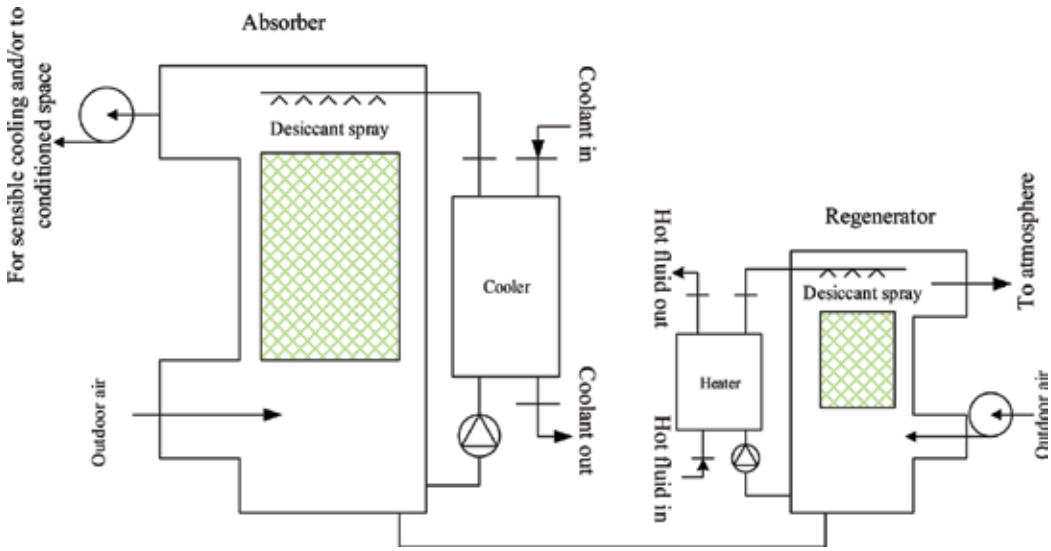

Figure 8. Basic configuration of liquid desiccant system [13].

for desorption of desiccant dehumidifier and continuous operation of the cycle. There are different modifications to the basic desiccant cooling cycles. A summary of different desiccant cooling cycles is:

- **Ventilation cycle**: In this cycle outdoor air is cooled and 100% return air from the conditioned room is utilized for regeneration process. The air leaving at point E is cooled in an evaporative cooler and is used as cold-sink for room return air as shown in **Figure 9**. The room return air is heated in a heat exchanger and then further heated using a heating medium up to a desired regeneration temperature.
- **Recirculation cycle:** this cycle compromises of the same components as ventilation cycle except 100% return air from the conditioned room is mixed with the process air stream at the inlet of desiccant wheel as illustrated in **Figure 10**. This cycle has a Thermodynamic advantage that it can process the air with greater availability for cooling. But this cycle has a higher cold-sink temperature as compared to the ventilation cycle.
- **Dunkle cycle**: This cycle is an effort to combine the thermodynamic advantages of both the ventilation and recirculation cycles. It is a recirculation cycle with an additional heat exchanger to improve the performance of the system. The cycle is shown in **Figure 11**.
- **Recirculation ventilated cycle**: Recirculation ventilated cycle is mix of ventilation and recirculation cycle in which 10% ventilation air mixed with the return air.
- **Wet-surface heat exchanger (WSHE)**: The other desiccant cooling cycle make use of a wet-surface heat exchanger (WSHE), wherein the incoming air can be cooled to its dew point temperature. In WSHE, water indirectly cools the process air and then this air is used to cool the return air from the room.

http://dx.doi.org/10.5772/intechopen.73166

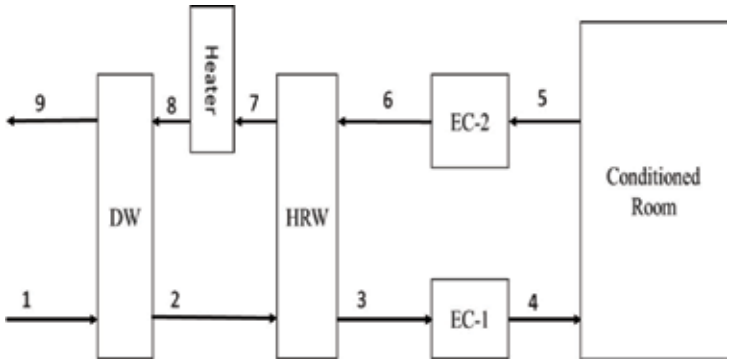

Figure 9. Desiccant evaporative cooling system operating on ventilation cycle.

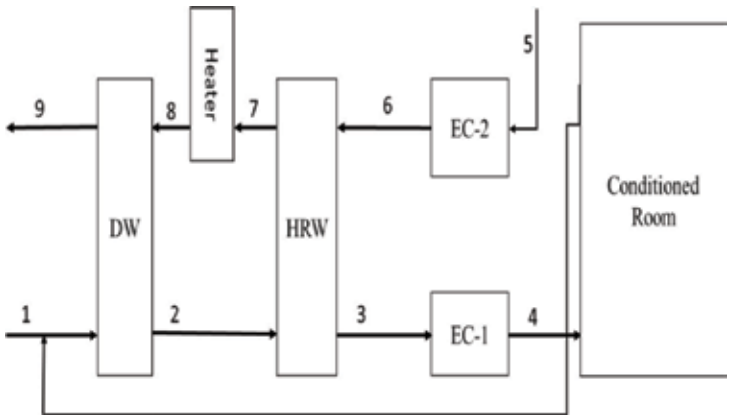

Figure 10. Desiccant evaporative cooling system operating on recirculation cycle.

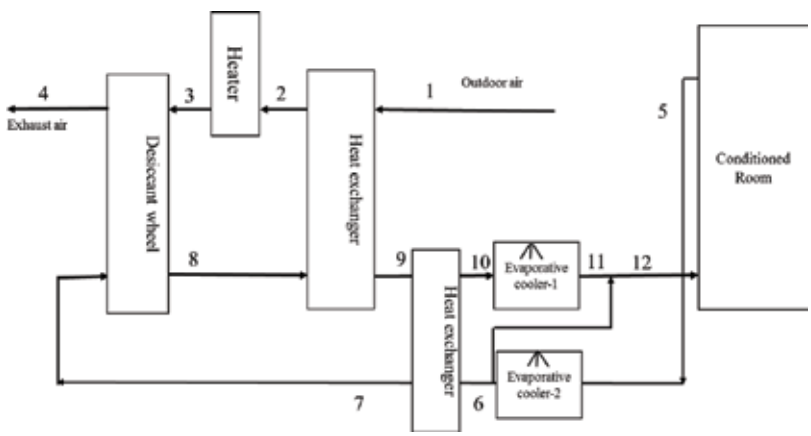

Figure 11. Desiccant evaporative cooling system operating on Dunkle cycle.

- **Novel conceptual cycle**: In novel conceptual cycle, mixed air is dehumidified and then this dehumidified air is sensibly cooled in a heat exchanger. After sensible cooling it is passed through WSHE.
- **Three mixed-mode cycles**: In this cycle the evaporative coolers which are used as cooling medium are replaced by regenerative/wet-surface heat exchangers.

5. Comparative analysis

5.1. Ventilation cycle

The basic configuration of a ventilation cycle is shown in **Figure 9**. In ventilation cycle, hot and humid process air passes through the rotating desiccant wheel and its dry bulb temperature increases and humidity decreases. The process air is then cooled by passing through a heat recovery wheel. The further cooling of process air is achieved using an evaporative cooler according to the set-values of supply air temperature and humidity. For ventilation cycle, the exhaust air stream from the conditioned space is cooled and humidified close to saturation using an evaporator cooler. The quantity of air coming at point 5 is normally equal to quantity of air entering at point 4. The exhaust air is sensibly heated to precool the process air. Finally, the regeneration air stream is heated and is passed through desiccant wheel for its regeneration, which allows the continuous operation of the dehumidification process. For ideal desiccant wheel the air at the exit of the wheel will be completely dehumidified and specific humidity at point 2 will be zero [14].

$$\omega_{2,\ ideal} = 0 \tag{1}$$

The heat recovery wheel is basically a counter flow heat exchanger. The desiccant wheel and heat recovery wheel latent effectiveness in term of specific humidity and energy balance for the adiabatic desiccant wheel can be represented as:

$$\varepsilon_{DW} = (\omega_1 - \omega_2)/(\omega_1 - \omega_{2,ideal}) \tag{2}$$

$$(\omega_1 - \omega_2)\, h_{fg} = (h_1 - h_2) \tag{3}$$

$$\varepsilon_{HRW} = (T_2 - T_3)/(T_2 - T_6) \tag{4}$$

In the evaporative cooler, air undergoes a process of adiabatic dehumidification. On psychrometric chart, this process follows constant wet bulb temperature line.

$$\varepsilon_{EC1} = (T_3 - T_4)/(T_3 - T_{w3}) \tag{5}$$

$$\varepsilon_{EC2} = (T_5 - T_6)/(T_5 - T_{w5}) \tag{6}$$

In case of equal process and regeneration air flow rates, energy balance on the adiabatic heat recovery wheel can be written as:

$$(h_2 - h_3) = (h_7 - h_8) \tag{7}$$

Sensible effectiveness of the desiccant wheel is given by:

$$\varepsilon_{DW,T} = (T_2 - T_1)/(T_8 - T_7) \tag{8}$$

After achieving the temperature and humidity at each state point of the cycle, the cooling capacity, regeneration load and coefficient of performance can be deduced from the following relations.

$$Q_{cool} = (h_5 - h_4) \tag{9}$$

$$Q_{reg} = (h_8 - h_7) \tag{10}$$

$$COP = Q_{cool}/Q_{reg} \tag{11}$$

5.2. Recirculation cycle

The basic configuration of a desiccant cooling system operating on regeneration cycle is shown in **Figure 10**. In recirculation mode all the process remains the same as that of ventilation cycle except the air leaving from the conditioned room is mixed with the process air at point 1 instead of circulating it on the regeneration side. On the regeneration side, fresh ambient air is used. For regeneration cycle the thermal COP of the system is given as:

$$COP = \dot{m}_p(h_1 - h_4)/\dot{m}_r(h_7 - h_8) \tag{12}$$

6. Results and discussion

The conditions of air at different points of the cycle operating on both cycles are obtained using the developed mathematical model in the preceding sections. The effectiveness of both evaporative coolers and heat recovery wheel is considered to be constant for this analysis. The conditions of the supply air are one of the important parameter which plays a major role on performance and amount of latent load removed from the room by the system. The climatic conditions used for this analysis and required temperature and humidity ratio of the supply air is presented in **Table 1**.

The obtained results for yearly average value of COP, required heat, and cooling capacity are presented in **Table 2**. It can be observed that, the system operating on ventilation cycle has higher value of average COP as compared to regeneration cycle. The difference in the performance of both cycles is because of required regeneration heat as illustrated in **Table 2**. The cooling load for both cycles remains almost same because of small difference in conditions of air at points 1 and 5. The difference of regeneration heat is because of temperature difference between point 7 and 8 (T_8 - T_7). In this analysis T_8 (regeneration temperature) is set to a constant value of 120°C. The temperature at point 7 has higher value in case of ventilation cycle as compared to recirculation cycle. This larger difference makes the required regeneration heat higher for recirculation cycle as compared to ventilation cycle. Note that, average values of performance parameters are calculated when $T_{ambient}$ = 35°C, regeneration temperature of 120°C, process air flow rate 1.5 kg/s, and both regeneration and process mass flow rates are equal. The detailed results for monthly COP of the system operating on both cycles are presented in **Figures 12** and **13**. The system operating under ventilation and recirculation cycle has a maximum COP of 0.81 and 0.52, respectively for the month of September.

	Outdoor air			Room supply air		
Month	**Dry bulb Temperature (°C)**	**Humidity Ratio (g_v/kg_a)**	**Wet bulb Temperature (°C)**	**Dry bulb Temperature (°C)**	**Humidity Ratio (g_v/kg_a)**	**Wet bulb Temperature (°C)**
April	30.14	13.19	21.10	17.31	9.81	15.19
May	33.21	14.27	22.05	18.74	9.91	16.70
June	39.54	15.71	24.69	18.52	10.11	15.88
July	41.51	20.55	28.97	17.44	10.23	14.10
August	37.28	20.39	27.94	18.32	10.45	15.23
September	37.01	23.52	29.50	18.51	10.12	16.90
October	34.34	15.53	24.47	17.43	9.55	15.77
November	28.71	16.34	23.50	18.54	9.23	15.13
December	23.53	12.94	18.88	18.16	8.88	15.01

Table 1. Climatic data and desired supply conditions.

Parameter	Ventilation Mode	Recirculation Mode
Q_{cool} (kW)	44.40	45.2
Q_{reg} (kW)	99.58	128.21
COP	0.461	0.354
Regeneration temperature (°C)	120	120

Table 2. Average performance parameters for desiccant cooling system operating on ventilation and circulation cycle.

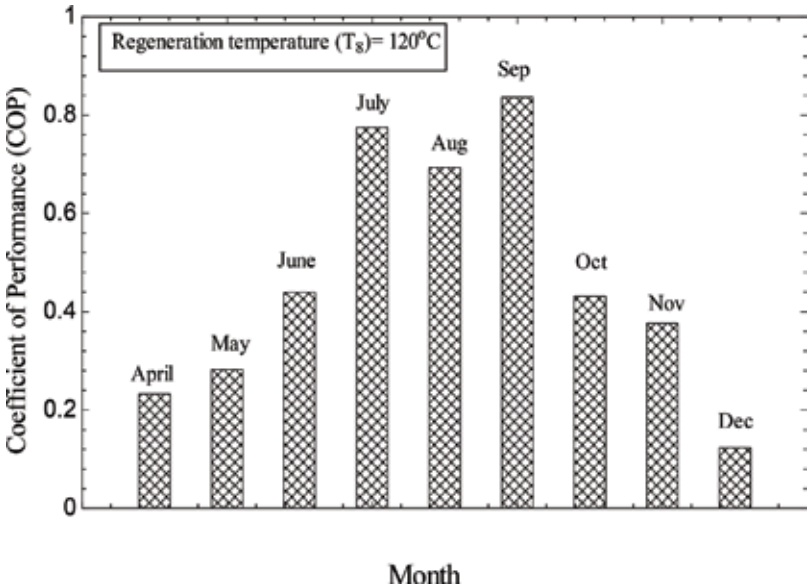

Figure 12. Monthly variations of COP for ventilation cycle.

http://dx.doi.org/10.5772/intechopen.73166

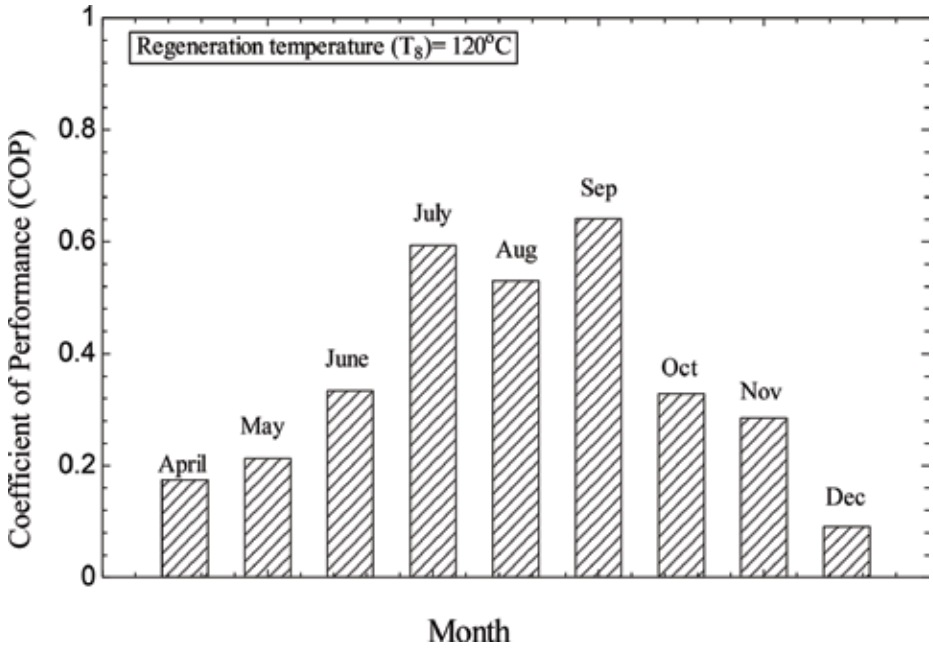

Figure 13. Monthly variations of COP for recirculation cycle.

7. Economic evaluation

In this section, an overview of economic aspects related to desiccant cooling technology has been presented. The economic evaluation of desiccant cooling system has been carried out by different researchers. Abdel-Salam and Simon [15] evaluated a membrane based liquid desiccant cooling system for its enviro-economic aspects. They compared primary energy consumption of four different systems. The obtained results showed that the primary energy consumption and total life cycle cost of desiccant cooling system was lower than conventional system by 19 and 12%, respectively. Addition of energy recovery ventilator improved the difference by 32% for primary energy consumption and 21% for total life cycle cost. Li et al. [16] compared vapor compression cooling system and hybrid of desiccant system for energy and economic evaluation. The results indicated that replacing the conventional system with hybrid system would reduce the size from 28 to 19 kW leading to annual effective energy savings of nearly 6760 kWh. However, the payback period would be 7 years because of the added initial investment costs.

The costs of system accessories will vary depending upon the required flow rates and cooling needs [9]. The sizing charts for fans and pumps are shown in **Figures 14** and **15**, respectively. It can be observed that cost of each accessory depends upon the required output. The small desiccant cooling systems have higher specific costs as compared to large units. A comparative analysis of system specific cost with respect to its size is presented in **Figure 16**. The specific installed system costs are 7300 EUR/kW for small-scale systems and in average 1900 EUR/kW for large-scale systems [17].

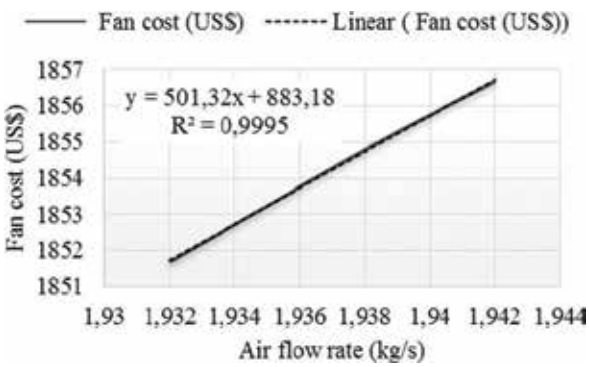

Figure 14. Cost of fan [9].

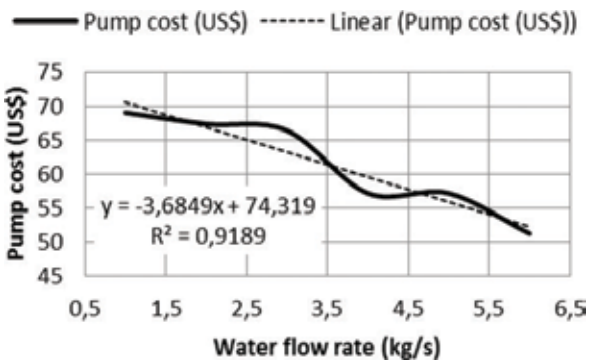

Figure 15. Cost of pump [9].

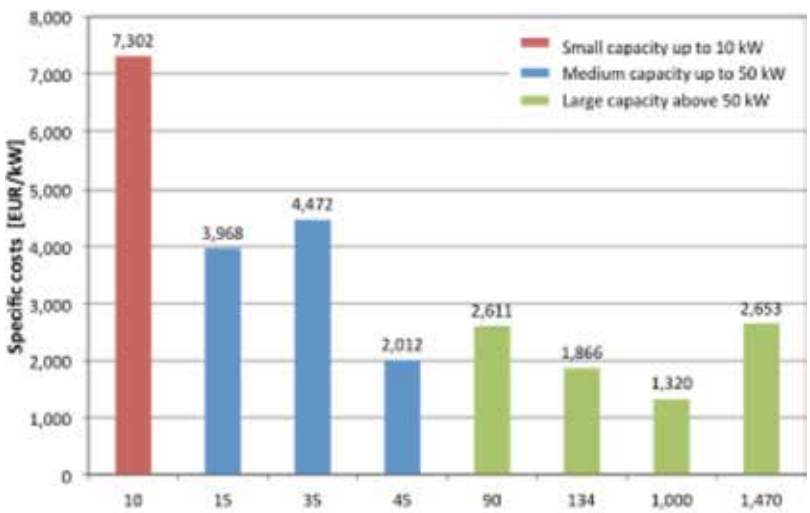

Figure 16. Specific costs of thermal cooling systems. Source: Green Chiller.

8. Recent developments and future needs

The performance and development of desiccant cooling systems strongly depends on the desiccant materials used. The thermo-physical properties of these materials affect the performance of the system significantly. The key parameter for the selection of a desiccant material is that it should have the ability to absorb and hold large amount of water vapor. It should be desorbed easily by providing heat input.

The properties such as density, vapor pressure, etc. of different desiccant materials can be enhanced by mixing two or more materials together. The mixed desiccants are termed as composite desiccants. Many researchers have studied the properties of composite desiccant materials in order to study their effects on dehumidification performance of the system. **Table 3** provides a summary of some experimental studies on desiccant cooling systems and lists the regeneration temperature and desiccant material used [18–24]. The literature review showed that most of the experimental studies were conducted with silica gel at high regeneration temperatures. There is currently limited research conducted with desiccant wheel other than silica gel.

Although, a number of developments have been made in desiccant cooling technology but a number of steps still needs to be addressed in order to make this technology more market accessible. Some of the future research and development needs are:

- Cost-effective, non-corrosive, and nontoxic liquid desiccant materials need to be developed.
- The effectiveness of regenerator needs to be improved using several approaches including multiple-effect boilers and vapor compression distillation. Different alternative energy sources should be utilized for regeneration purpose.
- Surface enhancements or extended surfaces such as fins should be used to modify the design of dehumidifier and regenerator for better heat and mass transfer.

Author	Desiccant material used	Regeneration temperature
Jia et al. [18]	Silica gel	60–120°C
White et al. [19]	Zeolite and polymers	50–80°C
Enteria et al. [20]	Silica gel	60–80°C
Eicker et al. [21]	Lithium chloride, Titanium dioxide, silica gel, silica gel and calcium chloride	45–90°C
Angrisani et al. [22]	Silica gel	60–70°C
Enteria et al. [23]	Silica gel, Titanium dioxide	60–80°C
Wrobel et al. [24]	Lithium Chloride	45–50°C

Table 3. Summary of literature for regeneration temperature and desiccant materials.

- Advanced indirect evaporative coolers should be integrated with liquid dehumidification system to make the system more commercial.
- The system should be developed for longer operation to avoid possible operating problems in industrial applications such as acidifying the desiccant, foaming, etc.

Research and development of liquid desiccant cooling system requires more efforts from experts in the area. Design activities needs to be developed to make this technology accessible to all people in different parts of the worlds.

9. Concluding remarks

The HVAC load can be reduced significantly using renewable energy based desiccant cooling systems due to lower requirement of input power for these systems and effective utilization of alternative resources of energy. These systems prove to be an effective alternative to conventional cooling systems which are energy inefficient and as well as minimize greenhouse gases emissions. In this chapter, a comparative study has been presented among two different configurations of a solar desiccant cooling system operating in the hot and humid climatic condition. The two desiccant cooling cycles namely, ventilation and recirculation are solved theoretically to analyze and compare the system performance. The results showed that COP of the system operating on ventilation mode is higher than the system operating on recirculation mode. Therefore, based on the condition of ambient air, solar desiccant cooling system under the ventilation mode is more suitable than the recirculation mode. This paper also analyzes monthly performance of the system operating under both modes. Furthermore, the analysis of the supply air condition shows that the system is able to provide human thermal comfort in humid climates and it can be an alternative for the conventional air conditioning system. The economic evaluation shows that the larger systems have lower cost as compared to smaller units.

Although progress has been made in the development of this alternative cooling technology but a number of steps still needs to be taken in order to make this technology more market accessible. More research should be conducted on other innovative desiccant cooling systems integration, taking into consideration the associated investment costs. The development in liquid desiccant technology is in progress and it has attaining stability in the market. Furthermore, in order to access this technology in comparison to conventional cooling systems, hidden costs of fossil fuels should be accounted. Understanding the hidden impacts of fossil fuels is critical for evaluating the true cost of conventional power generation systems and has to be communicated to the community.

Acknowledgements

The authors would like to acknowledge the support provided by King Abdulaziz City for Science and Technology (KACST) through the Science & Technology Unit at King Fahd University of Petroleum & Minerals (KFUPM) for funding this work through project No. 10-ENE1372-04 as part of the National Science, Technology and Innovation Plan (NSTIP).

http://dx.doi.org/10.5772/intechopen.73166

Nomenclatures

h	specific enthalpy (kJ/kg)
h_{fg}	specific enthalpy for water (kJ/kg)
$\dot{m}$	mass flow rate (kg/s)
Q_{cool}	cooling load (kW)
Q_{reg}	regeneration heat (kW)
T	dry bulb temperature (°C)
T_w	wet bulb temperature (°C)
Greek letters	
ω	humidity ratio (kg_v/kg_a)
ε	effectiveness
Subscripts	
a	air
DW	desiccant wheel
DCS	desiccant cooling system
HRW	heat recovery wheel
EC	evaporative cooler
p	process
r	regeneration
v	vapor
1, 2, 3….	state points

Author details

Muhammad Mujahid Rafique[1]* and Shafiqur Rehman[2]

*Address all correspondence to: mujahidrafique89@gmail.com

1 Independent Scholar, Toba Tek Singh, Pakistan

2 Center for Engineering Research, Research Institute, King Fahd University of Petroleum and Minerals, Dhahran, Saudi Arabia

References

[1] Rafique MM, Gandhidasan P, Rehman S, Al-Hadhrami LM. A review on desiccant based evaporative cooling systems. Renewable and Sustainable Energy Reviews. 2015;**45**:145-159

[2] Rafique MM, Gandhidasan P, Bahaidarah HMS, Shakir MA. Thermal and exergetic performance evaluation of an absorption type desiccant dehumidifier. Environmental Progress & Sustainable Energy. 2017. DOI: 10.1002/ep.12788

[3] Rafique MM, Rehman S, Lashin A, Al Arifi N. Analysis of a solar cooling system for climatic conditions of five different cities of Saudi Arabia. Energies. 2016 Jan 27;**9**(2):75

[4] Rafique MM, Gandhidasan P, Bahaidarah HM. Emerging energy efficient thermally driven HVAC technology: Liquid desiccant enhanced evaporative air conditioning. In: Desiccant Heating, Ventilating, and Air-Conditioning Systems. Singapore: Springer; 2017. pp. 229-256

[5] Rafique MM. A mathematical model for predicting the performance of liquid desiccant wheel. International Journal of Thermal and Environmental Engineering. 2016;**13**(2):101-105

[6] Rafique MM, Rehman S, Alhems LM, Lashin A. Parametric analysis of a rotary type liquid desiccant air conditioning system. Energies. 2016 Apr 21;**9**(4):305

[7] Rafique MM. A statistical analysis of desiccant dehumidifier for air conditioning application. International Journal of Hybrid Information Technology. 2015;**8**:245-256

[8] Uçkan İ, Yılmaz T, Büyükalaca O. Effect of operation conditions on the second law analysis of a desiccant cooling system. Applied Thermal Engineering. 2017 Feb 25;**113**:1256-1265

[9] Rafique MM, Rehman S, Alhems LM. Exergoeconomy of a desiccant enhanced evaporative cooling system using exergetic incremental function. Desalination and Water Treatment. 2017 Jun 1;**79**:30-39

[10] Das RS, Jain S. Experimental investigations on a solar assisted liquid desiccant cooling system with indirect contact dehumidifier. Solar Energy. 2017 Sep 1;**153**:289-300

[11] Watts N, Adger WN, Agnolucci P, Blackstock J, Byass P, Cai W, Chaytor S, Colbourn T, Collins M, Cooper A, Cox PM. Health and climate change: Policy responses to protect public health. The Lancet. 2015 Nov 7;**386**(10006):1861-1914

[12] Rafique MM, Gandhidasan P, Rehman S, Alhems LM. Performance analysis of a desiccant evaporative cooling system under hot and humid conditions. Environmental Progress & Sustainable Energy. 2016;**35**(5):1476-1484

[13] Rafique MM, Gandhidasan P, Ibrahim NI, Bahaidarah HMS. Recent developments in liquid desiccant based cooling systems. In: Abraham MA, editor. Encyclopedia of Sustainable Technologies. Elsevier; 2017. pp. 441-453

[14] Pons M, Kodama A. Entropic analysis of adsorption open cycles for air conditioning, part 1: First and second law analyses. International Journal of Energy Research. Amsterdam, Netherlands. 2000;**24**:251-262

[15] Abdel-Salam AH, Simonson CJ. Annual evaluation of energy, environmental and economic performances of a membrane liquid desiccant air conditioning system with/without ERV. Applied Energy. 2014;**116**:134-148

[16] Li YT, Lu L, Yang HX. Energy and economic performance analysis of an open cycle solar desiccant dehumidification air-conditioning system for application in Hong Kong. Solar Energy. 2010;**84**:2085-2095

[17] Mugnier D. Quality assurance and support measures for solar cooling-IEA solar heating and cooling. Energy Procedia. 2016;**91**:792-798

[18] Jia CX, Dai YJ, Wu JY, Wang RZ. Experimental comparison of two honeycombed desiccant wheels fabricated with silica gel and composite desiccant material. Energy Conversion and Management. 2006;**47**:2523-2534

[19] White SD, Goldsworthy M, Reece R, Spillmann T, Gorur A, Lee D-Y. Characterization of desiccant wheels with alternative materials at low regeneration temperatures. International Journal of Refrigeration. 2011;**34**:1786-1791

[20] Enteria N, Yoshino H, Satake A, Mochida A, Takaki R, Yoshie R, Mitamura T, Baba S. Experimental heat and mass transfer of the separated and coupled rotating desiccant wheel and heat wheel. Experimental Thermal and Fluid Science. 2010;**34**:603-615

[21] Eicker U, Schürger U, K€ohler M, Ge T, Dai Y, Li H, Wang R. Experimental investigations on desiccant wheels. Applied Thermal Engineering. 2012;**42**:71-80

[22] Angrisani G, Minichiello F, Roselli C, Sasso M. Experimental analysis on the dehumidification and thermal performance of a desiccant wheel. Applied Energy. 2012;**92**:563-572

[23] Enteria N, Yoshino H, Satake A, Mochida A, Satake A, Yoshie R, Takaki R, Yonekura H, Mitamura T, Tanaka Y. Performance of solar-desiccant cooling system with silica-gel (SiO_2) and titanium dioxide (TiO_2) desiccant wheel applied in east Asian climates. Solar Energy. 2012;**86**:1261-1276

[24] Wrobel J, Morgenstern P, Schmitz G. Modeling and experimental validation of the desiccant wheel in a hybrid desiccant air conditioning system. Applied Thermal Engineering. 2013;**51**:1082-1091

Edited by Chaouki Ghenai and Tareq Salameh

Air conditioning system is one of the major consumers of electrical energy in many parts of the world today. It represents between 40 and 70% of the energy consumption in commercial buildings. The demand of energy for air conditioning systems is expected to increase further in the next decades due to the population growth, the new economic boom, and the urbanization development. The rapid growth of air conditioning and electricity consumption will contribute further to climate change if fossil and nonrenewable resources are used. More energy-efficient and renewable energy-based air conditioning systems to accomplish space cooling are needed. This book intends to provide the reader with a comprehensive overview of the current state of the art in sustainable air conditioning technologies and focus on the most recent research and development on green air conditioning systems including energy-efficient and renewable energy-based air conditioning systems.

Published in London, UK

IntechOpen

ISBN 978-1-83881-331-4